Master thesis submitted for the partial fulfillment of
the Master of Marine Sciences at Utrecht University
December 2018

EFFECT OF VEGETATED FOREDUNES ON WIND FLOWS AND AEOLIAN SAND TRANSPORT

A field study of Aeolex II

Corinne Boehm (5813867)

Utrecht University

Utrecht University supervisors:
Prof. Dr. Gerben Ruessink
Dr. Christian Schwarz

MSC THESIS GEO4-1520

Effect of vegetated foredunes on wind flows and aeolian sand transport

A field study of Aeolex II

Student

Corinne Böhm (5813867)

c.bohm@students.uu.nl, corinne.boehm@gmail.com

MSc Marine Sciences, Utrecht University

Credits: 37.5 ECTs

Supervisors

Prof. Dr. Gerben Ruessink, UU (b.g.ruessink@uu.nl)

Dr. Christian Schwarz, UU (c.s.schwarz@uu.nl)

Utrecht University

Abstract

Coastal foredunes are important for coastal safety and biodiversity. The complex interplay between wind, morphology, vegetation and aeolian sediment transport across foredunes has been widely studied. This study aims to add to existing knowledge by studying the controls of foredune growth on high, densely vegetated foredunes. Field data were collected during a period of five weeks in Egmond aan Zee, the Netherlands (*AEOLEX II* campaign). This site is characterised by a wave-dominated beach with flat slope (1:30), approximately 20 m high foredunes with steep slope (1:2) and dense cover of European marram grass (*Ammophila arenaria*). Wind velocity, direction and turbulent kinetic energy (*tke*) were measured across the foredune, while sand transport was recorded on five days. Moreover, vegetation surveys were done across three transects, which were complemented with sedimentation data from LIDAR elevation maps. Results show that depending on the incident wind direction, the wind flow changes in both magnitude and direction. A similar pattern was observed for all onshore wind directions: the wind was first reduced and deflected to alongshore, followed by acceleration up to 310% and turning to perpendicular onshore. Highly oblique to alongshore directed flows were hardly altered at the foot but deflected up to 38° to more onshore at the crest. In absolute values the *tke* was directly proportional to the wind velocity. But relatively (*r*), it was largest at the dune foot for perpendicular onshore winds and on the slope at highly oblique to alongshore winds. Aeolian transport decreased substantially across the foredune. Fluxes at the upper dune foot increased first to 328% and subsequently decreased. Transport fluxes varied for different days, most likely due to the wind velocity and maximum fetch size. The vegetation assays showed that the foredune was covered densely (20 – 100%), reaching its maximum at the crest. The vegetation strongly influences the foredune, since most sedimentation was related to vegetation cover. The majority of wind flows were observed, resulting in a conceptual understanding on how wind changes across the foredune. Most of the findings are in line with previous studies. The study showed that the foredune has large influences, both on wind characteristics as well as on transport.

Acknowledgements

Firstly, I would like to thank both my supervisors Prof. Dr. Gerben Ruessink and Dr. Christian Schwarz for their support, constructive criticism and for the many answers to my questions. Thank you for your patience that allowed me to develop and grow on my own terms. Your enthusiasm was contagious and helped me to overcome moments of doubt. A special thanks to Gerben for making this project possible and organising the field campaign. Thanks to you we could not only gather a lot of interesting data, but shelter from the harsh wind, rain and saltating grains. An obvious thanks to Christian for the many meetings and the time that you spent discussing with me and pushing me into the right direction to improve over and over. I am lucky to have had such professional and kind supervisors. Also thanks to Dr. Jasper Donker for help and input in the field and throughout the project.

A big thank you to Team Egmond: Jorn, Jorn and Job with whom I spend the adventure of the field campaign. We shared the sunny as well as the so many windy days and evenings with chocolate covered pepernoten. Thank you all for helping me replacing car batteries on the dune top or counting grass helms.

I would also like to acknowledge the entire technical team ing. Marcel van Maarseveen, ing. Bas van Dam, Arjan van Eijk and Mark Eijkelboom. You explained the instruments to us, got them running in the field and helped keeping it so. You probably did so much more for us. Without you the data collection would not have been possible.

Lastly a thank you to all my friends. To name a few: Anastasia I owe you a tremendous gratitude for proof reading. Together with Fleur you supported and consoled me as friends and fellow students. Marina thanks to whom I always find motivation through the beauty of science. I would like to thank my family for supporting me during my studies and believing in me without expectations. Last but not least thank you Tirsan, no words can express my gratitude to you!

Table of content

Table of figures

Tables

1. Introduction

Coastal foredunes are shore-parallel sand dunes that form by aeolian deposition typically within vegetation on the backshore (Hesp, 1988, 2002; Zarnetske *et al.*, 2015; Davidson-Arnott *et al.*, 2018). There are various types of foredunes, but incipient and established foredunes can be defined into two main categories, each one having many morphological and ecological variations (Hesp, 2012). Their formation is closely linked to vegetation and to local coastal processes (Hesp, 1988; Davidson-Arnott *et al.*, 2018), in particular to aeolian sand transport (Anderson and Walker, 2006). Foredunes often play an essential role for coastal defence, being the first barrier against marine storms and flooding (de Winter, Gongriep and Ruessink, 2015; Miller, 2015). Storm surges are a main cause of foredune erosion, while foredune growth occurs due to aeolian sediment transport (Hesp, 1988; Zhang, Douglas and Leatherman, 2004; de Winter, Gongriep and Ruessink, 2015; Davidson-Arnott *et al.*, 2018). Moreover, foredunes function as a valuable ecosystem, hosting a large variety of species (Everard, Jones and Watts, 2010; Miller, 2015). Vegetation plays a crucial role in foredune build-up and stabilisation and is therefore an important determinant for the characteristics of a foredune, such as form or height (Sigren *et al.*, 2014; Keijsers, De Groot and Riksen, 2015). Many foredunes worldwide are covered by the pioneer species marram grass (*Ammophila arenaria*) (Petersen, Hilton and Wakes, 2011), and this also applies to the Netherlands (Arens, 1996; Petersen, Hilton and Wakes, 2011; de Winter, Gongriep and Ruessink, 2015). Marram grass has sand-trapping capacities and usually promotes high and topographically continuous foredunes with a steep stoss slope (Milne and Sawyer, 2002; Petersen, Hilton and Wakes, 2011).

There is a close interplay of vegetation and sediment transport on the foredune (Miller, 2015). Several aspects play a role in this. Firstly, the mere presence of the plants increases the roughness of the topography. Secondly, the trapped sediment eventually builds up and the dune morphology is altered. These two processes then affect the wind flow over the foredune, which itself is the driving force behind sediment transport mechanisms (Keijsers, De Groot and Riksen, 2015). Vegetation can however also hinder the delivery of sediment landward of the foredune (Petersen, Hilton and Wakes, 2011), which in many dune environments results in climax vegetation and a less dynamic ecosystem leading to less biodiversity (Arens *et al.*, 2013; Barchyn and Hugenholtz, 2013; Ruessink *et al.*, 2017).

Foredune dynamics and evolution are complex (e.g. Walker *et al.*, 2017; Davidson-Arnott *et al.*, 2018). These include aeolian processes on the beach, such as wind velocity, wind direction and surface moisture (Delgado-Fernandez, 2011; Bauer *et al.*, 2012), as well as nearshore processes of the foredune, such as vegetation cover and pattern (Delgado-Fernandez, 2011). The complexity of these interactions implies that growth and sand transport across the foredune are still not fully understood, especially regarding various wind conditions and different foredune types. Yet, there is great interest in improving the predictive capacity of foredune development (Davidson-Arnott *et al.*, 2018) for both environmental significance and coastal safety. The latter relies on the understanding of the processes underlying dune growth, which is critical for natural dune restoration after erosion events. This also would help to improve morphological models to predict the vulnerability of dunes. This is particularly significant in light of the projected increase in erosion events in the future. Long-term erosion rates are expected to increase in the face of accelerated sea level rise (Zhang, Douglas and Leatherman, 2004). Moreover, more extreme storm events in the North Sea may cause spontaneous erosion through storm surges (Beniston *et al.*, 2007). This is relevant for low-lying countries, such as the Netherlands, which is densely populated. It is therefore important to document and quantify transport events under various wind conditions on different foredunes and to link true vector quantities of the wind field with sediment transport (Petersen, Hilton and Wakes, 2011; Bauer *et al.*, 2012).

With this in mind, this project aims to document the interaction of vegetation and sediment transport on a high foredune and under various wind conditions, wind and wind-driven sediment transport across a foredune. In order to do so, a field campaign was conducted in October 2017 at Egmond aan Zee, the Netherlands, to study the matter on > 20 m high, densely vegetated foredune. Aeolian sediment transport was quantified and data collected *in situ*. These include the wind-field (velocity, direction, and turbulence), dune morphology, sediment transport and vegetation cover of the foredune.

The next chapter will provide a comprehensive background of vegetated coastal foredunes, as well as the different and most important processes that play a role in foredune growth and aeolian sediment transport across the foredune. Based on the literature review, the current shortcomings of previous studies are used to define a specific problem description and formulate research questions. This is followed by the methods of the field work during which wind velocity, direction and turbulence were measured, and sand transport and vegetation cover were determined. The study results are subsequently presented and are divided into two major sections: wind flows, and sediment transport, morphology and vegetation. The results will be discussed and put into context with previous studies. Ultimately, conclusions will be drawn as to how the vegetation on the foredune at its seaward site alter the physical settings that are responsible for aeolian sediment transport.

2. Background

2.1. Foredunes and their development

Foredunes develop during onshore winds by the accretion of aeolian transported sand that moves from the beach landwards and gets trapped in vegetation (Arens, 1996; Milne and Sawyer, 2002; Keijsers, De Groot and Riksen, 2015; Goldstein, Moore and Durán Vinent, 2017). Foredune development depends on complex interactions between coastal and beach topography, local wind characteristics, the frequency of erosion and storms (Goldstein and Moore, 2016), aeolian sediment transport, sediment availability (Hesp, 1988, 2002; Arens, Van Kaam-Peters and Van Boxel, 1995; Anderson and Walker, 2006; Hesp *et al.*, 2015; Zarnetske *et al.*, 2015), sand grading (Kuriyama, Mochizuki and Nakashima, 2005) and vegetation (e.g. Hesp, 1988; Davidson-Arnott *et al.*, 2018).

Since so many different factors can contribute to foredune morphology, it is challenging to identify the primary driving force behind dune development and recovery after erosion events (Goldstein, Moore and Durán Vinent, 2017).

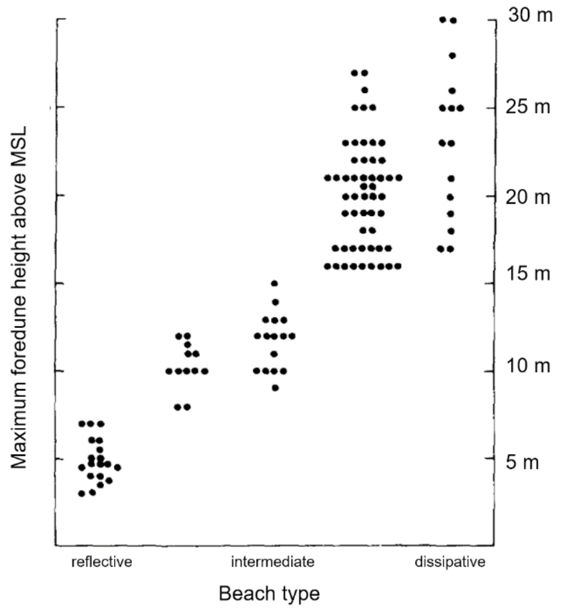

Figure 1. Relationship between beach type and maximum foredune height above mean sea level, found for Myall Lakes beaches, derived from data of ground surveys 100 m apart in the mid-region of selected modal beaches. Extracted and modified from Short and Hesp (1982).

The type of beach influences aeolian sand transport rates, which in turn have an effect on the potential size of the foredune (Short and Hesp, 1982). Dissipative beaches are frequently characterised by large-scale transgressive dune sheets, whereas reflective beaches are characterised by minimal dune development (Figure 1) due to high and low aeolian transport rates, respectively (Short and Hesp, 1982; Wright and Short, 1984). This MSc study was carried out at large dunes, found at high energy dissipative beaches along the Dutch coast (Ruessink, Kleinhans and van den Beukel, 1998).

More recently, Goldstein, Moore and Durán Vinent (2017) suggested that vegetation controls the maximum size of coastal dunes. The authors modelled the coevolution of topography and vegetation in response to both physical and ecological factors. They concluded that plant zonation, rather than sediment supply determines the maximum size of coastal dunes and therefore controls the coastal vulnerability to storms

(Goldstein, Moore and Durán Vinent, 2017). That vegetation is a major factor for maximal foredune height is supported by Arens (1996). The author found that once the vegetated foredune has established, the difference in height between beach and foredune increases to a point where it inhibits sand to reach the foredune. The high foredune would cause flow to be deflected, resulting in sand not being lifted up into suspension, so that a maximum height of vegetated foredunes establishes (Arens, 1996). Vegetation density acts as an important factor for foredune formation through an increase in roughness that causes a decrease in wind speed and the deposition of sediment (Hesp, 1989). Thereby, a positive feedback between vegetation and deposition can be recognised. Sand deposition encourages vegetation growth, which in turn leads to greater roughness and a decrease in wind speed thus enhancing deposition (Hesp, 1989). At decadal scales vegetation was found to play a larger role in foredune width changes than sand supply rates (Zarnetske *et al.*, 2015).

2.2. The vegetated foredune and wind flows

Airflow over the foredune is altered by topography and vegetation cover. Wind is accelerated due to flow compression when passing the foredune (Arens, Van Kaam-Peters and Van Boxel, 1995; Arens, 1996; Walker *et al.*, 2009; Bauer *et al.*, 2012). The acceleration effect is counteracted at the same time by the vegetation that causes an enhanced roughness and slows down the airflow. But although in many cases the vegetation increases the surface roughness on the dune slope, this is outweighed by the accelerating effects over the foredune slope and crest (Arens, Van Kaam-Peters and Van Boxel, 1995; Hesp *et al.*, 2005; Walker *et al.*, 2009). Consequently, within the vegetation canopy a deceleration is observed, whereas above the canopy the wind flow accelerates (Keijsers, De Groot and Riksen, 2015). Oblique and perpendicular onshore winds that are above 10 $m.s^{-1}$ are most favourable for foredune growth. For wind speeds lower than 10 $m.s^{-1}$ sand is deposited just before the dune foot, seaward of the vegetation boundary. Arens (1996) found a greater flow acceleration for a study site with a steeper topography and less vegetation (hence less roughness) than for less steep dunes. The steeper the slope, the greater the upward flow (or flow acceleration) over the foredune stoss site (Arens, Van Kaam-Peters and Van Boxel, 1995; Arens, 1996). This also occurs when the incipient wind direction shifts to more onshore (Arens, Van Kaam-Peters and Van Boxel, 1995; Walker *et al.*, 2006). According to Walker *et al*. (2006), a flow shift of 18° to more onshore lead to an acceleration of wind flows, due to greater streamline compression and topographic steering. Modelling (computational fluid dynamics (CFD) model) the effect of incipient wind direction on acceleration showed the same trend (Figure 2). Flow acceleration is on average 25% higher for onshore winds than for (highly) oblique winds (Hesp *et al.*, 2015).

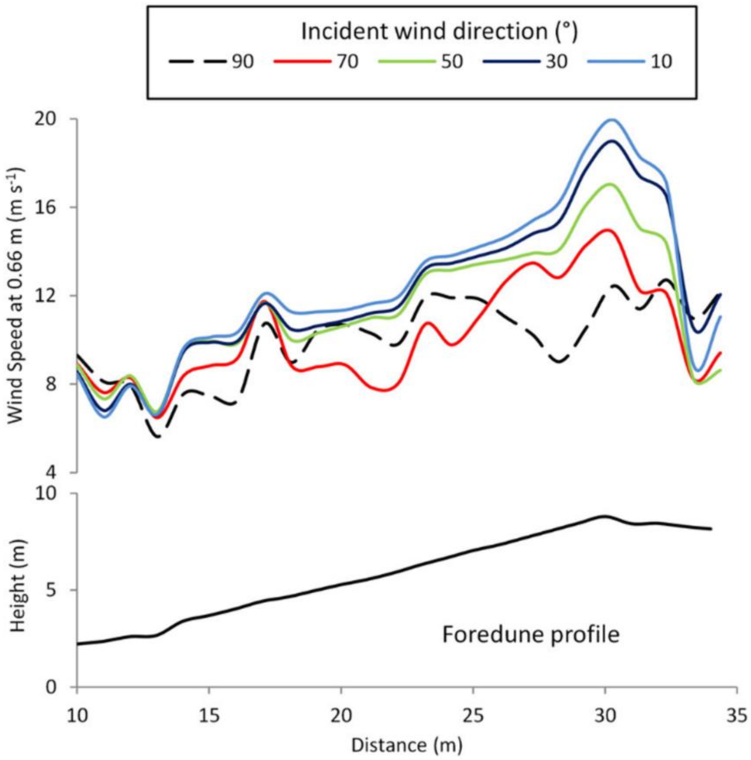

Figure 2. Modelled (CFD) near-surface wind speed responses for five incident wind directions (a) at 0.66 m above surface and b) showing the dune profile. Figure extracted from Hesp *et al.* (2015).

When flow acceleration was measured across the foredune towards the crest, surface stress was observed to increase and turbulent flows to decrease (Chapman *et al.*, 2013). However, Hesp *et al.* (2013) observed an increase of absolute turbulent kinetic energy (*tke*) with increasing wind speeds on the foredune crest (0.66 m above surface) with *tke* values ranging from 1.78 - 3.43 $m^2.s^2$ for 7.67 - 15.11 $m.s^{-1}$, respectively. Despite this, studies showed that the *tke* is relatively larger for smaller wind velocities (4 – 7.5 $m.s^{-1}$) (Chapman *et al.*, 2012, 2013) and greater at the dune foot (Chapman *et al.*, 2013).

As well as changes in wind velocity, it is important to consider wind deflection because deflection is linked to a deceleration of the wind (Walker *et al.*, 2006) and hence with the potential of the wind to transport sediment over the foredune and affect sedimentation patterns (Hesp, 2002; Walker *et al.*, 2006; Bauer *et al.*, 2012; Hesp *et al.*, 2015). At the same time, the more oblique the wind approaches, the smaller the effective slope so that there is less topographically-forced flow acceleration (Arens, Van Kaam-Peters and Van Boxel, 1995; Davidson-Arnott *et al.*, 2012). Davidson-Arnott *et al.* (2012) showed that a change in wind direction from oblique winds (30 - 45°) to onshore lead to a shift of foredune slope of 7 - 10° to 22°, which was paired with reduced transport. Walker *et al.* (2009) measured onshore topographic steering by 19° on the lower slope, while crest-parallel steering occurred on the upper seaward slope back toward the incident flow direction. Deflection can be considerable, but highly depends on the incoming wind direction: for instance, highly oblique onshore and shore perpendicular winds are less deflected (Bauer *et al.*, 2012). Walker *et al.* (2017) found that during very oblique incident flow conditions, there was significant deflection of flow (as much as 37°) from the backshore to the crest of a 12 m high foredune. Hesp *et al.* (2015) modelled (CFD model) wind flow patterns from scarp to crest over a foredune of 15 m height under all possible circumstances. This was possible, as the model had good correlations with observational results. They found maximum deflection of more than 20° to more shore perpendicular at moderate to high oblique winds of 30 - 60° (Figure 3).

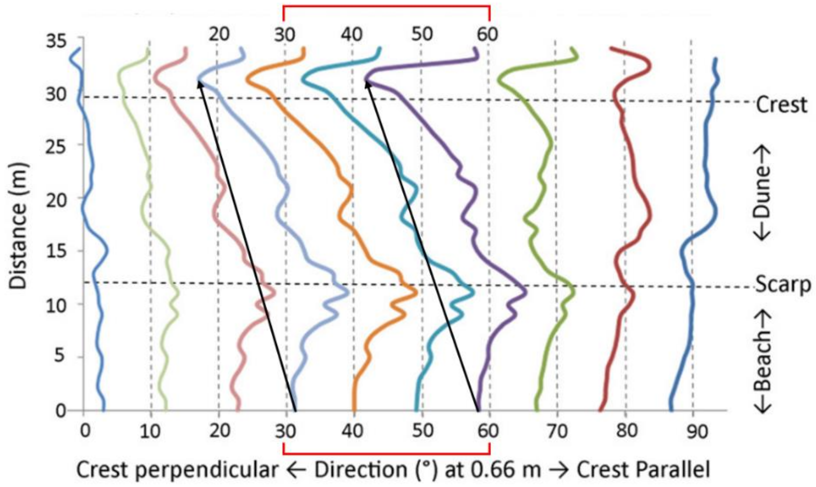

Figure 3. Modelled (CFD) direction of wind flow at 0.66m above the surface at 1m intervals across the foredune from the beach (at 0 m on the y-axis) to the dune lee slope (at ~35 m). Incident wind flow was modelled at 10° intervals. Red circles emphasize the large deflection of wind flows over the foredune. Extracted from Hesp et al. (2015) and modified.

Bauer et al. (2012) generalised the flow-form interaction in a conceptual model, based on field studies on wind flow and sediment transport across a beach–dune system (Figure 4). They found topographic steering over large foredunes (higher than 8 m). Perpendicular onshore winds (Figure 4.A) underwent flow acceleration, while highly oblique onshore winds (ca. 40° from crest-perpendicular) were deflected to more shore-normal (Figure 4.B). Their observations are in agreement with a number of studies, such as Arens, Van Kaampeters and Van Boxel (1995) and Walker *et al.* (2006). Hesp *et al.* (2015) also found that if the wind approaches a steep cliff at an angle of 45 - 90° the wind splits into alongshore and cross-shore component. When the wind approaches highly oblique (more than 60°), its velocity over the

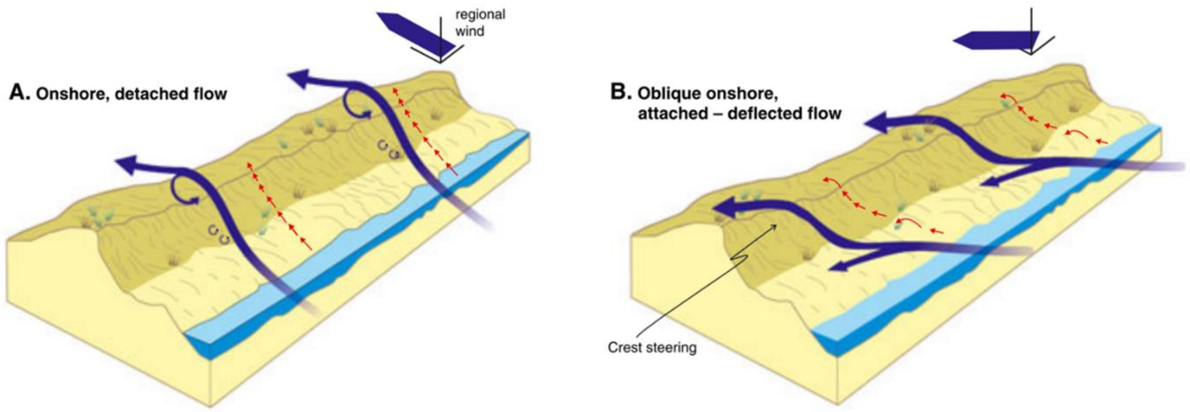

Figure 4. Conceptual model of flow–form interaction over large (> 8m) foredunes for different wind approach directions. Large solid arrows represent near-surface flows, modulated and steered by the local topography. Small arrows indicate possible sand transport. Retrieved and modified of Bauer *et al.* (2012).

foredune is not accelerated or even reduced (Hesp *et al.*, 2015). Both the acceleration and deflection might depend on dune height and dune slope, based on the comparison of the topography and vegetation cover on a low and a high foredune in the Netherlands (Hesp, 2002). Bauer *et al.* (2012) observed that the minor topographical elements of the beach and dune were altering near-surface flows with wind velocities ranging from 2.7 m.s^{-1} on the back-beach to 6.9 m.s^{-1} on the dune crest, and emphasise the importance of site-specific measurements in order to measure aeolian sediment flux.

In general it can be said that vegetation cover (and associated increase in roughness), the incipient wind flows (speed, direction and turbulence), as well as the specific topography of the foredune (e.g. steepness of slope) are important factors controlling the degree of deflection and magnitude of flow acceleration (Bauer *et al.*, 2012). Since the wind is the driving force behind the sand transport across the foredune, the aforementioned determine preliminary the transport rate. However, it does not seem entirely clear how these factors interact, due to site specific variations as well.

2.3. Sand transport across the vegetated foredune

2.3.1. The source: Aeolian sand transport on the beach

Aeolian transport is the down-wind transport of sand, controlled by several atmospheric, textural and surficial factors (Short and Hesp, 1982; Nickling and Davidson-Arnott, 1990). The characteristics of the wind flow (magnitude, direction and turbulence) together with soil moisture are governing factors for sediment transport across the beach. First the wind needs to exceed a threshold velocity for aeolian transport to be observed (Arens, 1996; Davidson-Arnott *et al.*, 2012; Sterk *et al.*, 2012). The threshold velocity varies within the literature, depending on the study area and conditions but is mostly stated around 10 m.s^{-1}. This also ranges from 6 m.s^{-1} when dry to 11 m.s^{-1} when wet (Arens, 1996) or 10 - 12 m.s^{-1} for different surface conditions (Sterk *et al.*, 2012). Wind turbulences are also a key driver in transport, as they determine the erosive capacity of wind (van Boxel, Sterk and Arens, 2004; Baas, 2006; Mayaud *et al.*, 2017). Turbulent eddies transport air and its properties with several orders of magnitude more effectively than molecular diffusion, resulting in it being a relevant transport mode for vertical fluxes (van Boxel, Sterk and Arens, 2004). When studying the turbulent flow associated with sand transport, the (turbulent) Reynold stress (RS) or the *tke* are commonly used. RS can be defined as the co-variance of the horizontal and vertical components of wind, multiplied with air density. It is therefore a downward flux of horizontal momentum. RS is observed if on average, horizontal speed of the air moving downwards is higher than the air moving upwards (van Boxel, Sterk and Arens, 2004). The turbulence intensity is the *tke*, based on the root-mean square of the fluctuating components of the wind flow (*u*, *v*, *w*). The relative importance of turbulence for aeolian sand transport however still remains unclear (Mayaud *et al.*, 2017).

Most of aeolian transport is driven by saltation, and to some extent by creeping and suspended load (Anderson and Walker, 2006). Saltation is limited to heights between 25 cm (Arens and van der Lee, 1995) and 30 cm (Horikawa and Shen, 1960) above surface. Deviations might be attributed to grain size or wind turbulences but were not specified in either of the aforementioned studies. In the vertical, transport decreases exponentially with height (Arens and van der Lee, 1995; Arens, 1996; Christiansen and Davidson-Arnott, 2004; Petersen, Hilton and Wakes, 2011). However, at different positions across the foredune, the decrease varies and can become less sharp higher on the foredune (Figure 5).

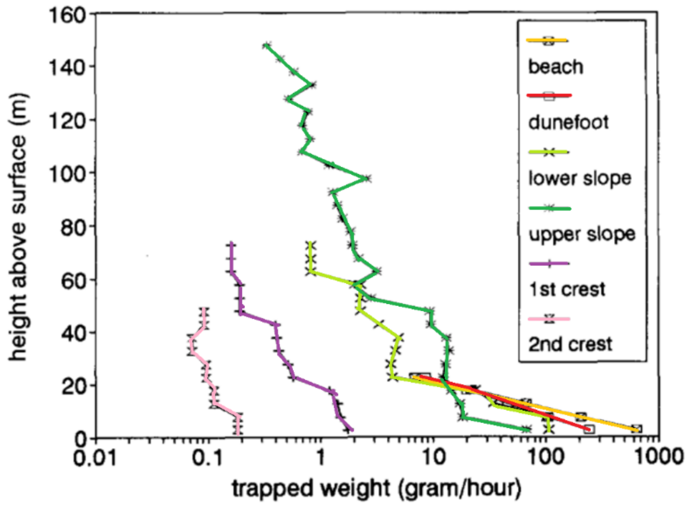

Figure 5. Sediment curves for different heights on a beach-dune, retrieved from (Arens and van der Lee, 1995). Traps were installed at different positions on the beach and the foredune and caught sand at different heights above the surface.

The spatial distribution of aeolian transport is a trade-off between wind-angle, beach geometry and critical fetch (Bauer and Davidson-Arnott, 2003). The maximum fetch depends on approaching wind angle and beach geometry and represents the largest fetch achievable. The actual fetch is the one occurring in the moment, while the critical fetch represents the minimum distance needed to get the sediment transport saturation (Bauer and Davidson-Arnott, 2003). The fetch effect occurs due to a downwind saltation cascade (Bauer and Davidson-Arnott, 2003; Bauer *et al.*, 2009). The number of saltating grains increases exponentially and asymptotically to a limiting maximum condition, given constant wind stress and a fixed average amount of grains that are dislodged by one single grain when landing again at the surface (Bauer and Davidson-Arnott, 2003; Bauer *et al.*, 2009). Beach features (moisture content, grain size, wind angle) during the saltation influence the fetch effect (Arens, 1996; Bauer and Davidson-Arnott, 2003; Bauer *et al.*, 2009), due to differences in saturation time and leading to varying saturation distances (i.e. the greater the saturation distance, the greater the fetch effect) (Bauer and Davidson-Arnott, 2003). For example, with a decrease in the sediment size, the aeolian sand transport rate increases (Kuriyama, Mochizuki and Nakashima, 2005). How the wind direction influences aeolian transport can be exemplified when wind shifts from perpendicular onshore to oblique onshore. The actual transport rate at the beach is then a trade-off between transport increase due to greater fetch effect and transport decrease due to the cosine effect (Bauer and Davidson-Arnott, 2003). The cosine effect is based on the assumption of mass conservation for oblique wind flows. The total sediment mass transport across a line downward of the wind on the beach is equal to the total sediment mass transport across the approximate shore parallel line of the foredune. However, the net transport per unit width will be smaller by a factor of the cosine of the incoming wind angle (Bauer and Davidson-Arnott, 2003). The greater the angle, the higher the reduction.

2.3.2. Aeolian sand transport across foredunes

Sand transport across the foredune depends on how much sand originates from the beach (for onshore winds). It is further influenced by changes in the wind field due to the sudden presence of dune topography (Short and Hesp, 1982). The wind flows respond to the topography change with flow separation and develop an internal boundary layer so that both the velocity gradients and surface shear stresses are reduced (Short and Hesp, 1982). Consequently, the aeolian sand transport rate decreases near the foot of the foredune (Short and Hesp, 1982; Kuriyama, Mochizuki and Nakashima, 2005) and drops exponentially landward of the foredune with a sharp decrease for lower wind speeds and a more gentle difference for high wind speeds (Arens, 1996). Sand transport rates depend on the wind speed so that greater (onshore) wind velocities induce greater sand transport and result in larger foredunes (Short and Hesp, 1982). The decline of sand transport up the stoss slope correlates to the incident wind speed. Low wind speeds lead to faster and more extreme gradients up the slope (Arens, Van Kaam-Peters and Van Boxel, 1995). Higher velocities induce aeolian transport in suspension leading to a less steep decline across the foredune and transport sand further landward (Arens, Van Kaam-Peters and Van Boxel, 1995). This effect was shown to increase proportional to the dune slope steepness. Flow acceleration over the foredune encourages a jet-like flow of sand, leading to transport in suspended form rather than saltation. In this way, sand can pass the foredune crest, regardless the dense vegetation. This distinct mode of transport can be referred to as *jettation* (Figure 6.c and Figure 6.d). For a scenario with a vegetated slope and high wind speeds (Figure 6.d), suspended sediment transport is especially relevant for sand transport to, across and over the foredune (Arens, 1996). However, when the dune is very high wind deflection leads to less suspended sediment transport (Arens, 1996).

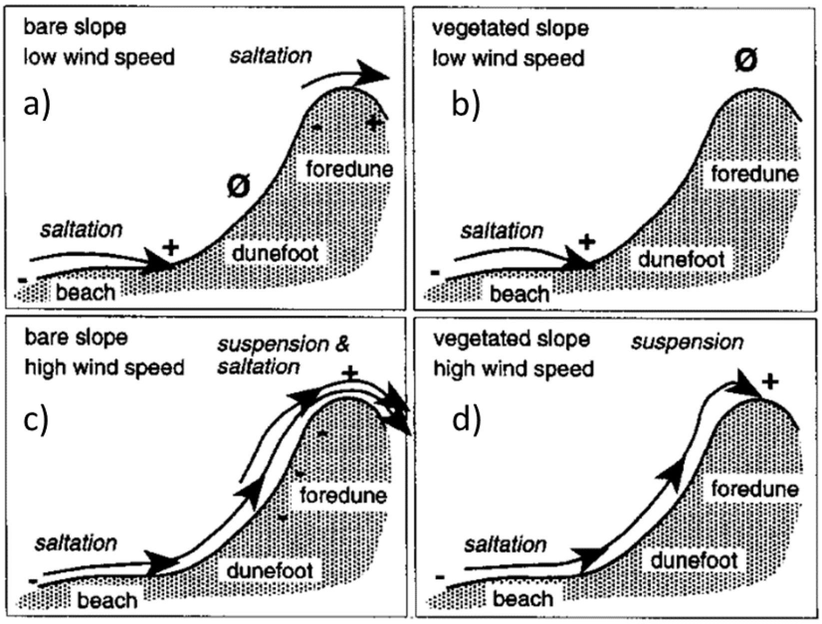

Figure 6. Transport mechanisms for aeolian transport of sand over foredunes, for bare and vegetated foredunes, with different combinations of wind speed (high-low). (+ indicates potential deposition, - indicates erosion; Ø indicates no transport.) extracted from (Arens, 1996).

Arens (1996) further showed the importance of wind direction: oblique and perpendicular onshore winds both cause sediment input to the foredunes, but the latter to a greater extent (40% and 64%, respectively). On the other hand, wind directed parallel to the foredune has little effect on the foredune development with possibly some erosion at the dune foot and some deposition during very strong winds (Arens, 1996). Besides the wind flow magnitude and direction, the aforementioned turbulences influence sand transport. Previous studies suggest that *tke* has stronger relationships with sand transport over coastal foredunes than RS, since there were large amounts of transport with small RS (Chapman *et al.*, 2013). The turbulence, i.e. the fluctuating parts of the wind components, are potentially essential for sand transport across the foredune. Firstly, they are responsible for the vertical uplift of particles to be transported in suspension (Arens, Van Boxel and Abuodha, 2002). Secondly, the turbulent flows are hypothesised to be an explanation for the sand transport through a zone of flow stagnation around the dune toe (Chapman *et al.*, 2012). The flow deceleration of wind flows at the dune foot does often not lead to a reduced transport, for which turbulence might be accounted (Chapman *et al.*, 2012). Due to concave streamlining of wind flows at the dune foot, turbulences can exceed the time-averaged stream-wise shear stress and by this encourage sand entrainment (Weaver and Wiggs, 2011; Chapman *et al.*, 2012, 2013). Thus, at the dune foot turbulent flows gain relatively more importance regarding sand transport than wind magnitude, which in turn gains more importance for sand transport on the upper part of the foredune (Weaver and Wiggs, 2011; Chapman *et al.*, 2013). When the foredune is vegetated, there is also vegetation-induced turbulences (Walker *et al.*, 2006; Chapman *et al.*, 2012), which is however difficult to quantify and distinguish from topographically induced turbulences, though thought to be an important parameter for transport (Chapman *et al.*, 2013).

Both the topographic effect of the foredune and vegetation cause a rapid decline of cross-shore aeolian sand transport (Arens, 1996; Kuriyama, Mochizuki and Nakashima, 2005). Vegetation densities of 20 - 30% are sufficient to reduce sediment transport and cause sediment deposition (Arens, 1996; Kuriyama, Mochizuki and Nakashima, 2005). A considerable range of vegetation cover (5 – 85%) leads to maximum deposition (Keijsers *et al.*, 2012). Spatial variations of the vegetation cover affect the transport and deposition further (Davidson-Arnott *et al.*, 2012), which is supported by Bauer *et al.* (2012). The authors observed twice in the field that transport events at the beach and dune slope occurred simultaneously, but were separated by a zone of practically no transport (lower slope). Beach and (upper) dune slope were thus decoupled and failed to exchange sediment (Bauer *et al.*, 2012). Christiansen and Davidson-Arnott (2004) studied landward sand transport over the foredune, including the role of a dune ramp. The studied foredune had suffered erosion during a storm leading to an non-vegetated dune ramp on its stoss site, so that sand was transported over the dune crest and only deposited in the densely vegetated foredune (Christiansen and Davidson-Arnott, 2004). The approximation of the square or cube of the bed shear velocity U* for modelling sediment transport can deviate considerably on the foredune (Davidson-Arnott *et al.*, 2012). This is due to microscale changes in topography and vegetation cover, as well as slight changes in wind direction (Davidson-Arnott *et al.*, 2012).

Measurements of aeolian sand transport over the densely vegetated foredune (species unknown) showed that landward sediment transfers could still be quite high with a deposition to the lee slope of up to 2.94 $m^3.m^{-1}$ in one month with strong onshore winds (Christiansen and Davidson-Arnott, 2004). Christiansen and Davidson-Arnott (2004) found further that deposition rates were however highly variable in space and time, finding a total annual lee slope deposit of 8 - 9 m^3 per metre beach width. Nevertheless, sand transport can also occur when the stoss site is densely vegetated (thus without bare dune ramp). This occurs mostly in suspended form (Arens and van der Lee, 1995; Arens, 1996; Petersen, Hilton and Wakes, 2011) (Figure 7). Petersen, Hilton and Wakes (2011) observed that for heights of up to 1.6 m above ground but in small quantities (Figure 8). Previous measurements detected a reduction in sediment transport between the foredune stoss side and the foredune crest of 71% (1.56 to 0.45 grams) at 0.5 m aboveground and of 25% (0.66 to 0.49 grams) at 1 m above ground. Behind the crest, transport decreased exponentially (Figure 8), which is consistent with earlier observations (Arens, 1996; Christiansen and Davidson-Arnott, 2004; Petersen, Hilton and Wakes, 2011).

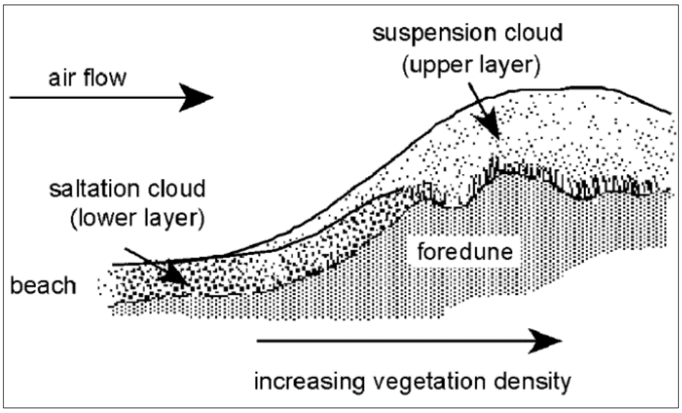

Figure 7. Aeolian transport mechanism over a vegetated foredune. Transition from saltation to suspension. Retrieved from Arens, Van Boxel and Abuodha (2002).

The suspended transport becomes more important than saltation on the foredune crest (Figure 8: Mast B with less transport at 0.5 m than at 1 m). Applying a CFD airflow model showed that the suspension cloud could reach up to 5 m high and possibly higher for wind velocities above 25 $m.s^{-1}$ (Petersen, Hilton and Wakes, 2011).

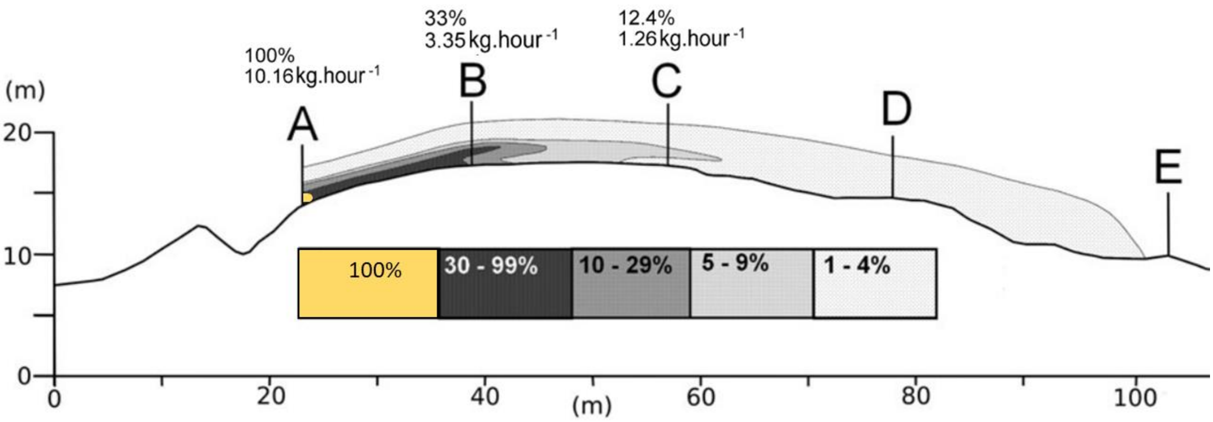

Figure 8. Sand transport rates in percentage, relative to mast A at 0.5 m (calculated from measurements recorded over 624 hours between 30th June and 25th July 2010). For mast A, B and C, the average suspended sediment transport rates ($kg.hour^{-1}$) as percentages of foredune crest transport are displayed on top for a period of 2.5 hours on 23rd November. Extracted and modified from (Petersen, Hilton and Wakes, 2011).

Sediment transport studies by Davidson-Arnott *et al.* (2018) over a 10 m high, steep and densely vegetated foredune (vegetated by marram grass) showed a vertical growth of ca. 1 m per decade, although sediment input and erosion were fairly balanced. The wind direction played a crucial role with oblique winds contributing more than onshore winds (Davidson-Arnott *et al.*, 2018).

Although most sediment is trapped within the canopy, longer term studies showed that sand can pass the vegetated foredune (when vegetated with marram grass) and is deposited on the lee side or landward of the foredune (Kuriyama, Mochizuki and Nakashima, 2005; Petersen, Hilton and Wakes, 2011; Davidson-Arnott *et al.*, 2012). This is partly due to high wind velocities, which cause a streamlining of the grasses and thereby reduce the roughness induced by vegetation (Bauer *et al.*, 2012; Davidson-Arnott *et al.*, 2012). Petersen, Hilton and Wakes (2011) found that this streamlining of the grass can also lead to modified saltation. Modified saltation is saltation that occurs on the lodged surface of high dune grass (here marram grass) that bends in the wind and acts as rebounder for sand grains (Figure 9). Single grains sink from suspension and continue their path via modified saltation on the bended marram grass. The authors suggested that high aeolian transport rates occur though modified saltation (Petersen, Hilton and Wakes, 2011). It is likely that sand transport over the fully vegetated foredune takes place either by means of suspension or modified saltation (Petersen, Hilton and Wakes, 2011; Hesp *et al.*, 2013; Keijsers, De Groot and Riksen, 2015). Davidson-Arnott *et al.* (2012) studied high-frequency sediment transport responses on a vegetated foredune (Greenwich, Canada) using 2D and 3D ultrasonic anemometers and Wenglor Laser Particle Counters to count transported sand grains. Their measurements across a foredune transect of increasing vegetation cover (9% to 40%) showed that wind velocities and sand transport are positively correlated with varying extent across the foredune. Although wind speeds were generally larger on the foredune than at the adjacent beach (by 2 – 3 $m.s^{-1}$), transport at the beach was for a multiple larger at all times. At the beach peak counts were of more than 1000 grains per second. The average transport for three stations at the beach were 19.2, 72.6 and 57.0 $kg.m^{-1}.h^{-1}$, compared to 0.09 $kg.m^{-1}.h^{-1}$ for the station on the middle of the foredune and 0.57 $kg.m^{-1}.h^{-1}$ for the crest station. While the largest transport events occurred often simultaneously with an increase in

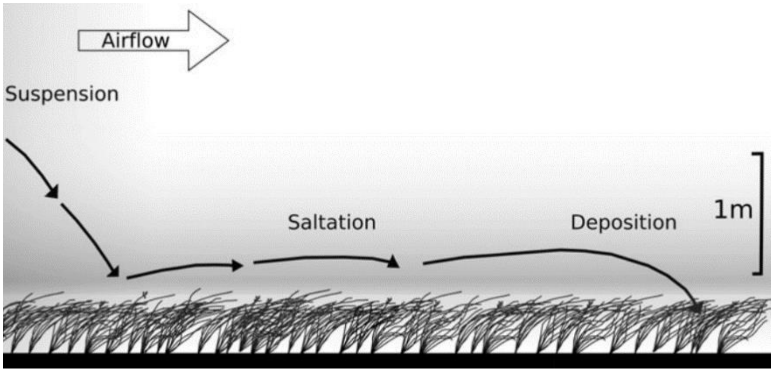

Figure 9. Modified saltation above the vegetation canopy. Extracted from (Petersen, Hilton and Wakes, 2011).

wind speed, peaks in wind speed did not necessarily induce peaks in transport. Wind gusts could induce large transport events of 40 counts per second during 10 - 15 seconds, however gusts of similar magnitude at the same period did also not produce such peak transport events (Davidson-Arnott *et al.*, 2012). Figure 10 shows an overview of one transport event (17 hours) with different wind conditions and measured sediment transport (continuity and magnitude) of the study of Davidson-Arnott *et al.* (2012). It shows that similar wind conditions may cause a considerably different net sediment transport. The results of Davidson-Arnott *et al.* (2012) stress the influence of small fluctuations of wind direction, moisture content and vegetation on sediment transport over the foredune.

transport event	Transport magnitude	Transport continuity	Wind speed (ms^{-1})	Wind direction
Start	negligible <0.1 counts s^{-1}	very low	3-6	oblique offshore
	small 0.5-2 counts s^{-1}	moderate	7	oblique offshore
	small 0.5-7 counts s^{-1} ←	moderate to high ←	8-13	oblique onshore
	moderate 5–20 counts s^{-1}	high	12-15	oblique onshore
	large 15->80 counts s^{-1}	high	13-16	oblique onshore
	moderate 5–20 counts s^{-1} ←	moderate to high ←	10-11	oblique onshore
	small 1–7 counts s^{-1}	moderate	10	oblique onshore
End	small <2 counts s^{-1}	low	7-9	onshore

Figure 10. Characteristics of wind flow and sand transport associated with temporal divisions within a transport event (03.05. 22:00 – 04.05. 15:15). Modified and extracted from Davidson-Arnott et al. (2012)

2.4. The role of vegetation in detail

Foredunes develop thus due to interactions of plants with flow processes and related aeolian sand transport. Pioneer species trap sediment on the foredune so that they grow vertically (Arens, 1996). A few examples of pioneer species are European and American searocket (*Cakile maritima* and *Cakile edentual)*, beach daisy (*Arctotheca nivea*)*,* bayhops (*Ipomoea brasiliensis*) and (European) marram grass (*Ammophila arenaria*). Their geomorphic role is undoubted and since the 19th century stressed (as cited in Hesp, 1989: Cowles, 1899). Aside from beach type and sediment supply previous studies have shown that vegetation also exerts an important role on foredune height by inducing a negative feedback between topography and wind flows that limits dune growth (Duran and Moore, 2013; Goldstein, Moore and Durán Vinent, 2017). Duran and Moore (2013) found that wave climate and corresponding beach type shift the vegetation limit, which is more inland for dissipative beaches with high waves, resulting in higher foredunes. The authors linked beach type and plant zonation in their role for shaping and determining the size of foredunes. Previous studies further showed that plant density exerts a major control on foredune height, with denser vegetation causing high and narrow dunes, while sparse vegetation causes low and wide dunes (Hesp, 1989; Stallins, 2016; Figure 11). *In situ* experiments showed furthermore that variations of plant height are just as influencing as plant density (Hesp, 1989).

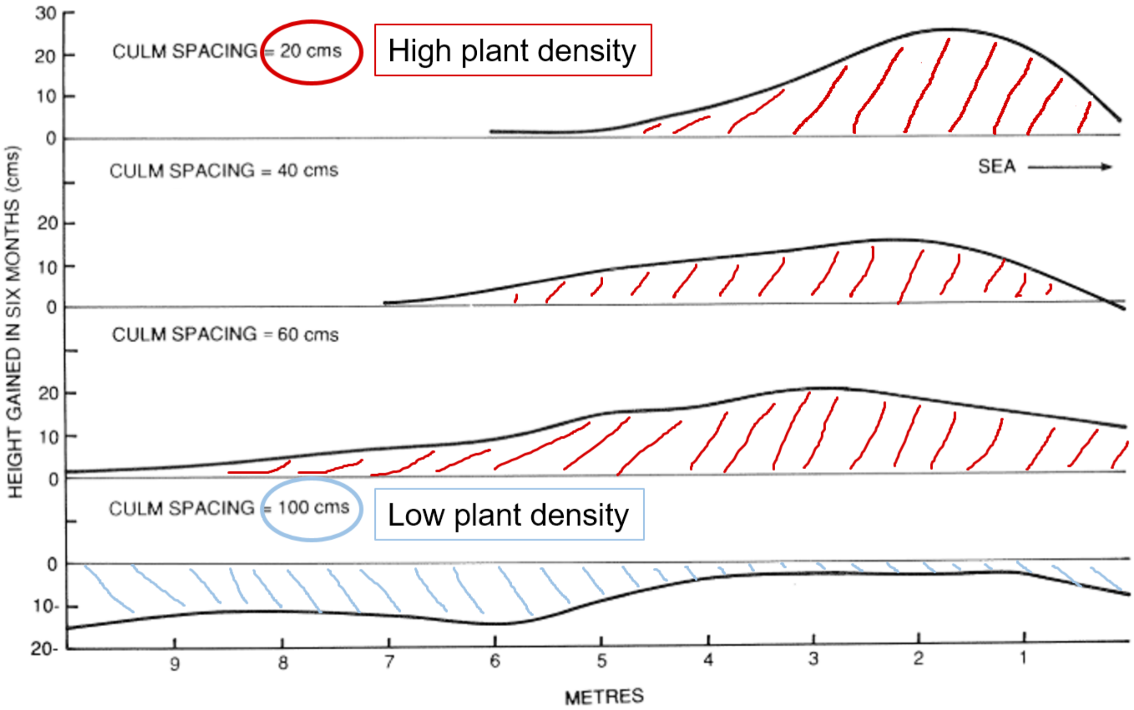

Figure 11. The effect of plant density on foredune accumulation and dune morphology. Plant density decreases from the top panel to the bottom and the gained dune height varies accordingly from steep and about 25 m high to erosion. Extracted and modified from (Hesp, 1989).

Vegetation causes a rougher surface and blocks wind substantially causing sand to be trapped (Hesp, 1989; Arens, Van Kaam-Peters and Van Boxel, 1995; Kuriyama, Mochizuki and Nakashima, 2005; Bauer *et al.*, 2012; Davidson-Arnott *et al.*, 2012). Previous studies showed that the wind velocity profile is considerably blocked by higher marram grass (Hesp, 1989) (Figure 12). Clear differences between longer (black) and shorter (green) vegetation at the exact same dune profile were observed, since the marram grass was cut after the first measurements.

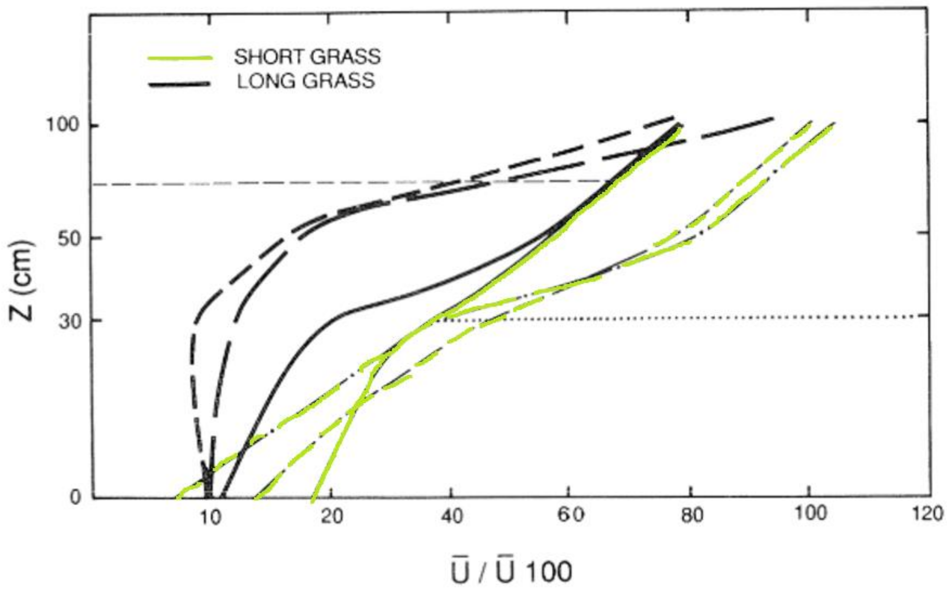

Figure 12. Difference in wind velocity profiles for short (30 cm; green) and long (80 cm; black) marram grass (Hesp, 1989).

Moreover, the surface beneath the plants is sheltered and impedes entrainment (Kuriyama, Mochizuki and Nakashima, 2005; Davidson-Arnott *et al.*, 2012). The length of vegetation determines whether transport occurs above and between the canopy (Hesp, 1989). With strong winds (more than 10 $m.s^{-1}$) however, the roughness owing to vegetation is decreasing as the stems are rigid at the bed only, while upper stems and leaves are more flexible and often bend with the wind streamlined (Hesp, 1989; Arens, Van Kaam-Peters and Van Boxel, 1995; Bauer *et al.*, 2012).

A decade long study by Keijsers, De Groot and Riksen (2015) showed that not only plant density and size but also vegetation patterns affect sediment transport Maximum sedimentation occurred for vegetation cover ranging from 5 – 85%, of which 20 - 80% are the most common cover for maximum deposition. Deposition took place predominantly (71%) within 5 - 20 m distance from the vegetation (Keijsers, De Groot and Riksen, 2015). Since higher vegetation cover (80 – 85%) was only found further landward on the dune, it lead to less sedimentation because sand was deposited within the lower dune parts. On average however the sediment trapping efficiency increases with increasing vegetation cover, even though 100% efficiency is never reached (Keijsers, De Groot and Riksen, 2015). Keijsers, De Groot and Riksen (2015) identified also a general sedimentation pattern across the foredune where deposition is large shortly after the first vegetation line (commonly at the dune foot), subsequently reaches a maximum somewhere landward of this line and decreases afterwards. The authors identified three different (long term) sedimentation profiles for three different scenarios of vegetation patterns (Figure 13). Firstly, a static and dense zone of vegetation causes a rather abrupt peak in sedimentation, secondly a foredune with incipient dune ridge triggers two sedimentation peaks, namely one just behind the incipient dune ridge and the second on the established foredune with little sedimentation in-between. The third scenario is of a more gradual vegetation cover that starts at the dune foot and increases across the foredune. It causes a more gradual sediment deposition on the slope because saltation can travel further up.

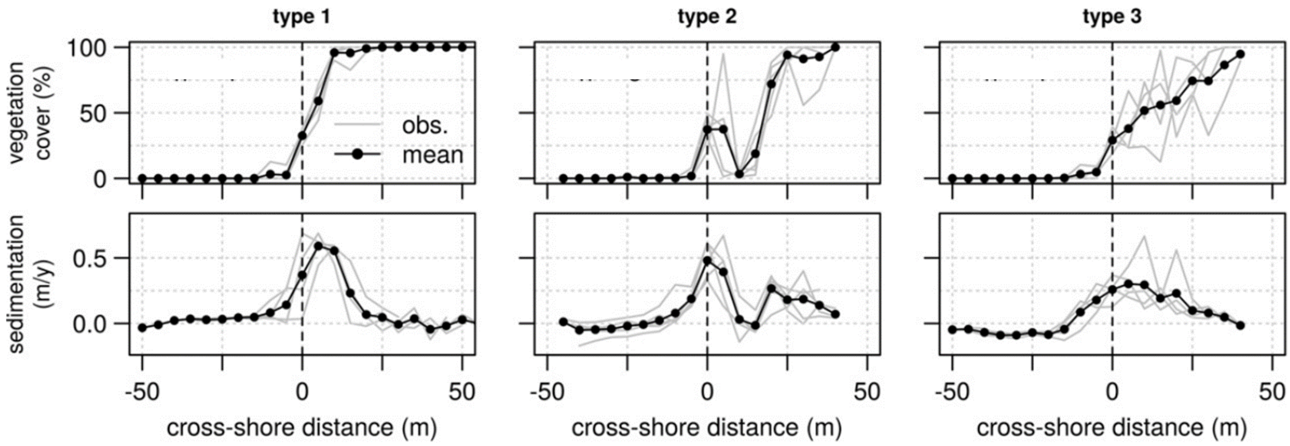

Figure 13. Different vegetation patterns on the foredune and their effect on sedimentation pattern. (1) no incipient dune and sudden increase in vegetation; (2) laterally continuous incipient dune with unvegetated dale ; (3) patchy incipient dune and gradual increase of vegetation on the foredune. Lower panels show the associated sedimentation profile. Extracted and modified from (Keijsers, De Groot and Riksen, 2015).

Regarding different species on the foredune, they affect the dune morphology and wind flows differently through differences in growth forms (Stallins, 2003; Zarnetske *et al.*, 2012). Small differences in species can have geomorphological effects, which was observed for two marram grass species, namely European marram grass (*Ammophilia arenaria*) and American marram grass (*Ammophilia breviligulata*) (Zarnetske *et al.*, 2012; Figure 14). The distinctive plants that live on the foredunes are usually dune-builders and burial tolerant species (as cited in Stallins (2016): Hosier 1973; Wood house 1982; Ehrenfeld 1990), which have different stress tolerances and requirements to sedimentation (Keijsers, De Groot and Riksen, 2015). A commonly known sand trapping plant that is associated with foredune accretion is marram grass which creates steeper dunes (Milne and Sawyer, 2002; Hilton, Duncan and Jul, 2005; Zarnetske *et al.*, 2012). This effect has been globally observed with marram grass stimulating high, steep and topographically continuous foredunes.

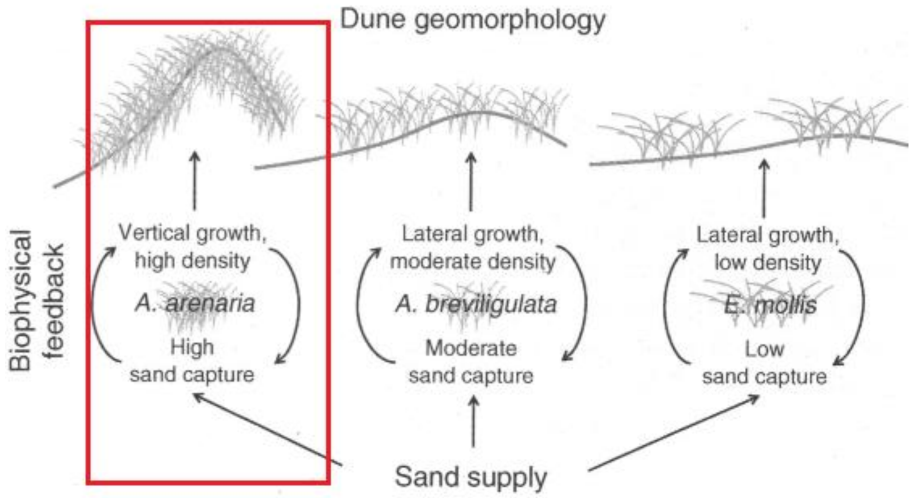

Figure 14. Sketch of dune geomorphology as response to biophysical feedback of different plant species, extracted and modified from Zarnetske *et al.* (2012).

The effect of vegetation on dune morphology can be variable over time. Zarnetske *et al*. (2015) suggest that different factors play the main role in foredune height depending on different time scales. Sand supply mainly influenced width and height at inter-annual timescales (56 – 80% and 64 – 69%, respectively). At decadal scales vegetation played a larger role in foredune width changes and sand supply rates were responsible for changes in height (88 – 90%). However, when shoreline change rates were smaller than 2 m annually, vegetation was the major influencing factor for both width and height at the decadal scale (Zarnetske *et al*., 2015). The role of vegetation can however only come to its play if sediment can be supplied from the beach, so that the factors sand budget and vegetation determine the dune geomorphology (Gutiérrez *et al.*, 2011).

2.5. Overview of studies and gathered knowledge

Table 1 presents a selection of the most extensive studies (chronological order) that cover findings about effects of vegetated foredunes on air flow patterns and characteristics.

Wind velocity		Incipient wind direction & deflection	Transport & dune accretion		Dune properties	Author(s)
10% increase at crest (2m above surface)	11 $m.s^{-1}$	oblique winds	100% deposition on slope	Dune growth of 3 $m^3.m^{-1}$	+/- 6 m high, slope of 5-10°; densely vegetated	(Arens, 1996)
	12-15 $m.s^{-1}$	perpendicular onshore	40% deposition on slope, 60% on dune			
50% increase at crest (0.5m above surface)	13 $m.s^{-1}$	oblique winds	73% deposition on slope		10.5 m high, slope of 20°; patchy vegetation	
	11 $m.s^{-1}$	perpendicular winds	N/A			
Use of relative wind speed: <1 decrease, >1 increase of wind speed	<1: foot (85%) >1: top (~110%)	Perpendicular onshore (~0°) & onshore (0-30°); deflected to normal up to 15°	Accumulation at dune foot (owing to deceleration) and transport in suspension over dune for winds ~10 $m.s^{-1}$		6 m high, Ø slope of 5°; Vegetation cover of 10% (foot), 50% (slope), 95% (top); species not specified, alongshore uniform Ø grain: 0.17 mm, orientation SW; Net sand budget: 5 $m^3.m^{-1}.yr^{-1}$	(Arens, Van Kaam-Peters and Van Boxel, 1995)
	<1: foot (90%) ~1: top (90-110%)	oblique onshore (30-70°)	Deposition at foot, transport across dune if > 10 $m.s^{-1}$			
	<1: foot (75-90%) <1: top (50-75%)	Highly oblique (70-90°) and alongshore (~90°)	Limited to beach and foot as transport occurs parallel to dune			
	<1: foot (50-90%) >1: top (110)	Offshore (170-180°)	N/A			
	<1: foot (90%) >1: top (120-150%)	Perpendicular onshore (0°) and onshore (0-30°), deflected to normal, > 15°	Erosion of lower slope and deposition landward		10 m high, Ø slope of 14°; No vegetation cover on stoss slope with 0% (foot), 10% (slope), 70% (top); exact species not specified but indication for *A. arenaria*, some alongshore variation Ø grain: 0.26 mm; Net sand budget: 15 $m^3.m^{-1}.yr^{-1}$	
	~1: foot (100%) >1: top (110-140%)	Oblique onshore (30-70°)	Deposition on slope			
	~1: foot (90-100%) <1: top (80%)	Highly oblique (70-90°) and alongshore (~90°)	N/A			
	<1: foot (50-80%) >1: top (120%)	Offshore (170-180°)	N/A			
	<1: foot (85%) >1: top (150%)	Perpendicular onshore (0°) and onshore (0-30°), deflected to normal, > 30°	Deposition at lower slope, No transport over foredune, despite speed-up at top and vegetation hinders erosion at top		23 m high, Ø slope of 11°; Dense vegetation cover of 0% (foot), >50% (slope), 95% (top); exact species not specified but indication for *A. arenaria*, alongshore irregular Ø grain: 0.18 mm; Net sand budget: 5 $m^3.m^{-1}.yr^{-1}$	
	<1: foot (95%) >1: top (120-140%)	Oblique onshore (30-70°)				
	<1: foot (90%) <1: top (70-90%)	Highly oblique (70-90°) and alongshore (~90°)				
	<1: foot (60-80%) >1: top (100-150%)	Offshore (170-180°), maximum deflection of 90°				

25 m.s^{-1} (storm event), threshold velocity: 9 m.s^{-1}	Nearly shore perpendicular (storm event)	Erosion of beach (2.8 m^{3}.m^{-1}) & dune cliffing; 0.52 m^{3}.m^{-1} (net deposition dune) vs 4.8 m^{3}.m^{-1} (predicted)	8-10 m high, irregular shape, dune ramp after storm dense vegetation cover, species unspecified; d50 = 0.2 mm	(Christiansen and Davidson-Arnott, 2004)
N/A	N/A	8-9 m^{3}.m^{-1}.yr^{-1} & indications for deposition landward		
N/A	Strong onshore winds	Max deposition of 2.94 m^{3}.m^{-1} in 1 month	3 m high, fairly regular shape, nearly vertical profile (scarped by storm) developed dune ramp; dense vegetation cover, species unspecified; d50 = 0.2 mm	
	N/A	7.14 m^{3}.m^{-1}.yr^{-1} (dune ramp) 8.99 m^{3}.m^{-1}.yr^{-1} (leeward of crest)		
Max 5 m.s^{-1} (at 10 m height); little correlation with aeolian transport (r=0.2)	Mostly onshore, seasonal variations: South-onshore in summer, N-onshore in winter (at 10 m height)	Aeolian transport strongly correlated (r=0.79) with vegetation index (height & cover per area); Cross-shore dune growth: 0.11 m.yr^{-1}	9 m, slope of 4-11°; main species: *C.kobomugi* and *C. soldanella* with varying cover 0-25% (seasonal) and 0-20 cm height; d50: 0.15-0.17 mm	(Kuriyama, Mochizuki and Nakashima, 2005)
Ø 7.2 m.s^{-1}, max. 15.9 m.s^{-1}, at 2.2 m above surface. Above-transport threshold: 6 m.s^{-1} (frequency: 19%); transport event: Ø 6.31 m.s^{-1} (backshore)& Ø 4.88 m.s^{-1} (crest) [6.31 m.s^{-1} (backshore) to 5.07 m.s^{-1} (toe) to 4.22 m.s^{-1} (lower slope) to 3.56 m.s^{-1} (upper slope) to 4.88 m.s^{-1} (crest)]	Oblique onshore (for transport) Transport event: Ø 274° (backshore) & Ø 259° (crest) [274° (backshore) to 281° (dune toe) to 293° (lower stoss slope) to 277° (upper slope) to 259° (crest): onshore topographic steering (+19°) on lower slope & crest parallel steering (-34°) on upper slope]	Alongshore transport observed during event, no further specification	8.5 m, slope of 20–25°, vegetated with *A. breviligulata* 0.2 – 0.8 m high, 4-70% cover. Toe with incipient terrace, followed by non- vegetated accretion ramp; Orientation 250°;	(Walker *et al.*, 2006)*
N/A	N/A	1.56 g at 0.5 m, 0.66 g at 1 m (foot); 0.45 g at 0.5 m, 0.49 g at 1 m (crest)	8-11 m high; thickly vegetated with *Ammophila arenaria*	(Petersen, Hilton and Wakes, 2011)
Max 31 m.s^{-1}		Max 10 kg.hr^{-1} (for 31 m.s^{-1})		
>15 m.s^{-1}	Onshore (< 30° from perpendicular)	0.09 kg.m^{-1}.h^{-1} (foredune), 0.57 kg.m^{-1}.h^{-1} (crest)	8-10 m high, 9-40% vegetated	(Davidson-Arnott *et al.*, 2012) *

Table 1. Overview of eleven relevant studies that incorporate the subjects of interest, namely vegetation, wind flow dynamics as well as sediment transport.

Ø 2-4.1 m.s^{-1} (back beach) Ø 5.8– 9.1 m.s^{-1} (crest)	Offshore: Near surface steering (crest), eddy recirculation (back beach); [oblique offshore: hybrid flow response]	Crest > back beach > slope; Ø 200-max 312 counts.s^{-1} (crest) Ø 50- max 200 counts.s^{-1} (back beach) None (slope) → decoupled transport beach and dune crest	8-10 m high, slope of 22°, nearly continuous cover of *A. breviligulata*, often with embryo dune, before study eroded & presence of dune ramp, Ø grain: 0.26 mm	(Bauer *et al.*, 2012) *
Ø 4.7 – 5.3 m.s^{-1}; 2.7 m.s^{-1} (backshore) to 6.9 m.s^{-1} (crest), flow deceleration at dune foot	Onshore: Little steering (<10°)	On lower slope close to threshold velocity (5.8 m.s^{-1}): 5-25 counts.s^{-1} (during 5 minutes)		
9 m.s^{-1} (back beach) 11 m.s^{-1} (crest)	Oblique onshore: Alongshore steering (beach & dune ramp/foot), crest-perpendicular: steering ~30°(crest)	back beach > crest> lower slope; > 1000 counts.s^{-1} (back beach) ~ 10-150 counts.s^{-1} (crest) None (lower slope) → decoupled transport beach and dune crest		
8.3-10.8 m.s^{-1}	Alongshore with onshore & offshore component (beach) steering to oblique onshore (~13°)& –offshore (20°) at crest			
N/A	Most common: oblique offshore (SW), some perpendicular onshore (N)	0.2-0.7 m.yr^{-1}; sedimentation at different vegetation covers, but no clear correlation with example 0.4 m.yr^{-1} at 1% cover	9 m, low & relatively steep, continuously vegetated slope & foot (with *A. arenaria*, *E. juncea*, *C. baltica*, *L. arenarius)*	(Keijsers, De Groot and Riksen, 2015)
			12 m, most gentle slope, vegetated slope, laterally continuous line at foot (with *A. arenaria*, *E. juncea*, *C. baltica*, *L. arenarius)*	
			15 m, vegetated slope, patchy at foot (with *A. arenaria*, *E. juncea*, *C. baltica*, *L. arenarius)*	
N/A	N/A	Dune growth averaged over decade: 0.07 m.yr^{-1} Maximal 0.15 m.yr^{-1} for dune with *A. breviligulata*,	3-9.4 m (Environmental Agency Protection and (EPA), 2000; Zarnetske *et al.*, 2015) large, densely vegetated and stabilised foredune (*A. arenaria*, *A. breviligulata*)	(Zarnetske *et al.*, 2015)
Simulation with 12.2 m.s^{-1} (incident, beach) to crest: Onshore (0°): ~20 m.s^{-1} Onshore (30°): 15-20 m.s^{-1} Onshore (60°): 10-15 m.s^{-1} Alongshore (90°): ~12 m.s^{-1}	Measured: 68° (toe) to 53° (scarp) to 47° (slope) to 35° (crest) Onshore (0°): no deflection 30-70°: most deflection (max at 45° with 19° scarp-crest) Alongshore: 0-5°	N/A	~10 m high, slope of 20°–25°, ENE-WSW orientation, vegetated by *A. breviligulata* (Ø 0.3 m at 2-45% cover)	(Hesp *et al.*, 2015)*
* related studies, due to long-term, multi-institutional collaboration, same study area (Greenwich Dunes, Prince Edward Island, Canada), reviewed by Walker *et al.* (2017): Davidson-Arnott *et al*., 2003, 2008; Walker *et al*., 2003, 2006, 2009; Hesp *et al*., 2005, 2009, 2013; Bauer *et al*., 2009; Davidson-Arnott and Bauer, 2009; Delgado-Fernandez and Davidson-Arnott, 2011; Chapman *et al*., 2012; Davidson-Arnott *et al*., 2012;; Ollerhead *et al*., 2013				

2.6. Problem description & Research questions

Previous studies are extensive and the general processes are understood in theory. However, most studies about aeolian sediment transport across vegetated foredunes measure transport either for a short period of time (usually several hours), or across foredunes that are maximally 10 – 15 m high, but often lower. In the Netherlands, dunes have an important role for coastal safety and biodiversity. But the densely vegetated foredunes of the North Sea coast are about 25 m high and have a steep stoss slope. Flow acceleration and wind deflection differ for different dune topographies and heights. How the wind flow develops over a high dune has important implications for sand transport across the foredune, yet this has not been studied often. What are the effects of wind approaching from different directions for a longer period of time? It is important to understand whether and to what extent transport is possible across such high foredunes. This allows to quantify the basis for future coastal management in the face of sea level rise for a country that lies for large parts below sea level. Many authors emphasise the importance of quantifying sediment transport rates across the foredune in relation to wind, vegetation and dune topography. This can then be used in models predicting dune growth and transport rates. Therefore, the local topographic features and variations in vegetation density need to be linked with wind vectors and coinciding sediment transport across the foredune. This Master thesis therefore focuses on the effect of dune topography and vegetation on wind flow characteristics and sediment transport across the foredune.

The study was conducted at the Dutch coast with high, densely vegetated foredunes. Thereby it assessed how the vegetation on the stoss site alters physical settings that are responsible for aeolian sediment transport. The conceptual model (Figure 15) displays the parameters that need to be known and related in order to understand aeolian sand transport across the foredunes of the study site. The relevance of this study lies in being part of the foundation for predicting dune growth after erosion events, as well as future dune development with altering environmental factors. As can be concluded from the overview in Table 1, a study about aeolian sand transport across high dunes (~ 25 m) and densely vegetated by marram grass has not been conducted in recent years (e.g. Arens, Van Kaam-Peters and Van Boxel, 1995). With this in mind, a main research question and two sub questions were formulated, as well as corresponding hypotheses:

How does vegetation on the foredune at its seaward site alter the physical settings that are responsible for aeolian sediment transport?

1) Airflows across the foredune: how does the wind change its velocity, direction and turbulence across the vegetated foredune?
Hypothesis 1: Depending on the incipient wind direction, it is hypothesised that airflows across the vegetated foredune will accelerate and deflect to more normal across the foredune. Furthermore, the turbulent flows is expected to decrease across the foredune.

2) What are the aeolian sand transport rates across a high and vegetated foredune?
Hypothesis 2: If there is aeolian transport recorded across the foredune, it is expected that the transport rate will decrease very fast shortly after the first vegetation around the dune foot. Most sediment is assumed to deposit at the dune foot, barely on the dune slope and none on the dune crest.

3) How is sand transport and deposition influenced by vegetation across the foredune?
Hypothesis 3: The vegetation cover is expected to influence sediment deposition. Species and vegetation cover in situ may play a role as they trap sand and simultaneously reduce wind flows that entrain sediment.

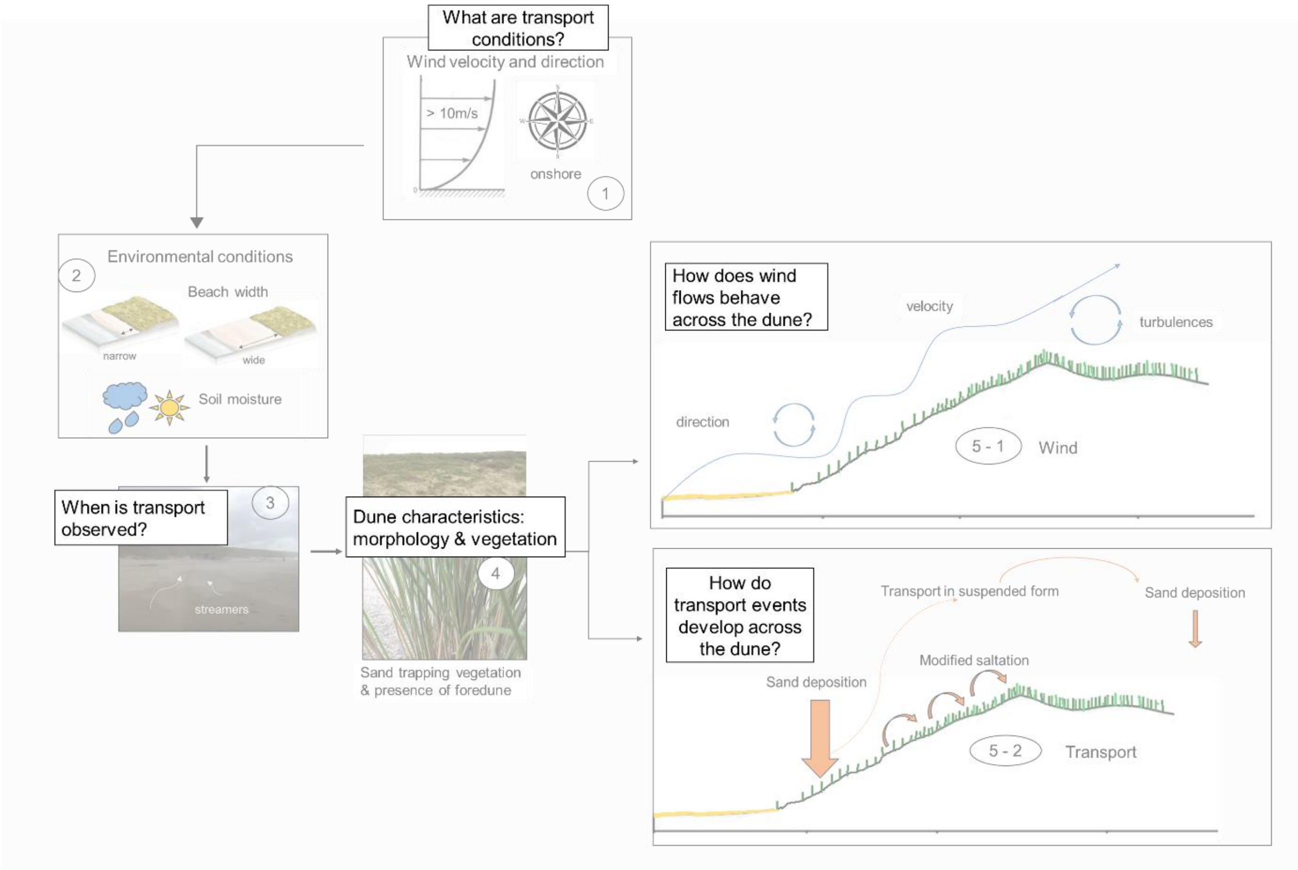

Figure 15. Conceptual model of questions that need to be resolved in order to answer the main research question.

3. Methodology

Field data were collected during a period of five weeks (02.10.2017 to 31.10.2017) in Egmond aan Zee (hereafter referred to as Egmond), the Netherlands, as part of *AEOLEX II* campaign. Wind direction, magnitude and turbulent kinetic energy (*tke*) were recorded continuously across the foredune using three ultrasonic anemometers. Sediment transport was quantified at five days (5th, 6th, 11th, 17th and 25th October) using sediment catchers. Vegetation was quantified along a study transect through a onetime assay.

3.1. Study area

The study area is at the Dutch North Sea coast (so-called Holland coast) near Egmond in Noord-Holland, the Netherlands. The coast is approximately orientated north - south, with an inclination of 8° relative to north (van Duin *et al.*, 2004). Although beach nourishments are done at Egmond, the study site is relatively undisturbed by this and shows natural dynamics. The studied cross-shore transect was 20 m south of the regional beach pole with km-indication of 41.0 (Figure 16).

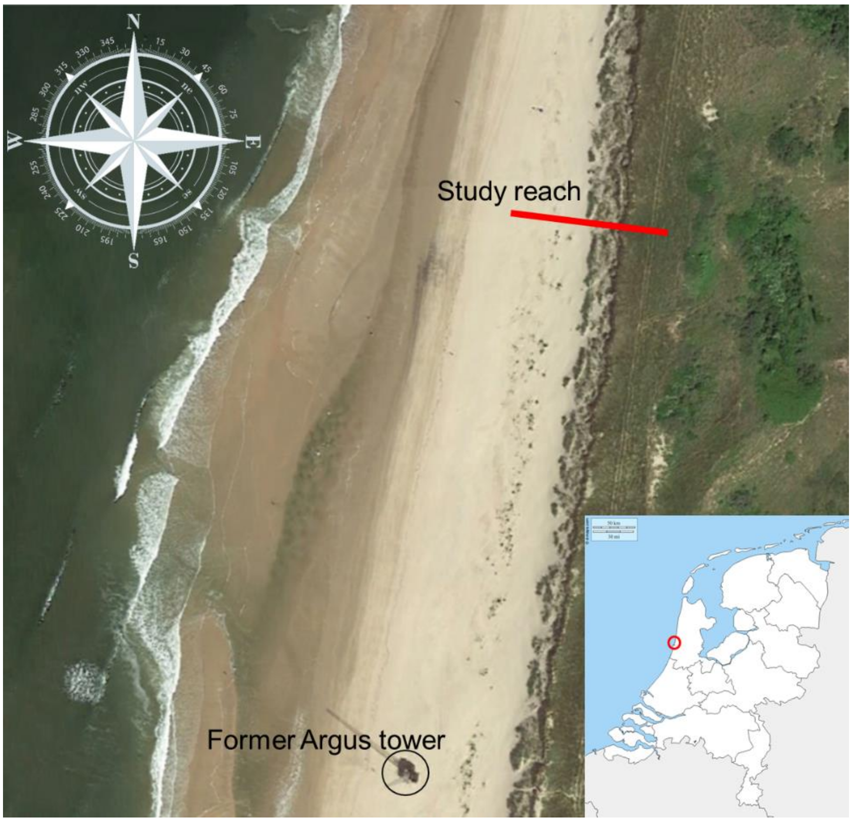

Figure 16. Location of study transect in red and its position in the Netherlands (inset). The former Argus tower (next to beach pole with km-indication of 41.25) was used as reference station throughout the study. Large image obtained from Google Earth, inset image from https://d-maps.com.

The ca. 100 m wide intertidal beach has a fairly flat slope of on average 1:30. The mean grain size at the beach is approximately 0.3 mm (de Winter, Gongriep and Ruessink, 2015). There are lateral continuous foredunes of about 25 m height with a steep stoss slope of 1:2.5 (Figure

17.a). The cross-shore transect (Figure 17.b) was selected as a representative foredune slope due to differences in vegetation patterns between the lower foredune stoss slope (patchy vegetation) and the upper stoss slope (densely vegetated) and due to little interaction from embryo dunes located at the offshore dune side, which had developed (Figure 17.c). The dense vegetation cover is likely to be responsible for the foredunes' steep stoss slope.

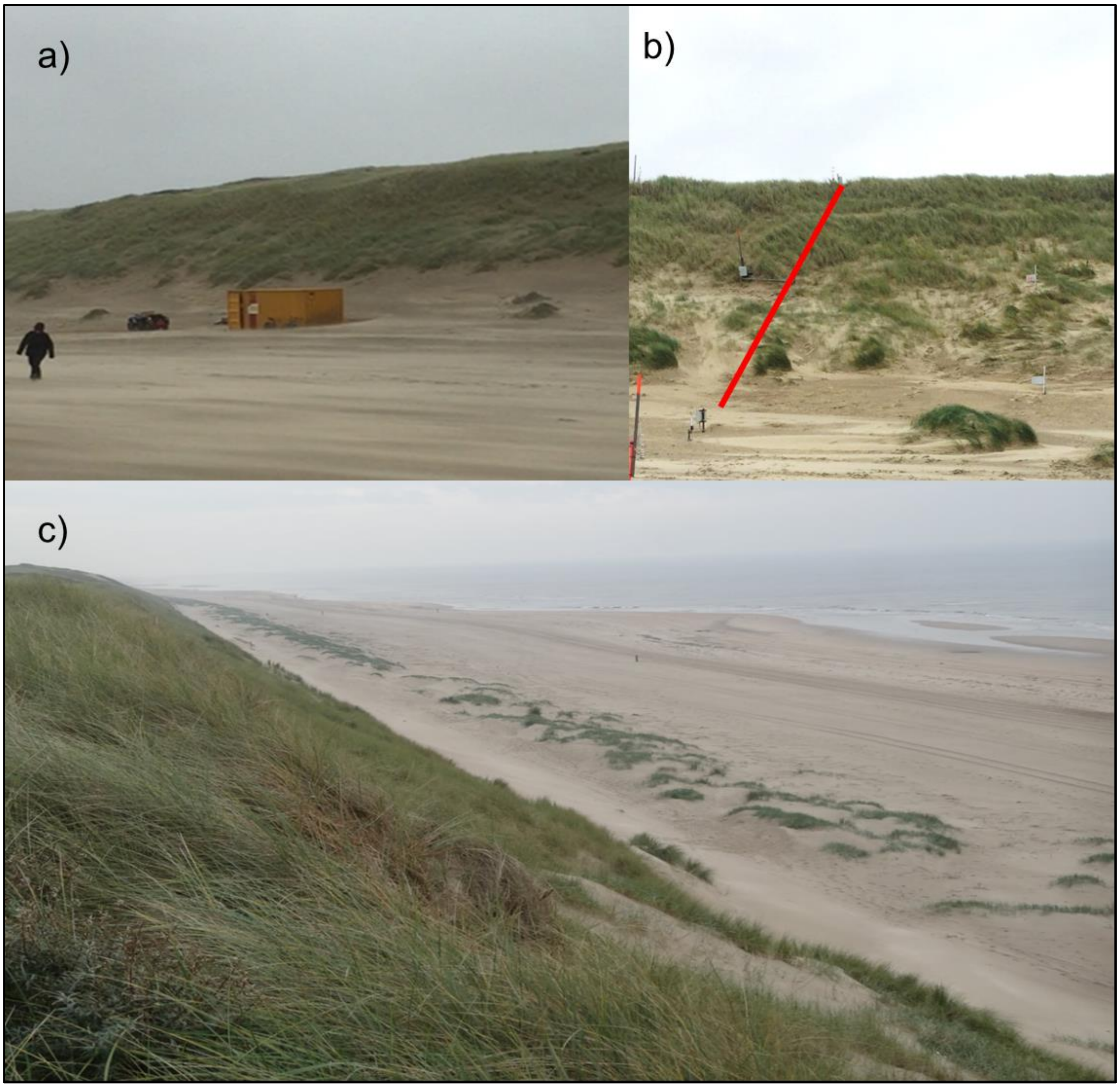

Figure 17. Dunes in study area. (a) The steep and densely vegetated foredune is displayed with a sea container and person for size reference, while (b) shows the main study transect (red line). Here, the lower foredune stoss slope has more patchy vegetation, while the upper stoss slope is densely vegetated. (c) shows the dune and the beach width viewed from the top of the dune (crest), as well as the presence of fairly continuous embryo dunes just south of the study transect.

The beach is wave-dominated and exposed to waves that approach from various direction ranging from southwest to north (Aagaard *et al.*, 2005) and an annual average significant wave height (H_s) of 1.3 m (years 1999 – 2011) (de Winter, Gongriep and Ruessink, 2015). The overall

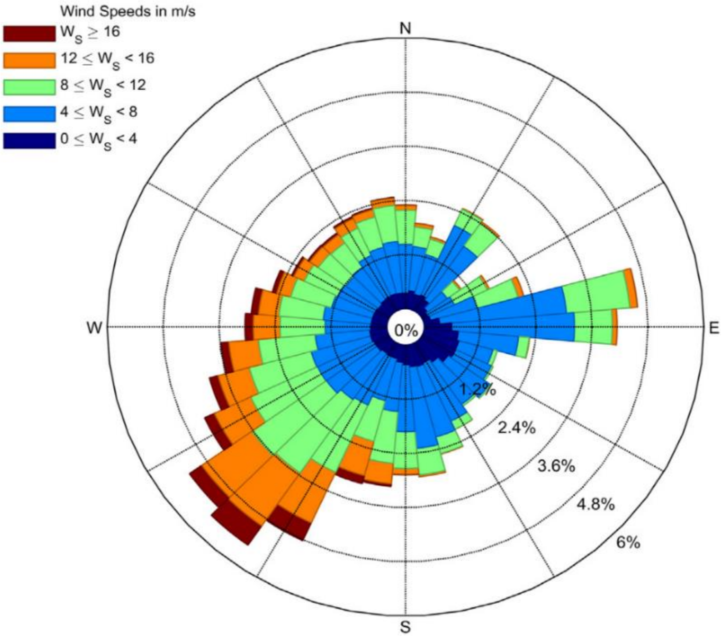

Figure 18. Wind rose of fourteen years (2001–2015) of Ijmuiden, 16 km south of the study area. The wind is measured at the station 225 of the Royal Netherlands Meteorological Institute KNMI. The wind data of Ijmuiden shows the overall wind climate of the study area. A similar station is used as reference station. Figure is extracted from Ruessink et al. (2017). The authors suggest that the peak of easterly winds might be attributed to a local phenomenon (presence of Noordzeekanal) as other wind stations in the area do not show a similar peak.

wind conditions of the region in which the study area is found are recorded at the IJmuiden weather station (station no. 225) of the Royal Netherlands Meteorological Institute KNMI (Ruessink *et al.*, 2017) (Figure 18). This station is situated ca. 16 km south of the study area close to the IJmuiden harbour mole at +13 m Normaal Amsterdams Peil (NAP). Southwest wind direction is dominant, with maximum velocities of 16 $m.s^{-1}$, which is onshore and oblique onshore, due to the coastal orientation of NW to SE (de Vries *et al.*, 2012; Ruessink *et al.*, 2017). October marks the beginning of the stormy season, which generally lasts until February (Arens, Van Kaam-Peters and Van Boxel, 1995). The Holland coast has generally a linear dune growth with 0 - 40 $m^3.m^{-1}.yr^{-1}$ and dune volume changes in the study area are positive, ranging between 5 and 15 $m^3.m^{-1}.yr^{-1}$ (de Vries *et al.*, 2012), which indicates aeolian transport into the foredune. The foredune is home to amongst others (European) marram grass (*Ammophila arenaria*), sand couch grass (*Elytrigia juncea*), lesser hawkbit (*Leontodon saxatilis*) and colonies of (European) sea rocket (*Cakile maritima*) (Provincie Noord-Holland, 2012). Thereby marram grass is the dominant species with a dense cover at the crest (Arens, Van Boxel and Abuodha, 2002).

3.2. Field measurements

3.2.1. Position of instruments

All measurements were taken at the stoss site and coordinates were recorded in RD2008, with reference to the former Argus tower (X/Y/Z: 102572/511553/0, 277.2° relative to north), that was next to beach pole with km-indication 41.25 (Figure 16). All x-coordinates point positively offshore and y-coordinates positively to the south, while z-coordinates are the elevation above NAP, which is approximately mean sea level. All coordinates are in metres. Axes of figures are reversed so that the seaside is orientated to the right hand side (west) and north to Magnetic

North. The cross-shore and dune beach profile of the study transect show a gentle sloping bare beach (1:40) and a steep stoss slope at the foredune (1:2) (Figure 19). The profile of the foredune was measured point-wise approximately every metre. This was done four times during the campaign using a RTK-GPS (Trimble). Three ultrasonic anemometers (SA1, SA2 and SA3) and four sand catchers (C) were all installed for the duration of the study (C1, C1.5, C2 and C3) with similar cross-shore position (Figure 19), but on different profiles (Figure 20) to avoid disturbance of the wind measurements.

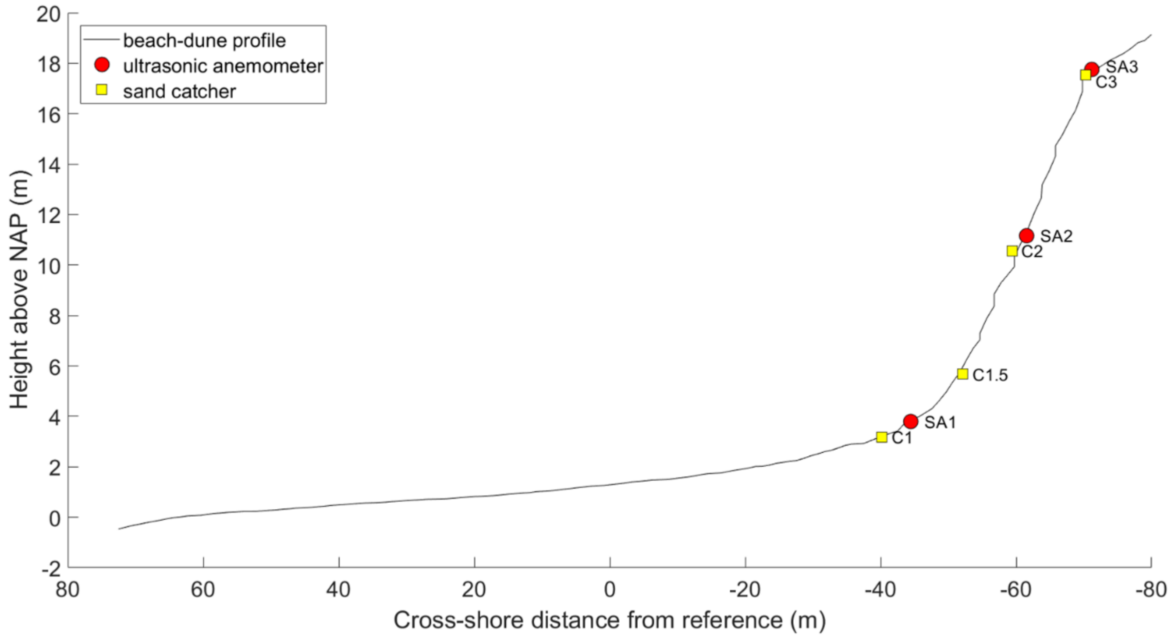

Figure 19. Beach and dune profile of the study transect. The sonic anemometers are displayed in red (SA1, SA2, SA3) and the sand catchers (C) in yellow. The SAs and catchers are not along the same cross-shore profile to avoid shading of the wind measurements by the presence of the catchers.

Figure 20. Picture of instruments at the study section. Yellow squares show the position of the sand catchers and red circles highlight the position of the SAs.

3.2.2. Wind measurements

For wind flow measurements, Ultrasonic Anemometers, Model 81000RE, R.M. Young Company, commonly referred to as sonic anemometers were used (Figure 21). They are referred to as SAs in this study.

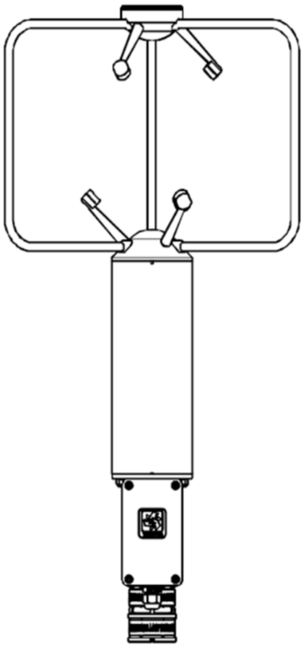

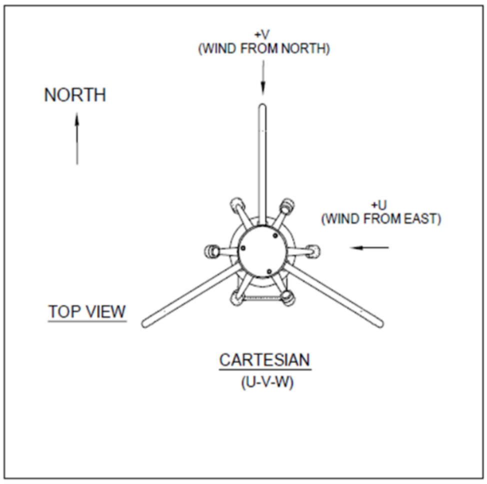

Figure 21. Left: sketch of ultrasonic anemometer (Ultrasonic Anemometer Model 81000RE, R. M. Young Company); right: a schematic top view of the instrument (R. M. Young Company, 2001).

SAs measure three dimensional wind velocity and speed, using the transit time of ultrasonic acoustic signals. From the speed of the sound, the sonic temperature is also derived, corrected for crosswind effects. For a wind speed range of 0 - 30 $m.s^{-1}$, it has a measurement resolution of 0.01 m/s and an rms ±0.05 $m.s^{-1}$. Van Boxel, Sterk and Arens (2004) studied ultrasonic anemometers in aeolian sediment transport research in detail. The three permanently installed SAs operated at a sampling frequency of 10 Hz during the entire campaign with small interruptions for data collection. The measurement volume of the SAs were at 90 cm from the ground and aligned to the beach pole of km-indication 40.75 (x/y/z = -35.4/-501.2/3.4) (Appendix 8.1, Table A2).

3.2.3. Sediment transport and morphology

To study aeolian sand transport across the dune, Modified Wilson and Cook sand catchers were used as proposed by Sterk and Raats (1996) (Figure 22). The catchers trap moving material at six different heights above surface between 0.05 m and 0.7 m. Each catcher consisted of six plastic bottles positioned at varying heights (Appendix 8.1, Table A2). Each plastic bottle (approximately 100 ml) has two glass tubes (inner diameter = 8 mm, opening = 50.3 mm^2) that enter through the lid. One tube allows air and sediment to enter, while the other opening allows air to escape. The bottles were mounted on an aluminium wind vane rotating around a fixed pole to assure orientation in the wind direction. Since saltation is limited to less than 50 cm above ground and transport is expected to decrease exponentially with height, the heights of the bottles were chosen according to a log distribution. The sand catchers have a trapping efficiency ranging from 49% (Sterk and Raats, 1996), 54.4% (Sterk *et al.*, 2012), 72 to 87% (Dong *et al.*, 2011) and up to 100%, and as such are considered the most efficient sampler in the field (Goossens and Offer, 2000). Since the trapping efficiency was not tested in a wind tunnel experiment previous to the study, information was provided by W. de Winter about her wind tunnel experiments with the same catchers and sediment of the study area, so that the efficiency was ascertained as 35%. The catchers used had a larger wind vane than those from Sterk and Raats (1996) (Figure 23). The operating period was timed on the second and the content of the traps was weighted before and after drying in an oven for 24 hours at 105°C. For weighting, a Sartorius analytical lab scale digital balance was used, similar to the model LC 2200 S MC1.

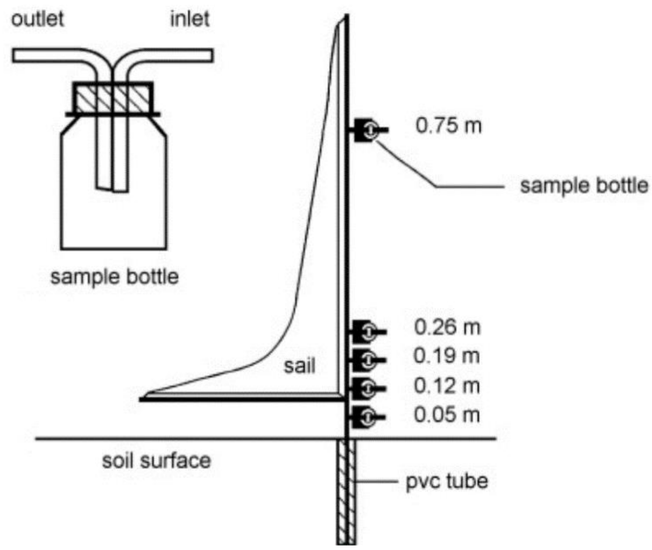

Figure 22. Sketch of a Modified Wilson and Cook sediment catcher, retrieved from Sterk and Raats (1996)

Figure 23. Sand catcher at operation at the dune foot (1) at height of embryo dunes, close to SA1

Four sand catchers were placed at fixed positions (Appendix 8.1, Table A3), which were chosen so as to not disturb the measurements of the SAs and to ensure free rotation of the wind vane. During one day of sand catcher measurements (11th October), an additional ultrasonic anemometer (SA1.5) was installed next to catcher C1.5. Every time the wind was expected to be larger than 10 m.s^{-1} and no or little precipitation was forecasted. This lead to five moments of data recording (Table 2).

Table 2. Sand flux measurements at five days and time of measurement per catcher in hh:mm:ss (MET)

Catcher No.	Date of measurement (day no.) 05.10.2017 (day 1)	06.10.2017 (day 2)	11.10.2017 (day 3)	17.10.2017 (day 4)	25.10.2017 (day 5)
C1	NA	12:54:21 - 14:52:35	10:38:40 - 16:30:00	09:27:00 – 14:03:00	10:59:00 - 15:24:00
C1.5	13:23:50 - 14:46:20	11:35:00 - 14:22:20	10:18:00 - 16:34:00	09:33:00 – 14:07:00	11:05:00 - 15:23:00
C2	13:21:30 - 14:49:20	11:44:58 - 14:27:25	10:12:45 - 16:38:00	09:38:00 – 14:09:00	11:14:00 - 15:31:00
C3	13:44:32 - 14:39:13	11:50:28 - 14:30:30	09:55:59 - 16:43:30	09:44:00 – 14:19:00	11:22:00 - 15:25:00

Morphological foredune changes were evaluated through two LIDAR surveys carried out by drone flights (Shore Monitoring & Research BV) before and after the campaign (23.09.2017 and 03.11.2017, respectively), resulting in elevation models, with 1 m cell size.

In order to compare the grain size of the caught sediment, the grain size distribution of the beach dune profile was analysed. For this, 17 samples were taken every five metres along the profile ranging from 0.09–17 m +NAP.

3.2.4. Vegetation

Plant density was estimated at the cross-shore transect every metre as described by Bonham (1989), by counting all individual stems within a 25 cm x 25 cm quadrant. Photographic documentation was taken for all counts on all transects (Figure 24).

Figure 24. Two example pictures of how stems were counted in a quadrant: a) sand couch (*Elytrigia juncea*) and b) European marram grass (*Ammophila arenaria*).

To account for natural deviations, rows of five quadrants were positioned per elevation (at 1 m intervals) with the middle quadrants aligned with the study transect (Figure 25). Two additional transects were studied to account for alongshore variability and to ascertain the representability of the main transect. They were 250 m and 500 m south at the beach pole with km-indication of 41.25 and 41.5, respectively. The foredune height and vegetation varied among transects so that a total count of 30 rows was done for transect 41.0, 14 rows for 41.25 and 10 rows for 41.5. Additional to the stem count, the width and length of five stems was measured. For each quadrant the plant species were determined and the dominant species ascertained.

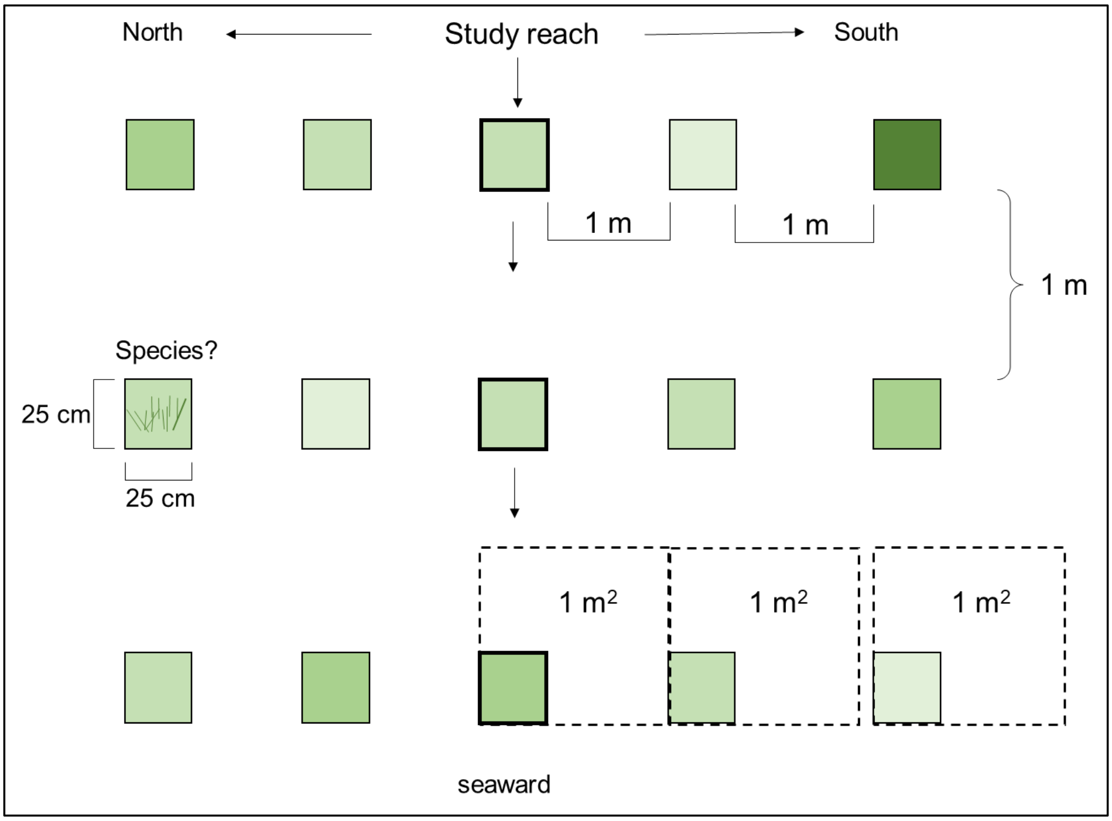

Figure 25. Conceptual sketch of vegetation count for density, plant height and species determination.

3.3. Data analysis

3.3.1. Wind flows

All entries were pre-processed: by a company quality assessment and additionally filtered that temperature changes within 5 seconds must be smaller than 2°C from the median. Data just before and after deployment of the SAs were removed.

Wind statistics were computed based on the recorded wind data (u, v, w) at high frequency (10 Hz). The axis were chosen that u is the horizontal wind velocity in east-west direction (positive from east) and v is the horizontal wind velocity in north-south direction (positive from north). The velocity component w is the vertical wind velocity (positive from below). Consistent with data processing by the Royal Netherlands Meteorological Institute KNMI, the time series of u, v and w were first smoothed into series of 3-s running means. The mean wind velocity ($\bar{u}$, $\bar{v}$, $\bar{w}$), the wind direction (θ) and wind gusts were then computed as ten minute averages based on the running means, while the turbulent kinetic energy (tke) was computed using the non-smoothed wind data. A visual quality control of the data for each deployment day was conducted for the ten minute averages, looking out for extreme jumps in wind velocity components to avoid the inclusion of disturbed measurements.

The following equations were used to obtain the wind magnitude (Eq.1), the turbulent kinetic energy (Eq.2) and the wind direction (Eq.3).

The wind magnitude was based on the mean wind components $\bar{u}$, $\bar{v}$ and $\bar{w}$:

$$\bar{u} = \sqrt{(\bar{u}^2 + \bar{v}^2 + \bar{w}^2} \qquad (1)$$

The turbulent kinetic energy was calculated as follows:

$$tke = \frac{1}{2} \times \left(\overline{(u')^2} + \overline{(v')^2} + \overline{(w')^2} \right) \qquad (2)$$

whereby tke is the turbulent kinetic energy as calculated by the mean (indicated by an overline) of the square of the fluctuating part of the velocity components (indicated by a prime (u', v', w')).

The wind direction was obtained with Magnetic North being 360°:

$$\theta = arctan(\overline{u, v}) * \frac{180}{pi} \qquad (3)$$

The dimensionless wind speed ratios between the SAs were used to express the change of the wind speed relatively as increase or decrease, based on incipient wind direction. To compare the wind statistics to non-disturbed wind flows, data of a proximate offshore measuring station (*IJgeul stroommeetpaal)* were used. The station of the Department of Waterways and Public Works (Rijkswaterstaat) lays ca. 16 km south of the study area and is ca. 1 km west of the southern harbour mole of IJmuiden, as well as 500 m south of the longitudinal IJgeul-axis. As the station is offshore, the wind flows are not influenced by the presence of a foredune or distinct topographical variations. It is therefore used as reference wind speed and direction. The height of the measuring is 10 m. In order to compare velocities between dune foot and reference station, the wind velocity data at the dune foot were corrected from 0.9 m above surface to 10 m above surface using the law of the wall, assuming a logarithmic velocity profile. The shear velocity u_* was calculated using the roughness length of $z_0 = 8 * 10^{-6}$ m, based on 1/30 law of the median grain size of the study area d50 = 250 µm as proposed by Bagnold (Dong *et al.*, 2001); and the von Karman constant κ = 0.41 (Eq.4). Based on the shear velocity at 0.9 m above surface, the wind velocity at 10 m height was calculated (Eq.5).

$$u_* = \frac{u_z}{ln\frac{z}{z_0}} * \kappa \tag{4}$$

$$u_z \frac{u_*}{\kappa}\ ln\frac{z}{z_0} \tag{5}$$

To study the development of turbulence across the foredune, the non-dimensional ratio (r) of the turbulent kinetic energy (k) and wind speed ($\bar{u}$) were calculated (Eq.6). The larger this ratio, the greater the turbulence relative to the wind speed.

$$r = \frac{\sqrt{k}}{\bar{u}} \tag{6}$$

For the wind direction, the horizontal velocity component of the SA was rotated into a north-south east-west coordinate system. Wind directions were recalculated so that -90° represents alongshore southern winds, 0° perpendicular onshore, 90° alongshore northern winds and 180°/-180° perpendicular offshore. All wind directions were recorded and pre-processed, but offshore wind directions were excluded from further analyses. This was done due to the research purpose: assessing wind and aeolian transport across the foredune, originating from the beach. The reference wind direction was assumed to be the same at 0.9 m and 10 m above surface.

3.3.2. Sediment transport

For all days of saltation, the contents of the vertical sand traps were weighted. From the weight and the noted operating time, the windblown mass flux per bottle in g.m^{-2}.s^{-1} was calculated as follows:

$$Q_b = \frac{1}{A}\frac{m}{t} \quad (7)$$

Whereby Q_b is the mass flux for each bottle, *A* is the circular surface of the pipe (50.3 mm^2), *m* is the caught sediment in grams per trap and *t* is the duration time of operation. Based on the sediment mass flux of the six bottles a vertical profile was drawn and an exponential curve was fitted to it. For this, a best-fit model was used for each catcher. The fitted curve was then integrated vertically over the height of 0 to 1 m to obtain the total mass flux Q_m in g.m^{-1}.s^{-1} at the location of the catcher (Eq.8). The calculated mass flux was multiplied by the trapping efficiency factor of $\frac{1}{0.35}$ (trapping efficiency 35%).

$$Q_m = \int_0^1 Q_z{}^{bz}\, dz * \frac{1}{0.35} \quad (8)$$

Additionally to the quantified sand transport, the dune volume before and after the field work was calculated. This was done for the study transect (41.0) and the additional two transects (41.25 and 41.5). The UAV data were used and interpolated and integrated for the cross-shore length of the stoss site at each transect. For this the average for 1 m from an alongshore width of 5 m was used and the foredune stoss slope per transect (Table 3). The same limits were used to determine the differences in height for the three transects from before and after the campaign to obtain elevation changes (accretion and/ or erosion).

Table 3. Limits (x and y) of cross-shore transects to calculate dune volume changes as well as elevation changes from before and after the campaign.

	Distance from reference (m)	
Cross-shore transect	X limit	Y limit
41.0	-80 : -30	-232 : -228
41.25	-65 : -30	-2 : 2
41.5	-50 : -15	248 : 252

3.3.3. Grain size distribution

On 11th October, a sufficient quantity of sand was caught for the analysis of grain size distribution at most catchers. Grain size distribution both for caught sediment and beach dune profile was done with the GRADISTAT particle size analysis software, as developed by Blott and Pye (2001). If the quantity of the caught sand was too little to be sieved, an optical determination was conducted, using a sand ruler (Figure 26).

Figure 26. Sand ruler used to determine grain size of caught sand within traps of sand catchers.

3.3.4. Vegetation

The plant density was determined for each quadrant and corrected for the surface area resulting in a stems per m^2. The mean of the five quadrants per elevation was used for further analysis. Due to the dense cover at the foredune crest, the vegetation cover in percentage could be determined relative to the coverage at the dune crest and the bare beach. The quadrant with the most numbers of stems at transect 41.0 (upper slope/ dune crest) was set as 100% as a reference (bare beach = 0%). For the two additional transects, the coverage relative to transect 41.0 was determined.

4. Results

The results from the study as part of the field campaign *AEOLEX II* are presented in the following chapter. Results from wind flows (overall wind flows, velocity, direction and turbulence) across the foredune are presented first, followed by the results from sediment transport, morphological analyses and vegetation quantification.

4.1. Overall wind flows

The recorded wind flows covered a large range of magnitudes and directions (Figure 27.a and Figure 27.b, respectively).

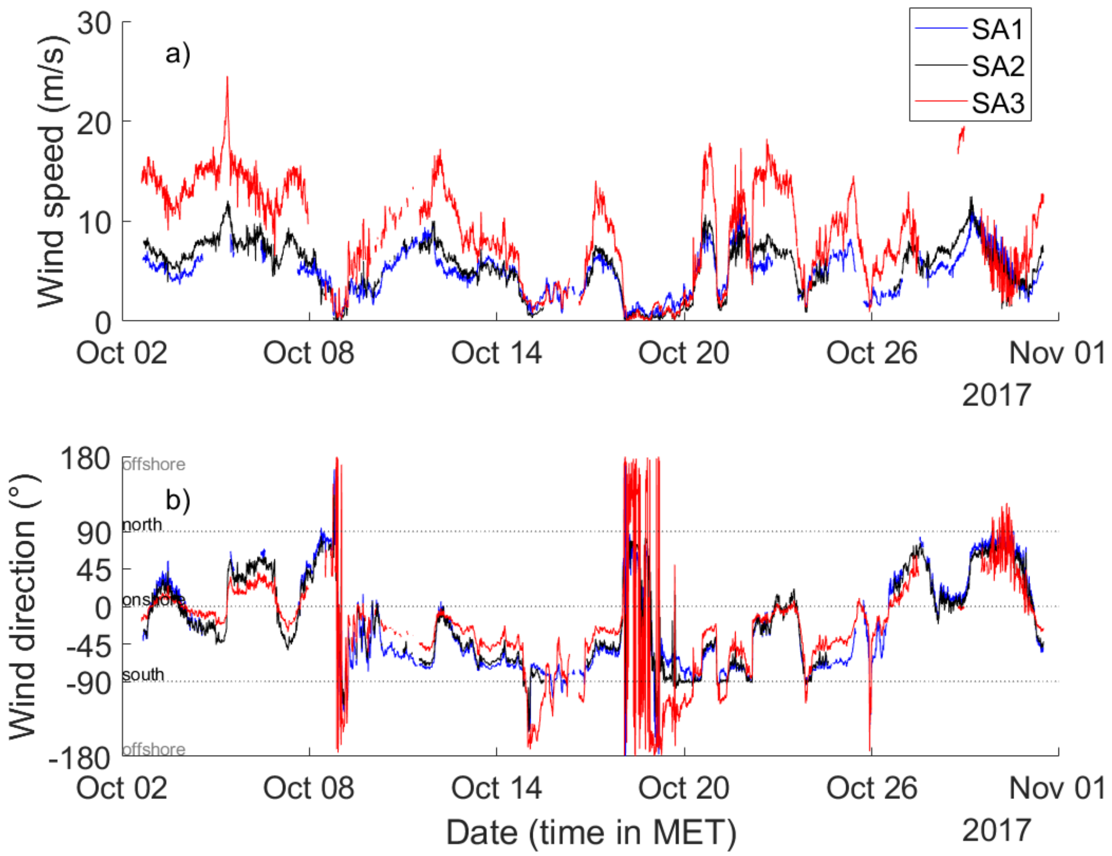

Figure 27. Overview of wind data for SA1, SA2 and SA3 for the whole study period. a) shows the wind magnitude (m.s.$^{-1}$) and b) the wind direction (°).

The wind roses (Figure 28) show clearly that the wind velocity increased from dune foot to crest (Figure 28.b and Figure 28.d, respectively). Compared to the reference (Figure 28.a), wind magnitude and direction varied clearly across the foredune. At the dune foot the lowest wind magnitudes were recorded: these were mostly below 8 m.s^{-1} and occasionally between 8 - 12 m.s^{-1}. A wide range of wind directions was recorded at the dune foot ranging from north to south (Figure 28.b). Wind flows approached mainly from a south-westerly direction and were of smaller magnitude. Offshore directed winds were barely recorded at the dune foot. On the mid slope, the wind velocity reached 12 m.s^{-1} four times during the study (Figure 28.c, orange line), during a north-western storm on 29th October. The wind direction on the mid slope varied similar to the dune foot (from north to south), covering alongshore, perpendicular and oblique onshore wind directions, while barely recording offshore flows. However, the wind approached the station more often from perpendicular onshore than at the dune foot. At the crest (Figure 28.d), the highest variability in wind velocities was observed with maximum magnitudes reaching up to 25 m.s^{-1}. Wind directions only varied between perpendicular-, and slightly oblique onshore, though offshore wind flows were similar to the reference station.

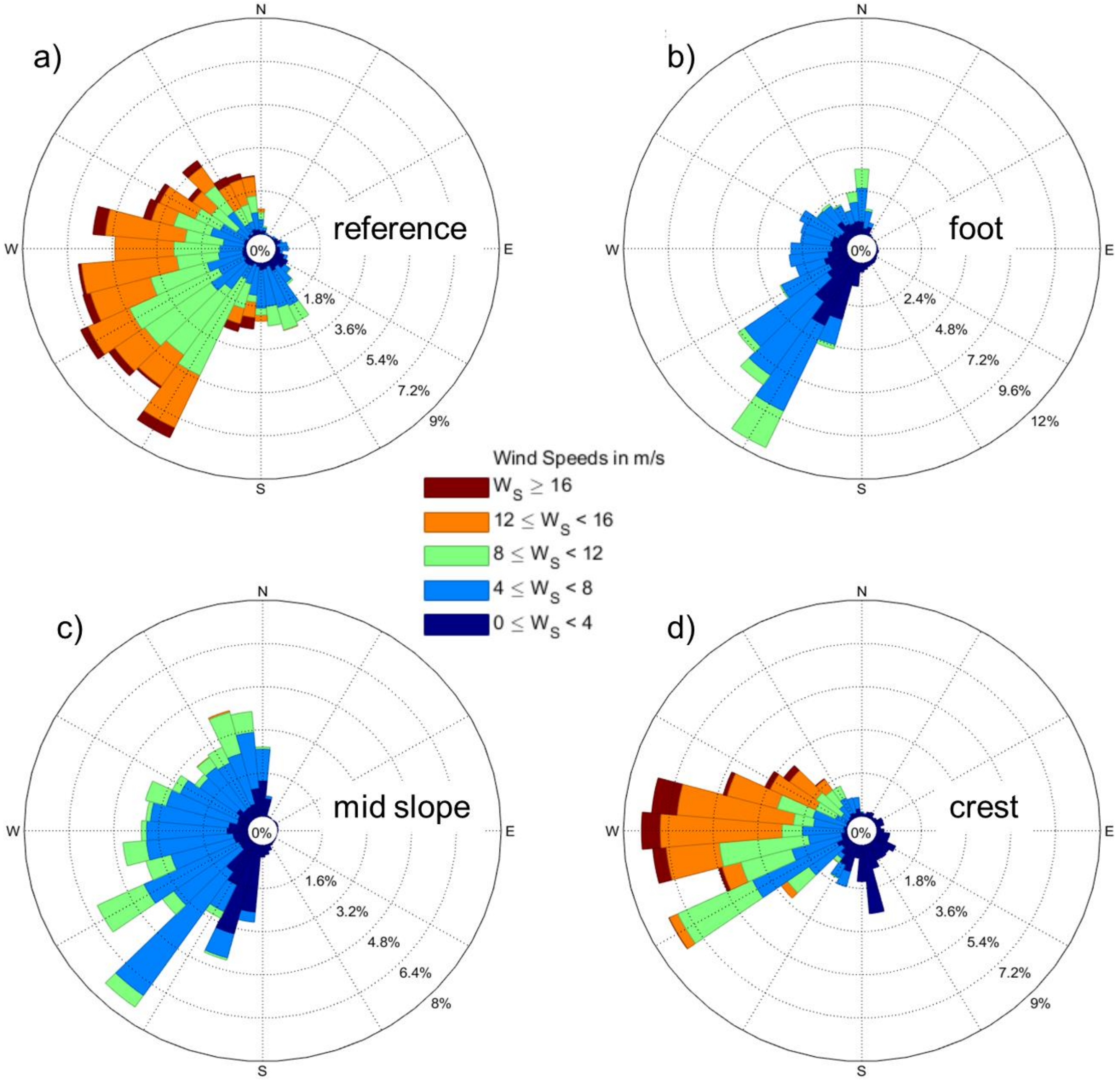

Figure 28. Wind roses from a) reference station, b) dune foot (SA1), c) mid slope (SA2) and d) dune crest (SA3). The colour indicates the velocity, and the frequency of the wind direction is indicated in percentage, increasing outwards.

4.2. Wind velocity

Wind velocities at the dune foot were corrected for height and compared to wind velocities measured at the reference station (Figure 29). There was a reduced magnitude of wind flows at the dune foot for approximately two thirds relative to wind speeds measured at the reference station (Figure 29). The largest velocity decrease was found for wind flows approaching perpendicular onshore up to an inclination angle of 25° (Figure 29, red symbols), while wind flows of highly oblique onshore to alongshore winds (between 65 - 90° inclination angle) from north and south were the least decelerated (Figure 29, black symbols). Oblique onshore winds flows were generally decelerated (25 - 65° inclination angle for both south and north, Figure 29, blue symbols).

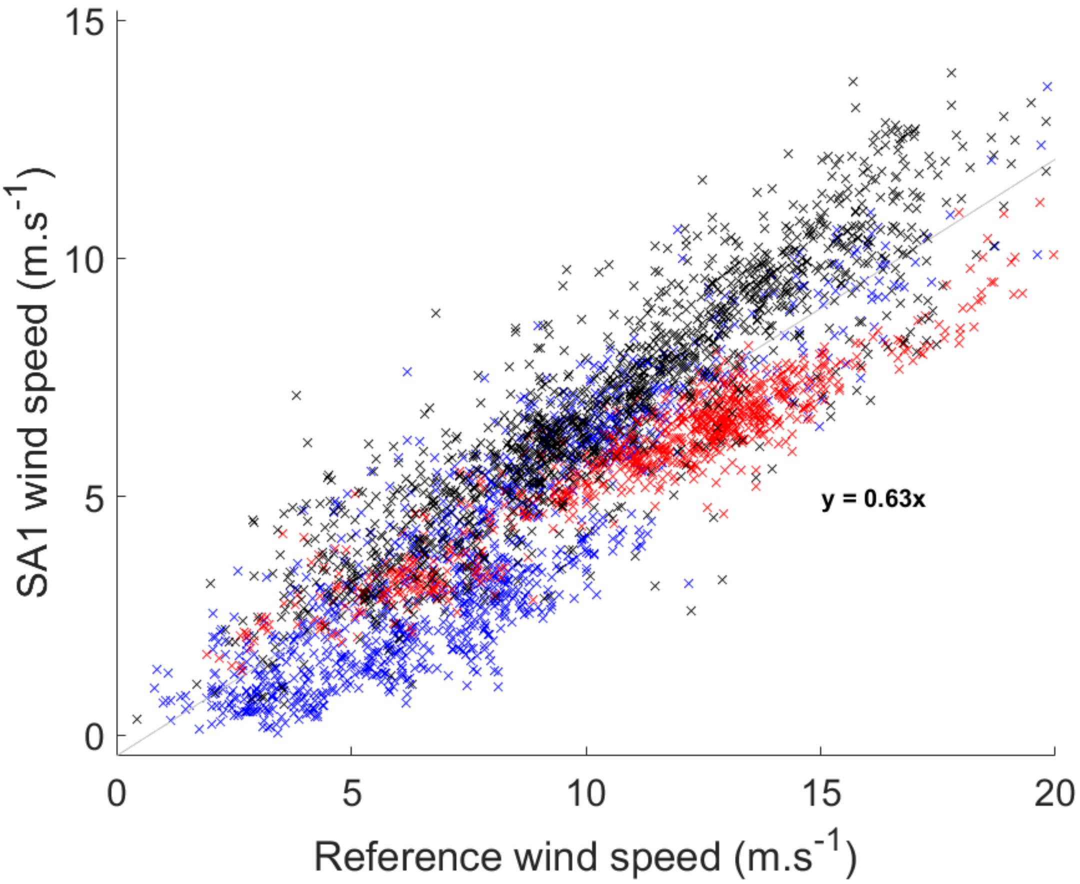

Figure 29. Comparison of wind velocities of reference station (IJmuiden) and dune foot (SA1). Black line indicates the least square line for all data, which is approximately two thirds (0.63). Red data points are perpendicular onshore winds of maximal 25° inclination angle; black data points are wind flows of highly oblique to alongshore wind directions (65 - 90° inclination angle for both south and north). Blue data points are oblique onshore wind flows of 25 - 65° inclination angle for both south and north.

The wind velocity increased across the foredune (Figure 28), but there were considerable variations in the magnitude of increase. The increase was studied relative from one ultrasonic anemometer to another one.

It became clear, that the increase did not show a strong dependency with wind speed itself (Figure 30). From dune foot to mid slope (Figure 30.a) the increase in wind speed is smaller than on the upper half of the foredune (Figure 30.b). The wind speed increase across the whole foredune slope (Figure 30.c) ranges up to 3 times higher and there seems little correlation with initial wind speed at the dune foot to it. Avery similar result (no obvious relationship) was obtained when comparing the relative increase with the wind speed of the reference station.

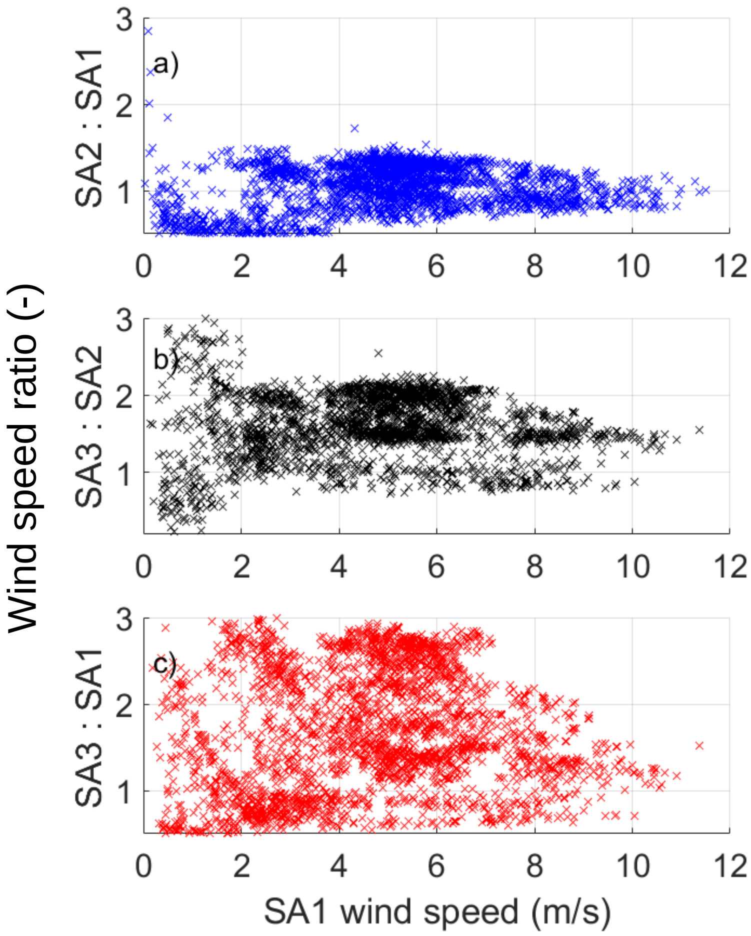

Figure 30. Wind speed ratios across the foredune, as a function of wind speed at the dune foot (SA1). a) shows wind velocities on lower slope, based on the ratio of SA2:SA1 with SA2 half way on the dune slope and SA1 on dune foot; b) shows the upper slope up to the crest (SA3) with the ratio of SA3:SA2; and c) shows the ratio wind speed of SA3:SA1 from dune crest to dune foot. All values > 1 indicate an increase in wind speed, while ratios < 1 indicate a deceleration of the wind speed.

The development of the wind velocity across the foredune was then studied based on incipient wind direction (Figure 31). On the lower slope, there was a small increase in wind velocity for onshore winds, on average by a factor of 1.1 (10%) (Figure 31.a). Largest increases above 1.3 (red dashed line) were found for wind directions extending from -22° to 14°, i.e. onshore. Oblique onshore winds accelerated on the lower slope but the wind slowed down for highly oblique wind directions (-76° south and 60° north). On the upper slope the wind speed predominantly increased (Figure 31.b). The largest increases occurred for onshore winds up to deviation of 22° from normal to south or north. For this onshore range, the wind velocities at the dune crest were larger than on the mid slope by more than a factor of 2 (+100%).

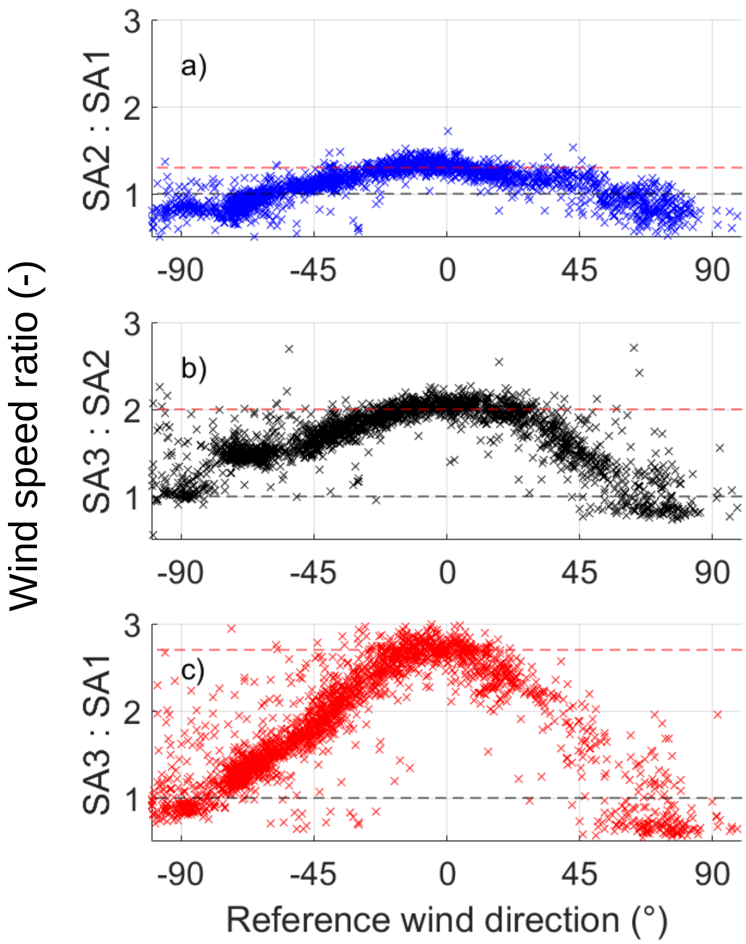

Figure 31. Wind speed ratios across the foredune, as a function of incipient wind direction using the offshore reference wind direction. a) shows wind velocities on lower slope, based on the ratio of SA2:SA1 with SA2 half way on the dune slope and SA1 on dune foot; b) shows the upper slope up to the crest (SA3) with the ratio of SA3:SA2; and c) shows the ratio wind speed of SA3:SA1 from dune crest to dune foot. The black dashed line at 1 indicates a ratio of 1, meaning same wind speeds at both stations. All values > 1 indicate an increase in wind speed, while ratios < 1 indicate a deceleration of the wind speed. All subplots include an extra reference line (red dashed line) that shows the wind velocity ratios for perpendicular onshore winds.

When the incipient wind direction was more oblique than -22° or 22°, the wind velocity still increased but to a lesser extent. On average, an increase by 1.7 (+70%) was measured. For highly oblique onshore winds from the south a small increase by 1.3 (+30%) was observed, while a decrease by a factor of 0.8 (-20%) was measured for highly oblique northwest winds (60-80°) (Figure 31.b). Across the entire foredune from foot to crest an acceleration was recorded (Figure 31.c). On average, wind velocity increased by 1.7 (+70%). For perpendicular onshore winds between -14° and 8° the wind speed increased by a factor of 2.8 (+180%) or greater, up to a maximum of 3.1 (+210%). With increasing obliquity of the approaching wind, the acceleration was reduced. Alongshore winds from south (-80° to -90°) decreased by a factor of 0.8 (-20%), while oblique to highly oblique onshore winds from north (60-90°) showed a decrease by a factor of 0.7 (-30%) (Figure 31.c).

4.3. Wind direction

The development of the wind direction across the foredune was seemingly independent of the wind speed for speeds above 5 m.s^{-1} (Figure 32.a - c). The absolute values of deflection (i.e. regardless the direction of bending) showed more variations and were greatest for wind velocities below 5 m.s^{-1} for all stations. The absolute deflection seemed however dependant of the incipient wind direction at the dune foot and the dune crest (Figure 32.d and f).

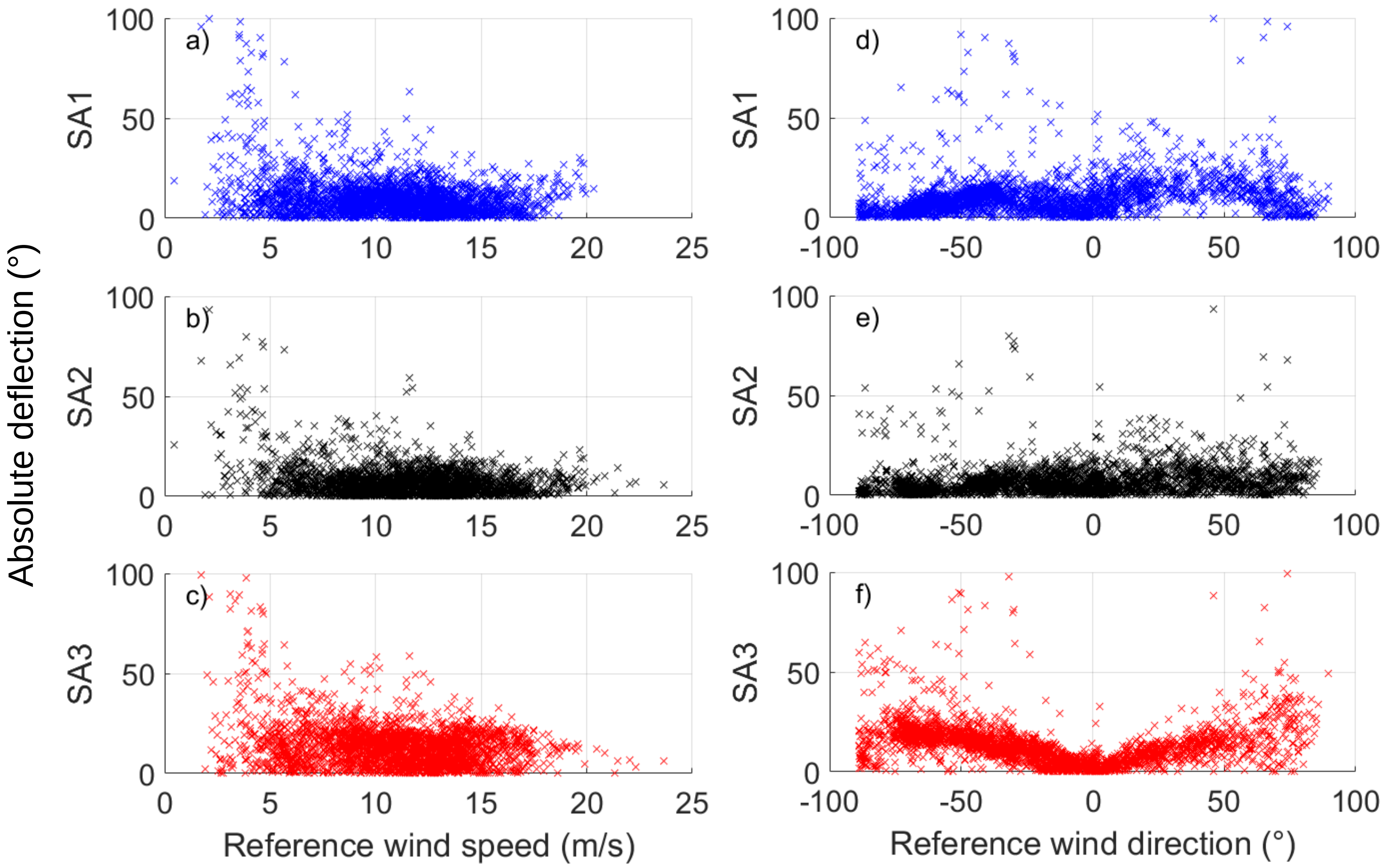

Figure 32. Absolute values of deflection (°) of the wind direction as a function of the reference wind speed (a -c) and as a function of the reference wind direction (d - f). The subplots a) and d) show the dune foot (SA1); b) and e) the mid slope (SA2); and c) and f) the dune crest (SA3).

At the dune foot, maximum deflection was observed for oblique onshore winds between 25 - 65° reaching up to 20° of deflection (Figure 32.d). The absolute deflection did not seem to be dependent on the wind direction at the mid slope (Figure 32.e). However, at the dune crest a largest deflection of the wind flow was observed for highly oblique and alongshore wind directions (Figure 32.f). The direction of deflection across the three stations was compared as a function of the reference wind direction (Figure 33). At the dune foot (SA1), wind flows were deflected towards alongshore directions most of the time (84%) (Figure 33.a) and perpendicular onshore winds were practically absent (Figure 28.b). Wind flows were deflected by on average of 11° (median = 9°), but largest deflection could be as much as 41° for an incident direction of 17° (Figure 32.d). The main wind direction (S or N) remained the same. However, the observed deflection to more alongshore was more pronounced for north-western than for south-western winds and the greatest deflection was found for incident wind angles of 20 - 60°. Perpendicular onshore winds (-5° to 5°) were deflected more alongshore to the north.

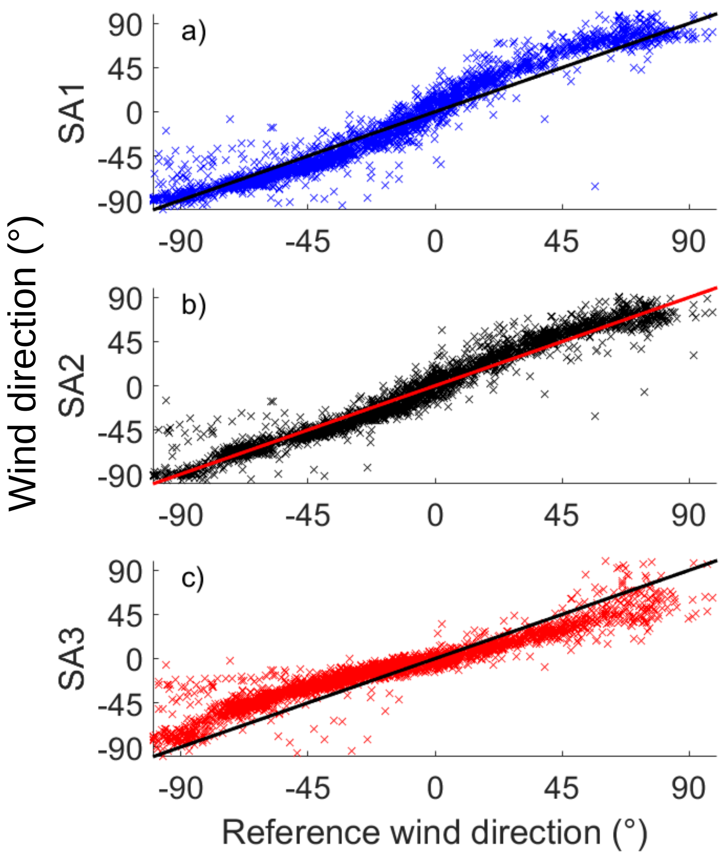

Figure 33. Comparison of wind direction across the foredune, as a function of the reference wind direction with a) the wind direction at the dune foot (SA1); b) on the mid slope (SA2); and c) on the crest (SA3). The line indicates the identity line. Perpendicular onshore = 0°, alongshore = -90° (S) and 90° (N).

The wind at the mid slope (SA2) turned generally more alongshore, compared to the reference (Figure 33.b). On average, the wind was deflected by 7° and large deflections of up to 37° were recorded for slightly oblique onshore wind of 22° (Figure 32.d). Nonetheless, wind directions were most similar to the reference station (Figure 28.c), especially when the wind approached from southern wind directions (-90° to -20°). Perpendicular onshore winds (-5° to 5°) were deflected to more alongshore, in accordance with the incipient wind direction. Northern winds were deflected stronger to more alongshore at the mid slope, similar to the deflection at the dune foot. At the dune crest the wind flows were mainly deflected towards onshore directions (88%) (Figure 33.c). Compared to the reference wind direction the direction changed by 14° on average (median = 13.5°) and up to 38° to more crest-normal for highly oblique incident wind directions (74°). Alongshore winds were rarely recorded (Figure 28.d). While the data cloud was S-shaped at the dune foot, this trend was mirrored at the dune crest: the deflection to alongshore at the dune foot changed across the foredune to cross-shore at the dune crest. Maximum deflection occurred for oblique onshore wind directions of 30 - 70°.

Compared to the wind flows at the dune foot, the wind turned more onshore on the lower slope (between foot and mid slope). On the upper slope (between mid slope and crest) the majority of wind directions (94%) turned more onshore. A maximum deflection of 19° and 28° on the lower slope (relative to the dune foot) was recorded for wind directions of NW (26°) and S-SW (-67°), respectively. On average, flow was deflected by 5° from foot to mid slope. On the upper slope, deflection became more pronounced so that wind was steered from mid slope to crest by on average 15° and maximal 31° for wind directions of NW (53°) and SW (-48°). The change of wind direction across the foredune from foot to crest was consequently largest because of the flow alterations at the dune foot. Across the foredune from dune foot to dune crest, wind was steered to more onshore (96%) most of the time and by an average of 20° (median = 23°). The maximum deflection from foot to crest was 33° for N-NW (74°) and 32° for S-SW (-59°) wind flows, thus oblique to highly oblique onshore winds.

4.4. Turbulent kinetic energy

4.4.1. Absolute turbulent kinetic energy

The *tke* increased with increasing wind velocity at all SAs across the foredune (Figure 34). At the dune foot (Figure 34.a) and on the mid slope (Figure 34.b), the *tke* increased with increasing wind velocity, based on the average *tke* for varying velocity ranges (Table 4). At the dune crest (Figure 34.c) the *tke* also increased with increasing wind velocities but the increases were less pronounced and there was a larger scatter. For wind velocities of 1 – 6 $m.s^{-1}$ the dune crest had the largest *tke*. The *tke* at the dune crest was subsequently lower than on the mid slope and the dune foot at higher wind speeds (Table 4). The *tke* was greatest on the mid slope for velocities of 6 – 15 m.s^{-1}. Largest absolute *tke* was measured at the dune crest with a value of 10.7 m^2.s^{-2} (at wind speed of 13 m.s^{-1} and wind direction of -50°).

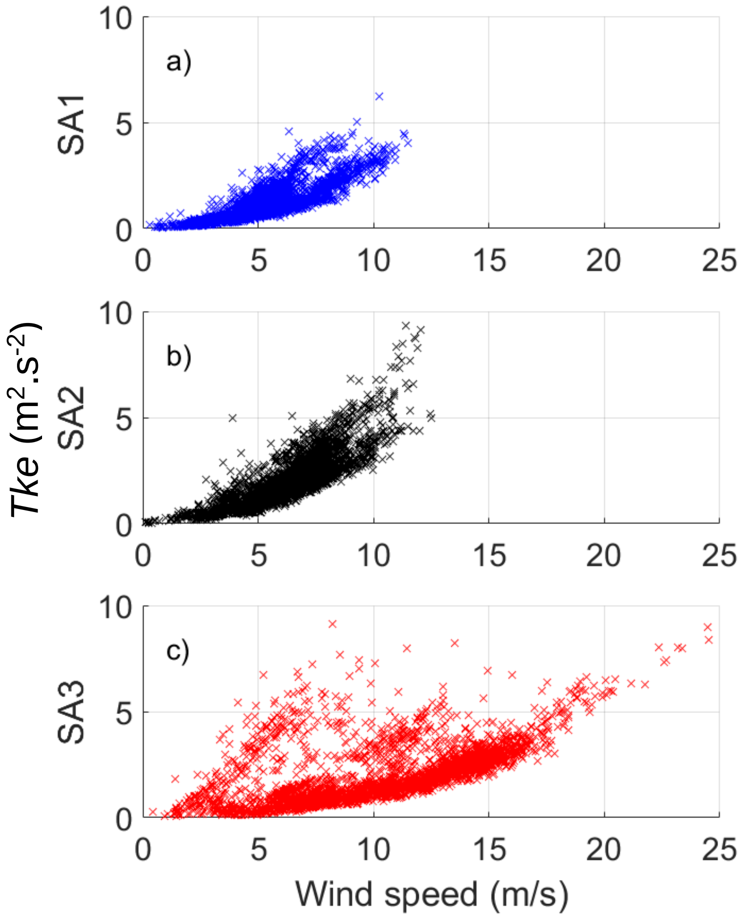

Figure 34. Measured *tke* as a function of wind speed at a) dune foot (SA1); b) mid slope (SA2); and c) dune crest (SA3).

Table 4. Average *tke* values for different wind velocities at different stations across the foredune for all data. The blue shading indicates the largest and the grey shading highlights the second largest *tke*.

Wind velocity (m.s^{-1})	Mean *tke* (m^{2}s^{-2}) Dune foot	Mid slope	Dune crest
1 - 2	0.3	0.3	0.5
2 - 3	0.4	0.5	0.9
3 - 4	0.6	0.9	1.1
4 - 5	0.9	1.1	1.4
5 - 6	1.3	1.5	1.6
6 - 7	1.6	2.1	1.3
7 - 8	2.0	2.7	1.3
8 - 9	2.5	3.3	1.7
9 - 10	3.0	3.9	1.7
10 - 15	3	5.3	2.4
15 - 20	NA	NA	3.5

The *tke* was further not seemingly dependant on the incipient wind direction (Figure 35). For all positions on the foredune, a large scatter was observed while no clear trend for any direction.

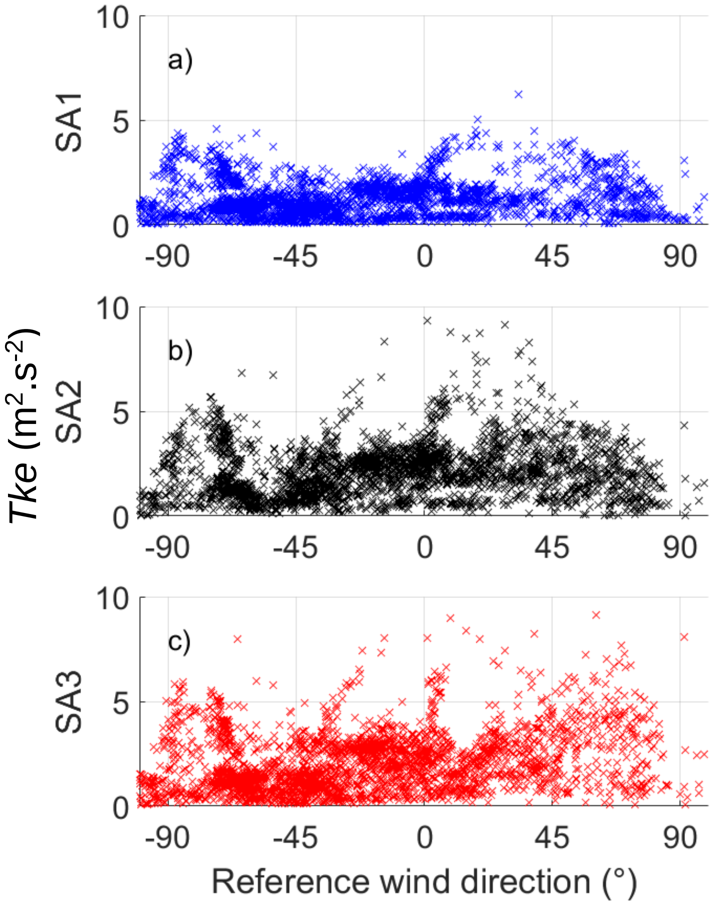

Figure 35. Measured *tke* as a function of the reference wind direction at a) dune foot (SA1); b) mid slope (SA2); and c) dune crest (SA3).

4.4.2. *r* – Dimensionless ratio of turbulent kinetic energy and wind speed

The dimensionless ratio *r* showed little dependence on wind velocity, except for velocities of 0-2 m.s^{-1} at the dune foot (SA1) and on the mid slope (SA2) (Figure 36a and Figure 36.b, respectively). Above 2 m.s^{-1}, *r* fluctuated mainly between 0.18 and 0.4 and the differences between the dune foot (Figure 36.a), the mid slope (Figure 36.b) were minimal, although *r* was overall 0.05-0.1 higher on the mid slope. There was more scatter at the dune crest (Figure 36.c) for wind velocities smaller than 10 m.s^{-1}. Overall, *r* was smallest on the dune crest. For wind velocities smaller than 2 m.s^{-1}, *r* was on average 0.28 with 10% quantile of 0.19 and 90% of 0.4 at the dune foot. at the mid slope *r* increased to 0.5 on average with 10% and 90% quantile of 0.29 and 0.84, respectively, whereas at the dune crest an average of 0.4 was found with 10% and 90% quantile of 0.23 and 0.49, respectively.

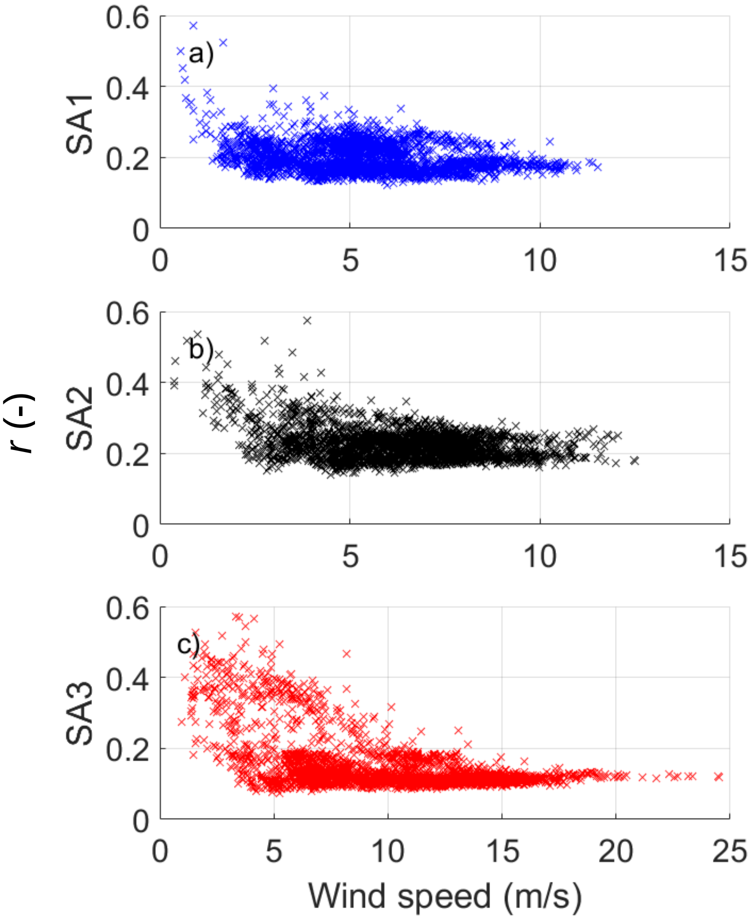

Figure 36. Dimensionless ratio *r* between square root of *tke* and wind speed for a) dune foot (SA1); b) mid slope (SA2); and dune crest (SA3). *(Note: maximum values are not included in Figure for better visualization).*

With flow across the foredune, *r* decreased and there were clear differences for varying wind directions (Figure 37). On the dune slope wind was seemingly more turbulent than at the dune crest and to some extent more turbulent than at the dune foot.

At the dune foot, *r* varied from 0.17 to 0.25 and was mainly above 0.2 (Figure 37.a; Table 5). At the mid slope, *r* was largest compared to the other stations and all wind directions lead to *r* above 0.2, except for oblique onshore winds from the south (Figure 37.b; Table 5). At the dune crest, *r* was smallest and only larger than 0.2 for highly oblique onshore winds from north and alongshore winds (Figure 37.c; Table 5). Onshore winds resulted in greatest *r* at the dune foot, while this occurred for alongshore winds on the dune slope and crest. At the dune foot and on the slope, *r* was twice as large as at the crest for onshore winds (-20° to 20°). Oblique onshore winds generated the smallest *r* at the dune foot and on the dune slope, whereas (perpendicular) onshore winds were associated with the smallest *r* at the dune crest. North and north-west winds had on average a higher *r* than south and south-western winds (ca. twice as often *r* > 0.2).

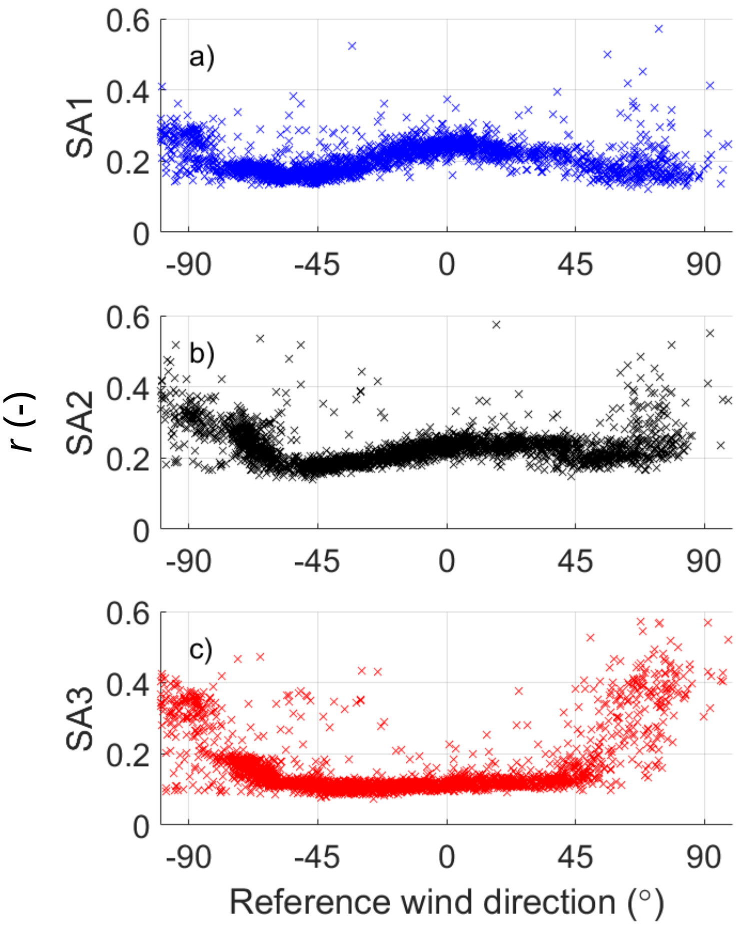

Figure 37. Dimensionless ratio *r* ($\sqrt{tke}/speed$) dependant on wind direction (°) at a) dune foot (SA1); b) mid slope (SA2); and c) dune crest (SA3). The wind direction -90° (south) and 90° (north) are dune parallel winds (i.e. alongshore), while 0° is perpendicular onshore.

Table 5. Averages of dimensionless ratio r ($\sqrt{tke}/speed$) for varying wind directions, categorised into perpendicular onshore, onshore, slightly oblique onshore, oblique onshore and highly oblique onshore as well as alongshore wind directions.

Wind direction		Mean *r*		
		Dune foot	Mid slope	Dune crest
Perpendicular onshore	-5° to 5°	0.25	0.23	0.12
Onshore (South)	-20° to -5°	0.23	0.22	0.11
Onshore (North)	20° to 5°	0.24	0.24	0.12
Slightly oblique onshore (South)	-35° to -20°	0.2	0.2	0.11
Slightly oblique onshore (North)	35° to 20°	0.22	0.24	0.13
Oblique onshore (South)	-55° to -35°	0.17	0.18	0.12
Oblique onshore (North)	55° to 35°	0.21	0.22	0.17
Highly oblique onshore (South)	-75° to -55°	0.17	0.24	0.15
Highly oblique onshore (North)	75° to 55°	0.2	0.27	0.32
Alongshore (South)	-75° to -90°	0.22	0.29	0.26
Alongshore (North)	75° to 90°	0.18	0.26	0.4

4.5. Sediment transport, morphology and vegetation

4.5.1. Sediment fluxes

Sand transport varied considerably both between catchers and days (Table 6.a, Figure 38 and Figure 39). The catcher just landward of the embryo dunes on the upper dune foot (C1.5) trapped the most sediment, while the catcher at the dune crest (C3, same height as SA3) caught the least sand.

Table 6. Mass fluxes of different catchers (C1; C1.5; C2 and C3) and different operation days (day 1: 5th October; day 2: 6th October; day 3: 11th October; day 4: 17th October and day 5: 25th October) and corresponding wind conditions during the operation time of sand catchers. a) Total mass fluxes (g.m^{-1}.s^{-1}) and mean fluxes per catcher (g.m^{-1}.s^{-1} and % relative to dune foot); b) Saltation height (cm); c) reference wind direction; d) average wind velocity; e) mean *tke* and f) mean *r*.

Catcher No.	Day 1	Day 2	Day 3	Day 4	Day 5		
Sand transport							
	a) Total mass flux in g.m^{-1}.s^{-1}					Mean mass flux g.m^{-1}.s^{-1}	%
C1	NA	10.93	30.16	6.73	1.61	12.35	100.0
C1.5	11.80	48.53	119.07	23.11	0.11	40.52	328.0
C2	1.64	0.74	7.69	0.30	0.03	2.08	16.8
C3	0.62	0.03	0.18	0.05	0.02	0.18	1.4
	b) Saltation height in cm for flux of 1 g.m^{-1}.s^{-2} ** height of maximum flux (maximum flux in g.m^{-1}.s^{-2})*					Mean height in cm *(including *)*	
C1	NA	18	20	10	13	15.5	
C1.5	24	38	37	16	*9.4* (0.09)*	29 *(25)*	
C2	*6.5* (0.07)*	*6.5* (0.3)*	60	*6.5* (0.16)*	*5.5* (0.03)*	60 *(17)*	
C3	6	0	*62* (0.07)*	*62* (0.07)*	0	6 *(43)*	
Corresponding wind conditions							
	c) Reference wind direction in ° (reference wind velocity in m.s^{-1})						
	26 (15)	46 (13.2)	-68 (14.3)	-41 (9.7)	-1 (8.7)		
	d) Wind speed at corresponding SA in m.s^{-1}					Corresponding SA	
C1	6.6	6.7	8	5.6	5.1	SA1	
C1.5			*11 (SA1.5)*			-	
C2	8.8	7.7	7.5	6.3	NA	SA2	
C3	15.7	11.2	11	10.5	9.7	SA3	
	e) *tke* at corresponding SA in m^{2}.s^{-2}						
C1	3.7	3.2	2.9	1.1	0.9	SA1	
C1.5			*1.9 (SA1.5)*			-	
C2	5.3	3.9	3.6	1.5	NA	SA2	
C3	6.8	3.6	4.1	1.4	1.3	SA3	
	f) *r* from corresponding SA dimensionless						
C1	0.28	0.24	0.2	0.17	0.19	SA1	
C1.5			*0.13 (SA1.5)*			-	
C2	0.26	0.22	0.24	0.18	NA	SA2	
C3	0.16	0.15	0.17	0.1	0.1	SA3	

The mass flux at the dune foot (C1) ranged from 1.6 $g.m^{-1}.s^{-1}$ (day 5) to 30.2 $g.m^{-1}.s^{-1}$ (day 3) and caught the second most sand with on average 12.35 $g.m^{-1}.s^{-1}$. Mass fluxes for the catcher at the upper dune foot (C1.5) ranged from 0.1 $g.m^{-1}.s^{-1}$ (day 5) to 119.1 $g.m^{-1}.s^{-1}$ (day 3). Mass fluxes for this catcher were the largest with on average 40.52 $g.m^{-1}.s^{-1}$. Only on day 5, the catcher on the dune foot (C1) indicated greater mass fluxes than C1.5. At the catcher on the dune slope (C2), mass fluxes ranged from 0 $g.m^{-1}.s^{-1}$ to 7.7 $g.m^{-1}.s^{-1}$ (day 5 and day 3, respectively). On the top of the dune (C3) mass fluxes were in the order of milligram and reached a maximum of 0.6 $g.m^{-1}.s^{-1}$ on day 1. Relative to the dune foot catcher (100%), the mass flux across the foredune increased to more than 300% just below the vegetation, subsequently dropping to 16.8% half way on the dune slope and reaching its minimum on the dune crest (1.4%). At the bare beach on day 3, transport fluxes were by up to a fourfold larger, namely 168% (lower beach), 238% (lower – mid beach) and 446% (upper beach).

The catchers also showed variations regarding the saltation height (Table 8.b). The saltation height ranged up to a maximum of 60 cm on the mid slope (C2, day 3), but was overall largest at the higher dune foot catcher C1.5 with on average of 29 cm (25 cm, when including the height of the maximum flux of 0.09 $g.m^{-1}.s^{-1}$ on day 5). At the dune foot (C1) an average of 15 cm was found, ranging from 10 – 20 cm (day 4 and day 3, respectively). Only on day 5, the saltation height at the dune foot (C1) was higher than at the upper foot (C1.5). The mid slope (C2) showed barely any transport, except for day 3. A transport of 1 $g.m^{-1}.s^{-2}$ was only reached once at the dune crest (C3) at 6 cm above ground. On day 3 and day 4, the maximum values (0.07 $g.m^{-1}.s^{-1}$) were found in the uppermost trap at 62 cm above ground. Saltation height on the bare beach was similar to the dune foot catchers at approximately 25 cm. Differences were also found between measurement days. At the dune foot, saltation height was largest on day 2 and day 3. During the five transport events, different wind conditions prevailed (Table 8.c-f). Wind directions were slightly oblique onshore and oblique onshore from north on day 1 and 2, respectively, highly oblique onshore and oblique onshore from south on day 3 and 4, respectively and perpendicular onshore on day 5 (Table 8.c). At the dune foot (C1) wind velocity during transport events ranged from 5 – 7 $m^{-1}.s^{-1}$, on the mid slope (C2) from 7 – 9 $m^{-1}.s^{-1}$ and at the dune crest from 12 – 16 $m^{-1}.s^{-1}$ (Table 8.d). The *tke* was largest in absolute values on the mid slope and dune crest and ranged from 0.9 – 6.8 $m^2.s^{-2}$ (Table 8.e). The dimensionless ratio *r* was largest on the mid slope and the dune foot and ranged from 0.1 on the crest to 0.28 on the foot (Table 8.f).

On day 3 (Figure 38), data of an additional SA was available at the height of C1.5 (upper dune foot), which indicated a wind speed of 11 $m.s^{-1}$, a *tke* of 1.9 $m^2.s^{-2}$ and *r* was therefore 0.13.

A decrease of transport with height was observed for all catchers but on the crest. Both catchers at the dune foot showed a clear decrease of trapped sand with height. On the mid slope (C2) the decrease was less rapid. On the dune crest (C3) trapped sand increased with height on day 2, day 3 and day 4 (Figure 39.c) and decreased with height on day 1 (Figure 39.a) and day 5 (Figure 39.d). However, on day 1 the uppermost bottle caught more sand than the subjacent one. For all catchers, the uppermost trap had negligible transport: the maximum was found at the mid slope (C2) on day 3 with 0.9 $g.m^{-1}.s^{-2}$.

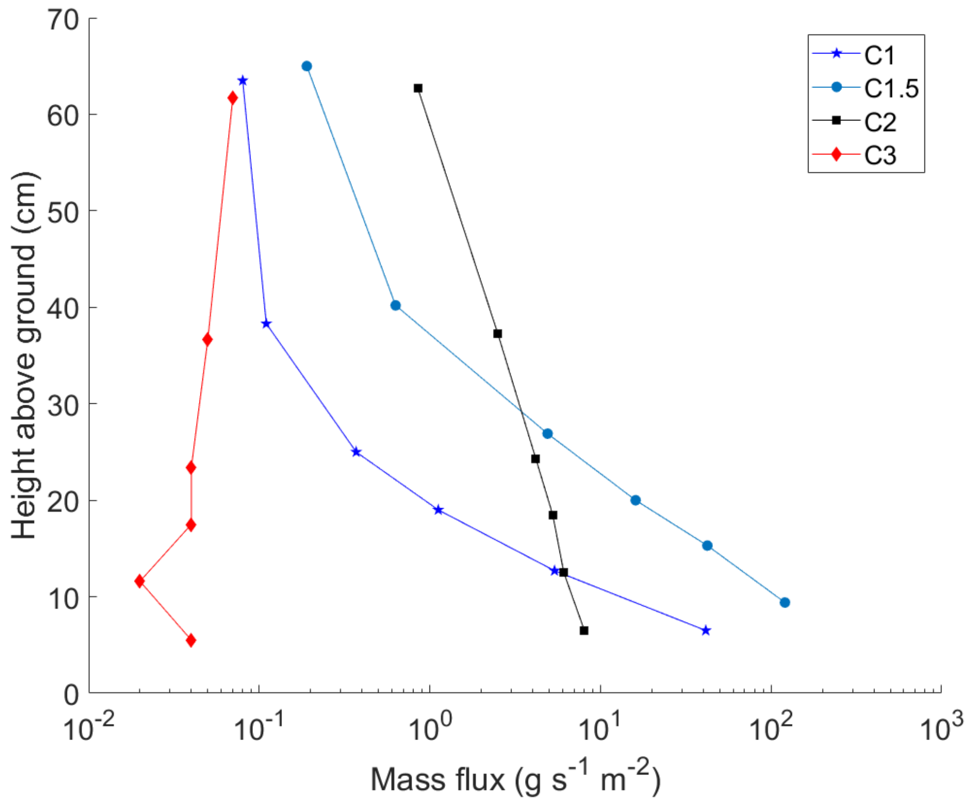

Figure 38. Sand transport as mass flux per height across the foredune on day 3 (11^{th} October) for dune foot (C1), upper dune foot (C1.5), mid slope (C2) and dune crest (C3).

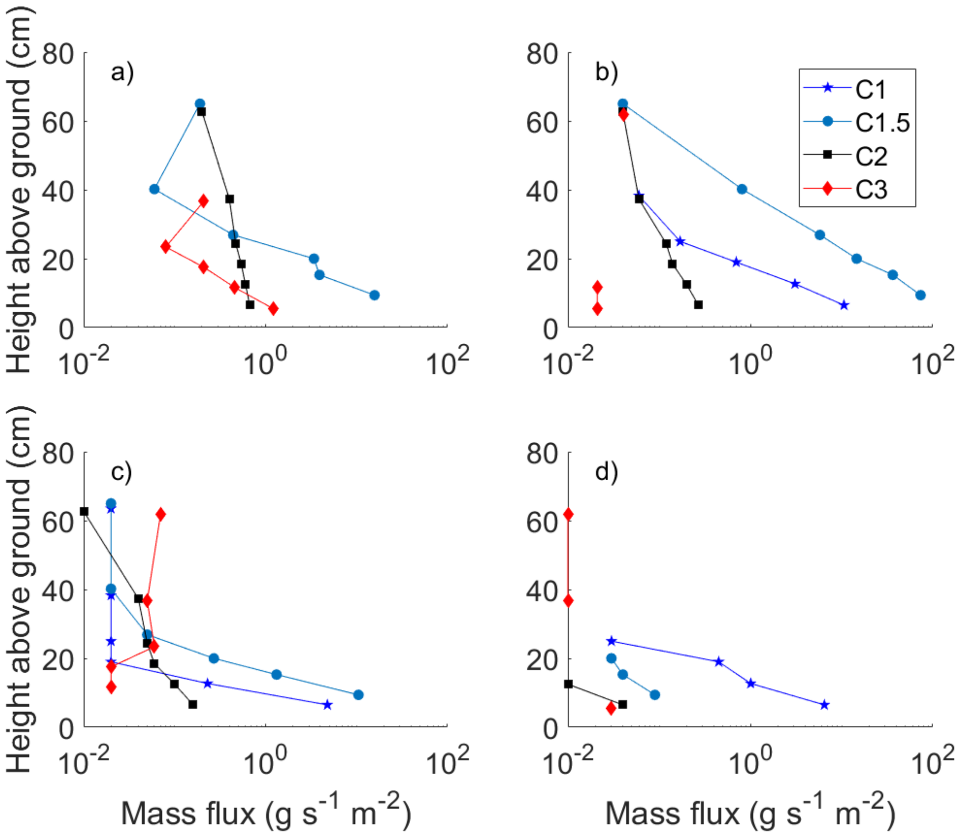

Figure 39. Sand transport as mass flux per height across the foredune on a) day 1 (5th October); b) day 2 (6th October); c) day 4 (17th October); and d) day 5 (25th October) for dune foot (C1), upper dune foot (C1.5), mid slope (C2) and dune crest (C3).

4.5.2. Grain size distribution

Grain size distribution of bed sediment in the cross-shore direction showed a decreasing trend both from shore landwards and with increasing elevation (Figure 40). The grain size distribution of trapped sand showed this trend as well. However, the smallest grain size was found at approximately 2.5 m above NAP (at - 30 m cross-shore), both for sand on the beach (217 µm) as well as for trapped sand (212 µm). This is approximately the height where embryo dunes were found south of the study transect (3 – 5 m above NAP). For the beach dune profile, grain sizes ranged from medium, well sorted sand and symmetrical distributed (most seaward intertidal area) to fine sand, which was very well sorted and coarse skewed (dune crest) with a median (d50) of 307.2 µm to 229.5 µm, respectively. The mean grain size of the profile was 257 µm. All of the trapped sand was very well sorted and coarse skewed.

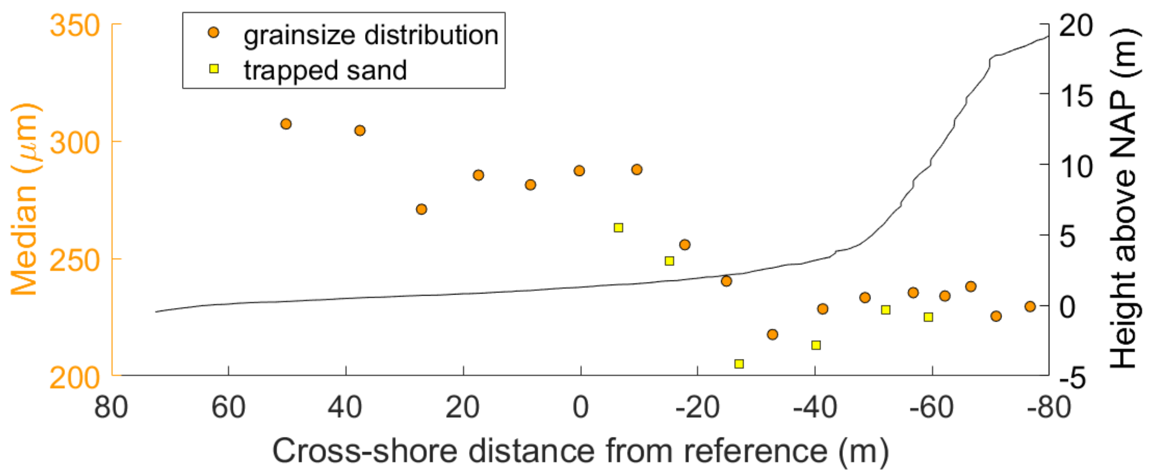

Figure 40. Grain size distribution for beach dune profile as well as trapped sand from sand catchers.

4.5.3. Morphology

The volume change during the study period was positive for all transects. The least change in volume occurred at the main study transect (41.0), while the largest volume change took place at 41.25. The foredune along the main study transect from dune foot to dune crest gained a total volume of 0.58 m^3, leading to a deposition of 0.012 $m^3.m^{-1}$. Transect 41.25 had a total gain of 2.77 m^3 and consequently a deposition of 0.079 $m^3.m^{-1}$. Transect 41.5 gained 0.054 $m^3.m^{-1}$ and 1.87 m^3 in total from the dune foot to the crest. The elevation change varied both across the foredune and for each transect (Figure 41). However, all transects showed sediment accumulation around the dune foot. At transect 41.0 accretion and erosion alternated (Figure 41.a). A positive change at the dune foot to a maximum of 17 cm (-35 to -46 m) was followed by erosion of 10 cm at the upper dune foot (-46 to -53 m). Subsequently, sand accumulated up to 13 cm on the lower slope (-53 to -60 m) and there was a small positive change of approximately 5 cm on the upper slope (-60 to -70 m). The foredune underwent erosion of up to 31 cm at the dune crest (-70 to -75 m). At transect 41.25 (Figure 41.b) most accretion occurred at the lower dune foot (-30 to -42 m) with 33 cm and up to 9 cm on the foredune slope (-52 to -65 m). Erosion of a maximum of 5 cm occurred on the lower slope (-49 to -52 m). At transect 41.5 (Figure 41.c) sand accretion of up to 28 cm occurred at the dune foot (-22 to -33 m) and approximately 5 cm eroded on the lower slope (-35 to -38 m). The upper slope and the foredune crest (-43 to -50 m) eroded up to a maximum of 21 cm.

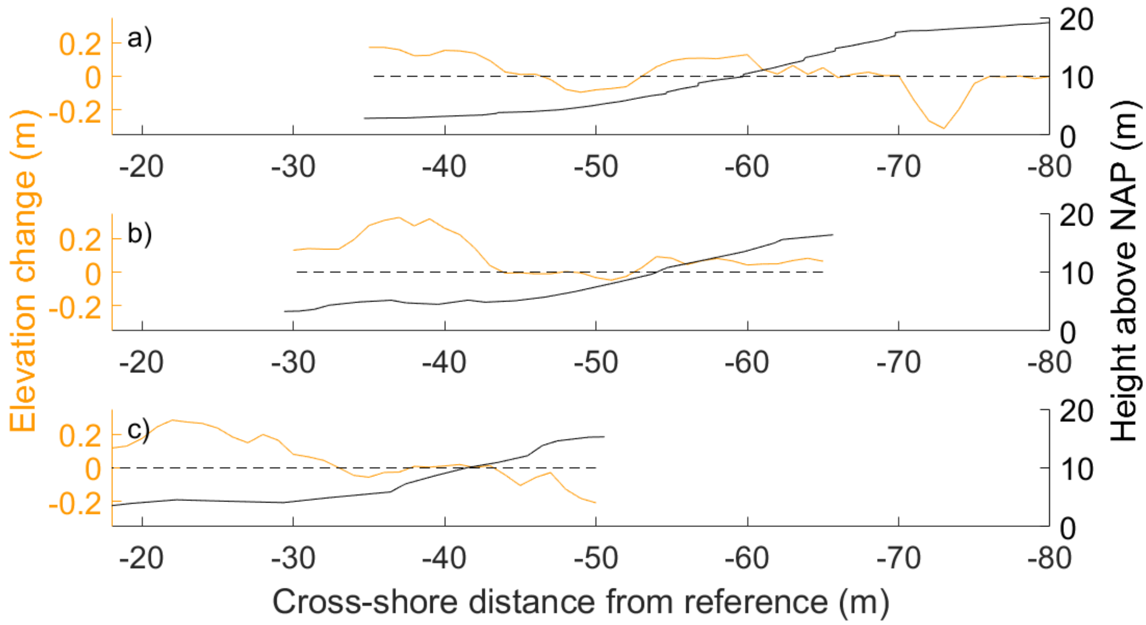

Figure 41. Elevation change (accretion and erosion) in metres during the study period and foredune profiles of a) 41.0; b) 41.25 and c) 41.5. Striped line shows the reference line of 0 m elevation change.

4.5.4. Vegetation

While the main study transect did not have an embryo dune on its seaward side, the two additional profiles (41.25 and 41.5) had a vegetated embryo dune in front of the dune foot at --32 to -42 m and 18 to -28 m cross-shore distance from reference, respectively (Figure 42). At the main study transect, all of the most common species were observed (marram grass, sand couch, lesser hawkbit and sea rocket). At all transects sand couch grass was the dominant species around the dune foot up to 6.9 m above NAP for transect 41.0, 5.3 m and 4.4 m above NAP for 41.25 and 41.5, respectively. A dense cover of marram grass followed on the lower and upper foredune slope and crest. The vegetation cover on the foredune varied amongst transects (Figure 42). Photographs can be found in Appendix 8.2. The vegetation cover for transect 41.0 was the greatest on the dune crest (100%). A coverage of 67% and 27% were observed at the dune crest of transects 41.25 and 41.5, respectively. Transects 41.0 and 41.25 showed more similarity than transect 41.5, with regards to both vegetation cover and dune profile. Maximum vegetation cover at transects 41.0 and 41.25 was found at the crest, while for transect 41.5 a maximum of 54% was found on the mid slope, whereas the crest was less densely covered. Transects 41.25 and 41.5 both had a vegetated embryo dune (1 - 8%) at 3 – 5 m above NAP, followed by a bare upper dune foot, while the main transect only had a bare dune foot. All three transects were vegetated on the slope (20 - 70%), ranging between approximately 7 – 16 m above NAP. Vegetation cover was only greater (95 - 100%) for transect 41.0 at 18 m above NAP.

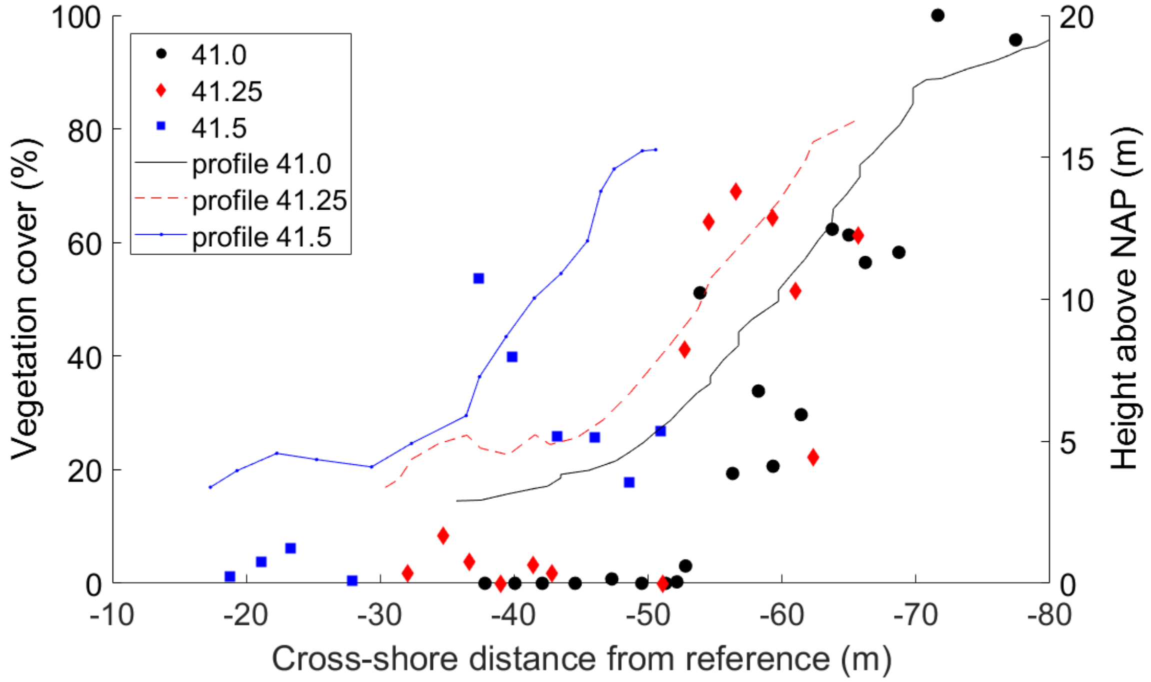

Figure 42. Vegetation cover in percentage of each profile, marked as dot for transect 41.0 (black), diamond for 41.25 (red) and square for 41.5 (blue)

4.5.5. Spatial variation of vegetation cover and morphology

The spatial variation of the vegetation cover varied with height above NAP at each transect (for details see section 4.5.4) and will be compared with changes in elevation throughout the field campaign. Overall, a vegetation cover of 0 – 10% was found at 3 - 6 m above NAP, 20 – 70% at 7 – 17 m above NAP and more than 95% at 18 m above NAP.

At transect 41.0 (Figure 43.a) positive and negative elevation changes occurred at 0% vegetation cover at the dune foot. With increasing height of the foredune (6 – 10 m +NAP) an increasing vegetation density (20 – 51%) was observed to a maximum sand deposition of 13 cm. Above 12 m NAP the vegetation cover stayed steady at approximately 60% and was associated with a smaller elevation increase of 5 cm. A vegetation cover of 95% (or more) occurred simultaneously with maximal erosion at 18 m above NAP. At transects 41.25 and 41.5 (Figure 43.b and Figure 43.c, respectively) a vegetation cover of 1 – 10% and maximum sand deposition were observed at the embryo dune at 5 m and 4 m above NAP, respectively. At 6 – 7 m above NAP there was no vegetation and no or a negative elevation change (0 – 5 cm). For transect 41.25 vegetation cover stayed steady at approximately 60% and was associated with small elevation increases. An area of little vegetation (22%) at 15.5 m above NAP did not alter the positive sedimentation trend. At transect 41.5, increasing height above NAP did not lead to an increased vegetation cover and was associated with erosion from up 11 m above NAP.

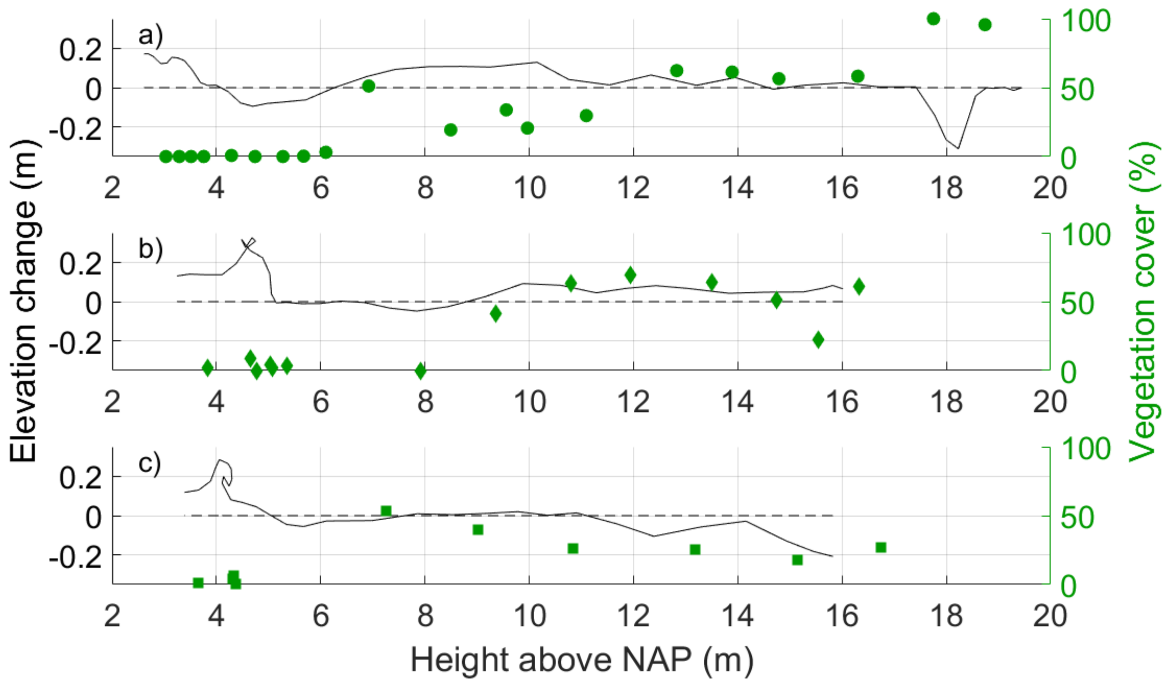

Figure 43. Elevation change and vegetation cover as a function of height above NAP in metres for transects a) 41.0; b) 41.25 and c) 41.5

4.5.6. Relationship between vegetation cover, morphology and mean transport

For the main study transect (41.0) the relationship between vegetation cover and elevation change (Figure 44.a) as well as sand transport (Figure 44.b) could be assessed. At the bare dune foot, relatively large sand transport was recorded, together with a positive elevation change. On the upper dune foot, just below the vegetation (at -52 m distance from reference), the largest sand transport was found with 305% but at the same time erosion was observed. On the dune slope the vegetation cover increased and the mass flux decreased to 16.8%, while elevation increased by 13 cm. At the dune crest where the vegetation cover was 100%, hardly any sand transport was observed (C3), while there occurred the most erosion.

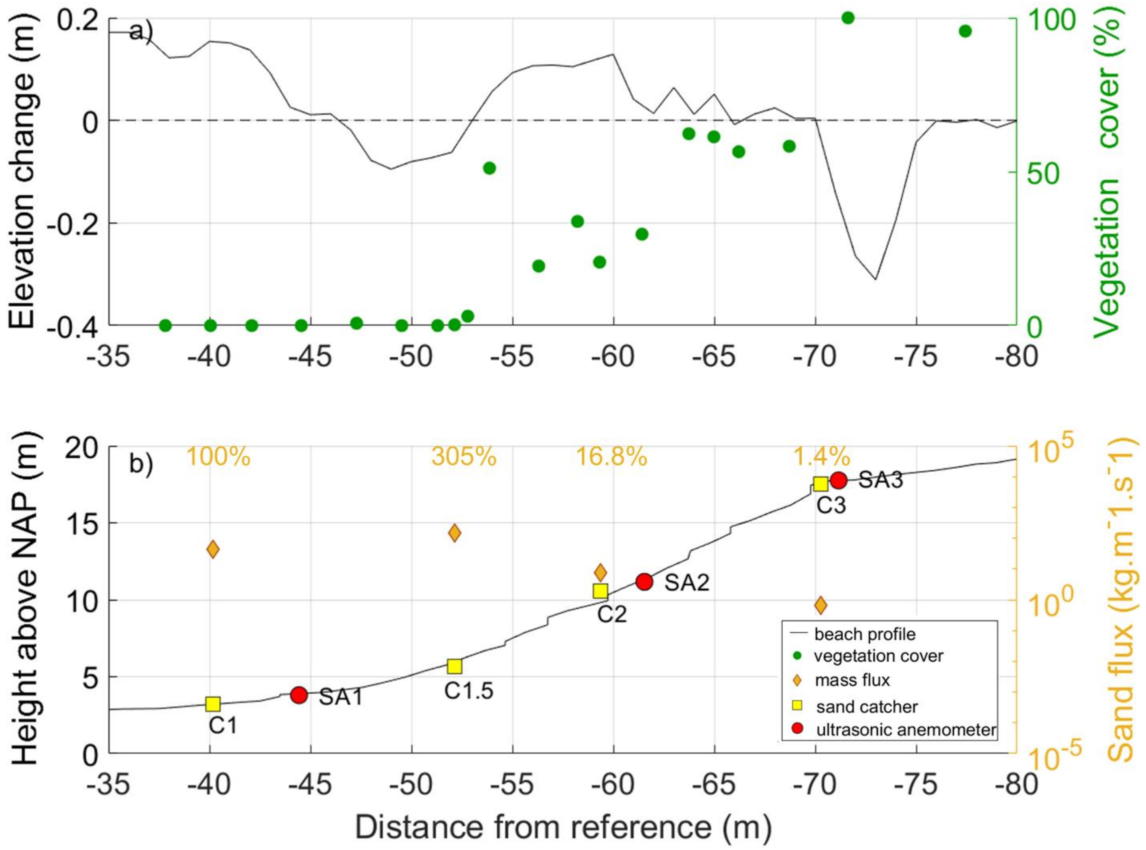

Figure 44. Relationship between mean sand transport, vegetation cover and morphology for main study transect 41.0 with a) vegetation cover (%) and elevation change (m); b) sand flux (kg.m^{-1}.s^{-1}) and dune profile with position of sand catchers (Cs) and ultrasonic anemometers (SAs)

4.5.7. Summary table of results

Table 7. Summary of findings about effects of vegetated foredune on air flow patterns and transport fluxes under various wind conditions.

Wind velocity		**Incipient wind direction & deflection**		**Transport & dune accretion**	**Dune properties**
Ø at: Reference: 10.2 m.s^{-1} Dune foot: 4.7 m.s^{-1} Mid slope: 5.5 m.s^{-1} Dune crest: 8.6 m.s^{-1} Max at: Reference: 23.7 m.s^{-1} Dune foot: 11.5 m.s^{-1} Mid slope: 12.5 m.s^{-1} Dune crest: 24.5 m.s^{-1} *In general: Flow stagnation at dune foot, streamline compression and acceleration toward crest.*		All onshore wind directions covered. *In general: alongshore deflection at dune foot and crest-normal deflection toward crest.*		Average sand fluxes: dune foot: 100% (12.35 g.m^{-1}.s^{-1}), upper dune foot: 328% (40.52g.m^{-1}.s^{-1}), slope: 16.8% (2.08 g.m^{-1}.s^{-1}), crest: 1.4% (0.18 g.m^{-1}.s^{-1}). Stoss site growth of main transect : total of 0.58 m^{3} (50 m) ; 0.012 m^{3}.m^{-1} Stoss site growth of transect 41.25: total of 2.77 m^{3} (35 m); 0.079 m^{3}.m^{-1} Stoss site growth of transect 41.5: Total of 1.87 m^{3} (35 m); 0.054 m^{3}.m^{-1}	Main study transect: 23 m high, steep slope of 27° and densely vegetated by marram grass (*Ammophila arenaria*). Transect 41.25: 17 m high, steep slope of 21° with max 69% cover of marram grass. Transect 41.5: 15 m high, steep slope of 19.5° with max 54% cover of marram grass.
Acceleration 170% to 200%	9.7 m.s^{-1} (foot: 5.6 m.s^{-1}, slope: 6.3 m.s^{-1}, crest: 10.5 m.s^{-1})	oblique onshore winds: deflected alongshore at foot (up to 30°), crest-normal at crest (7-24°)	-41° (SW)	C1: 6.73 g.m^{-1}.s^{-1}, C1.5: 23.11 g.m^{-1}.s^{-1}, C2: 0.3 g.m^{-1}.s^{-1} , C3: 0.05 g.m^{-1}.s^{-1}	
	13.2 m.s^{-1} (foot: 6.7 m.s^{-1}, slope: 7.7 m.s^{-1}, crest: 11.2 m.s^{-1})		46° (NW)	C1: 10.93 g.m^{-1}.s^{-1}, C1.5: 48.53 g.m^{-1}.s^{-1}, C2: 0.74 g.m^{-1}.s^{-1}, C3:0.03 g.m^{-1}.s^{-1}	
Acceleration 280% to 310%	8.7 m.s^{-1} (foot: 5.1 m.s^{-1}, slope: NA, crest: 9.7 m.s^{-1})	perpendicular onshore: deflected alongshore at foot (up to 10°), steered back to crest-normal at crest	-1° (W)	C1: 1.61 g.m^{-1}.s^{-1}, C1.5: 0.11 g.m^{-1}.s^{-1}, C2: 0.03 g.m^{-1}.s^{-1}, C3: 0.02 g.m^{-1}.s^{-1}	
	15 m.s^{-1} (foot: 6.6 m.s^{-1}, slope: 8.8 m.s^{-1}, crest: 15.7 m.s^{-1})		26° (WNW)	C1: NA, C1.5: 11.8 g.m^{-1}.s^{-1}, C2: 1.64 g.m^{-1}.s^{-1}, C3: 0.62 g.m^{-1}.s^{-1}	
Acceleration 130% (SSW) Deceleration 80% (NNW)	14.3 m.s^{-1} (foot: 8 m.s^{-1},upper foot: 11 m.s^{-1}, slope: 7.5 m.s^{-1}, crest: 11 m.s^{-1})	Highly oblique winds	-68° (SSW)	C1: 30.16, C1.5: 119.07 g.m^{-1}.s^{-1}, C2: 7.69 g.m^{-1}.s^{-1}, C3: 0.18 g.m^{-1}.s^{-1}	
Deceleration 70% to 80%		Alongshore winds (-80 to -90° and 80-90°)		NA	

5. Discussion

5.1. Wind velocity

A large range of wind velocities and directions were measured throughout the field campaign at Egmond aan Zee. Comparing the wind velocity at the dune foot (SA1) with the reference station showed clearly a flow reduction at the dune foot especially for perpendicular or slightly oblique onshore winds. For highly oblique and alongshore directed winds, the least deceleration at the dune foot was found compared to the reference station. These findings were expected as they were described by Walker *et al.* (2017), studying flow form interactions across a foredune. For all winds that were onshore (-80° to 80°), the wind speed increased (i.e. wind accelerated) across the foredune. The increase was on average 170% and reached up to 310% between the dune foot and the dune crest. The scale of increase varied for different wind conditions. The acceleration across the foredune was seemingly not dependent on the initial wind speed at the dune foot. Only for wind velocities smaller than 2 $m.s^{-1}$, a greater acceleration than for other wind velocities was noticeable on the upper slope (SA2 to SA3), which might be due to a steeper slope of the upper half of the dune. However, a clear relationship was found between the wind acceleration and the incipient wind direction (based on the reference wind direction). Generally, the more the incipient wind was directed perpendicular onshore, the greater the acceleration across the foredune. With increasing obliquity, the acceleration decreased. This is in agreement with previous studies, which also found that: the more onshore, the larger the acceleration (Arens, Van Kaam-Peters and Van Boxel, 1995; Walker *et al.*, 2006). The acceleration for onshore winds could be most likely attributed to flow compression as commonly stated amongst literature (Arens, Van Kaam-Peters and Van Boxel, 1995; Arens, 1996; Hesp *et al.*, 2005; Walker *et al.*, 2009; Bauer *et al.*, 2012; Chapman *et al.*, 2013). A shift from oblique onshore (-45° and 45°) to more perpendicular onshore (< 22°) winds resulted in higher flow acceleration of 50 – 100%. This is larger than the suggested 25% increase by (Hesp *et al.*, 2015) using a CFD model. The larger acceleration of this study could be because of the higher dune with 25 m compared to 10 m used in the model. The doubling in dune height could be an explanation for a more pronounced streamline compression and accordingly higher acceleration for onshore winds. However, other findings showed that the magnitude of acceleration (ca. 150%) were of the same order for a dune of 10 m and 23 m, which was attributed to an increased roughness and deflection of flow (Arens, Van Kaam-Peters and Van Boxel, 1995). The authors measured the wind flows however higher than the 0.9 m used in this study and over a dune with a steepness of approximately 1:5. Considering the large speed up across the foredune in Egmond, there was little effect of increased roughness and flow deflection seemed not to reduce the acceleration. The steep foredune slope of 1:2 could have been responsible for this. The flow compression was largest on the upper half of the foredune since the wind speed ratio from mid slope to the dune crest (SA2 to SA3) was larger than form dune foot to mid slope (SA1 to SA2). Additionally, there was a small asymmetry between wind directions from north and south. For highly oblique northwest winds (60-80°) a decrease of 20% was found, while this did not occur with southwest winds. Purely alongshore winds from south showed a decrease of wind velocity of 20% and alongshore winds from north 30%. The lessening of acceleration for increasingly oblique wind flows is in agreement with the CFD model results of Hesp (2015) as well as findings of Walker *et al.* (2017), who showed that wind velocity can decrease for highly oblique wind flows (more than 60°).

No clear effects due to the vegetation cover across the dune could be detected. Through in situ experiments and CFD modelling a comparison at the same dune profile and under the same wind configurations with and without vegetation could resolve this. Without this comparison, the findings of this study imply that the acceleration effect due to the dunes' topography outweighed the decelerating effects due to increased roughness owing to vegetation. This is commonly observed (Arens, Van Kaam-Peters and Van Boxel, 1995; Hesp *et al.*, 2005; Walker *et al.*, 2009) and was according to expectations.

5.2. Wind direction

The wind direction changed across the foredune. In general, steering to a more alongshore flow was detected at the dune foot (SA1) relative to the reference. Subsequently the wind turned back towards the initial direction on the lower slope (SA2) and was eventually steered to more perpendicular onshore direction on the upper slope (SA3). Deflection angles varied vastly and were not clearly dependent on the initial wind velocity, although velocities (at all positions of the dune) lower than 5 $m.s^{-1}$ displayed a larger range of wind deflection and underwent the largest deflection in absolute terms. This occurrence might be attributed to more turbulent characteristics of wind flows with smaller wind velocities. At the dune foot steering was on average 10° but could be up to 100°, which is similar to the maximum values of 90° found in earlier studies for similar foredunes (Arens, Van Kaam-Peters and Van Boxel, 1995).

The deflection was clearly dependant on the initial wind direction. Oblique onshore wind directions at incident angles of 30 - 70° showed the greatest deflection across the dune toward crest-normal. This range of wind directions is widely demonstrated to cause the most deflection in previous studies (Walker *et al.*, 2017). Topographic steering on the dune was 14° on average to more crest-normal and by as much as 38° for oblique flows (relative to reference). Highly oblique onshore winds were less deflected when approaching from south, while highly oblique and alongshore flows from north were also strongly deflected. The observations for the southern winds (maximum deflection for oblique onshore winds) are in agreement with previous studies (Arens, Van Kaam-Peters and Van Boxel, 1995; Bauer *et al.*, 2012; Hesp *et al.*, 2015; Walker *et al.*, 2017). The magnitude of deflection for the northern winds is similar to findings by Walker *et al.* (2009), who observed 35° for alongshore flows and 29° for oblique flows. Since the wind steered back toward crest-normal from the previous alongshore deflection at the dune foot, the differences between foot and crest were even more pronounced. There were furthermore differences in the magnitude of deflection for same incident wind angles of northern and southern direction. Northern winds were steered stronger to the alongshore at the dune foot, while southern winds were deflected stronger to crest-normal at the dune crest. On the mid slope, northern winds were still more alongshore relative to the reference direction, while this was not the case for southern winds. Since the wind directions were rotated, taking into account the inclination of the coastline, the asymmetry of deflection for winds approaching from the north and south could be due to a deviation of the coastal orientation from the applied 8° inclination from north, which were based on previous studies in the area (van Duin *et al.*, 2004). Also the effect might be attributed to the local topography of the dune and the beach dune profile. As south of the dune foot (in proximity of SA1), embryo dunes were found, this might have altered the wind flows beforehand, which was not the case for northern winds.

5.3. Turbulent kinetic energy

There was an increase of absolute *tke* with increasing wind velocities with values up to 3.5 $m^2.s^2$ at the crest for velocities above 15 $m.s^{-1}$. This is similar to observations of Hesp *et al.* (2013), who found a *tke* of 1.8 - 3.4 $m^2.s^2$ for velocities of 8 - 15 $m.s^{-1}$, respectively. But relative to the wind velocity, the *tke* decreased as a result of acceleration and streamline compression of wind flows across the dune toward the crest. This was studied by means of the dimensionless *r*. The trend of the reduced *r* on the crest was expected, on the basis of earlier studies (Chapman *et al.*, 2013). That the largest *r* was found for the station at the mid slope however was against expectations since the deceleration of wind flows at the foot theoretically enhances turbulence (Chapman *et al.*, 2013). Calculating *r* for the results of Chapman *et al.* (2013) revealed that it was largest for smaller wind velocities (4 – 7.5 $m.s^{-1}$) and greater at the dune foot. The velocity range was comparable with the velocity range of this study of 1 – 7.5 $m.s^{-1}$ resulting in largest *r*. Similar to the asymmetry of changes in wind speed and direction, the turbulent flows, were not symmetrical for the same inclination angles but with different approaching wind directions: When wind originated from northern directions *r* was larger than for the same southern directions. This is most likely because northern winds are inherent more turbulent. This was derived from available wind gust data and seemed sound since wind gusts are related to *tke* (Kumer *et al.*, 2016) and thus also *r*. Comparing the wind gust data revealed that mean and maximum gusts for northern onshore winds were larger than for southern onshore winds for all three ultrasonic anemometers of the dune (Table 8). The northern winds are hence less stable, resulting in the observed asymmetry for wind approaching at same incident angle from north and south.

Table 8. Wind gusts (mean and maximum values) in $m.s^{-1}$ that could explain the larger *tke* and *r* for northern onshore winds compared to southern onshore winds.

	SA1		SA2		SA3	
	S	N	S	N	S	N
mean	7.83	8.46	8.61	9.57	11.94	13.07
max	17.52	18.16	16.62	18.53	25.94	29.28

The findings of larger *tke* and *r* on the mid slope (SA2) than at the dune foot (SA1), might be a result of vegetation induced turbulences. Although, difficult to quantify and distinguish from topographically caused turbulences, it can play an important role (Walker *et al.*, 2006; Chapman *et al.*, 2012). Since vegetation is absent at the dune foot, but present on the mid slope, vegetation cover might therefore be responsible for these findings. Another factor could have been the wind direction that was still turning back to more crest-normal on the slope. At the crest the wind became possibly more streamlined than on the slope, resulting in smaller relative turbulences.

5.4. Sediment transport, morphology and vegetation

5.4.1. Sand fluxes across the foredune

Sand catchers were placed whenever wind velocities were forecasted to be above 10 $m.s^{-1}$. This was defined as threshold velocity for aeolian transport and was approximately accurate. Yet transport events were observed for wind speeds below it with a reference wind speed that ranged from 8.7 – 15 $m.s^{-1}$. Overall fluxes varied considerably and decreased rapidly with dune height as well as across the foredune. These findings are in accordance to on available literature (Arens and van der Lee, 1995; Arens, 1996; Christiansen and Davidson-Arnott, 2004; Petersen, Hilton and Wakes, 2011). Across the foredune from foot to crest, sand fluxes decreased on average by 99%. Petersen, Hilton and Wakes (2011) observed a decrease by 71% (of trapped sand at 0.5 m above ground) over the stoss face to the crest, which would be similar to comparing the mid slope catcher (C2) with the dune crest catcher (C3). For the transport at approximately 0.5 m above ground, a reduction of 40 - 98% was observed, but sand caught at this height was in the order of milligrams or less, therefore not very reliable to compare. The total flux reduction between the two catchers was 92%. Sand fluxes measured by Davidson-Arnott *et al.* (2012) were of similar magnitudes than our study with only the flux on the slope being contradictory. Sand fluxes at the Greenwich Dunes ranged from 19.2 – 72.6 $kg.m^{-1}.h^{-1}$ at the beach and 0.09 $kg.m^{-1}.h^{-1}$ and 0.57 $kg.m^{-1}.h^{-1}$ on the slope and crest, respectively. At the dune foot in Egmond fluxes ranged from 44.46 $kg.m^{-1}.h^{-1}$ (C1) to 145.87 $kg.m^{-1}.h^{-1}$ (C1.5) and on the slope (C2) and crest (C3) 7.49 $kg.m^{-1}.h^{-1}$ and 0.65 $kg.m^{-1}.h^{-1}$ were measured, respectively.

5.4.2. Saltation height

The saltation height was variable and ranged from 10 – 38 cm above ground at the dune foot and was on average 15.5 cm and 29 cm for C1 and C1.5, respectively. The commonly specified height of 25 – 30 cm for aeolian transport (Horikawa and Shen, 1960; Arens and van der Lee, 1995) was found at the beach with 25 cm. Saltation was limited to the dune foot, except for one transport event (day 3), where larger sand fluxes reached the mid slope (C2) at 60 cm above ground. The increase in saltation height on the lower and upper slope and a less sharp decline of transport with height was previously observed by Arens and van der Lee (1995). Although aeolian transport in suspension or modified saltation was not measured, it was possibly observed in situ on the dune crest, since sand would reach ones face standing up and it is commonly suggested to be the main transport form at the dune crest (Petersen, Hilton and Wakes, 2011; Hesp *et al.*, 2013; Keijsers, De Groot and Riksen, 2015).

5.4.3. Dissimilarities between days

The different transport events had varying wind velocities and directions, but generally the wind direction seemed to play a larger role for sand transport than wind velocity. Greater wind velocities (above 13 $m.s^{-1}$) together with obliquity of the approaching wind caused more sand transport and resulted also in higher saltation heights. Another aspects that needs to be considered is the moisture content of the beach, since it can influence the aeolian transport considerably (Bauer and Davidson-Arnott, 2003; Duran and Moore, 2013; Davidson-Arnott *et al.*, 2018). If comparing the tide between the different days there were quite some differences (Figure 45).

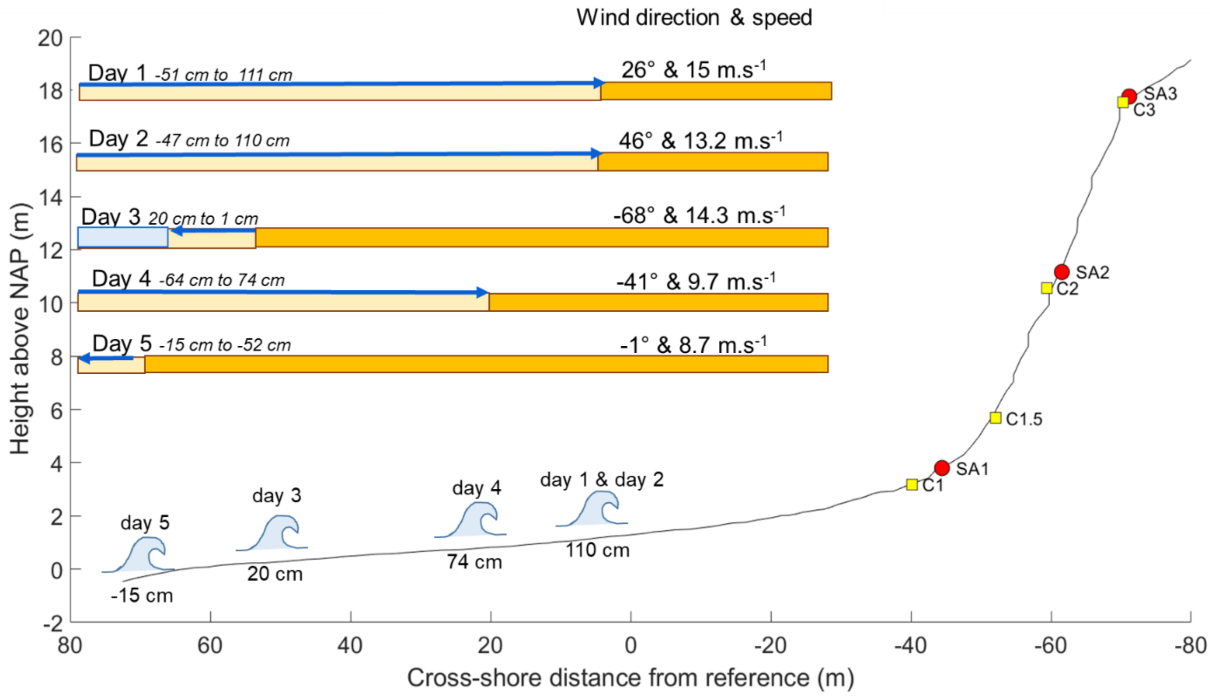

Figure 45. Beach width, based on tidal elevation (above NAP) for different days. Wave symbols show the tidal elevation that was reached on the day. Bars show the beach width that was submerged in blue that was under tidal influence (falling or rising tide) in yellow; and the width that stayed entirely dry in orange. Respective wind direction and wind speed (both measured at reference station) are indicated.

While the tide was rising on day 1, day 2 and day 4 during the measurements of sand fluxes, it was falling on day 3 and day 5. When sketching the tidal elevation of each day, it can be seen that the beach width that stayed dry was considerably wider for some days. On day 3, the water level was 50 cm lower (relative to NAP) and on day 5 more than 1 metre. Since the beach profile is gentle (1:40), a difference of water level height of 50 – 100 cm reduced potentially the maximum. The wind speed was somewhat larger on day 1 (15 m.s^{-1}) than day 2 (13.2 m.s^{-1}) with accordingly larger *tke* and *r* across the dune, but transport was less on day 1 than on day 2 (Table 6). At the dune foot (C1), the oblique winds (day 2) caused larger transport, while on the foredune (C2 and C3), transport was greater for more crest-normal wind flows (day 1). This might be attributed to the cosine and fetch effect as described by Bauer and Davidson-Arnott (2003). The maximum fetch was larger for day 2, since wind approached more oblique than on day 1. This resulted in a transport increase for the dune foot catchers, while catchers on the dune experienced a transport decrease due to the cosine effect (due to deflection). During the transport event on day 3, the greatest sand flux was registered. The wind direction was highly oblique onshore from the south (-68°) and the reference wind velocity was 14.3 m.s^{-1}. The link between the highly oblique wind direction and the large maximum fetch due to the low tidal levels could explain the large transport fluxes on day 3. Transport was smallest for day 5 with perpendicular onshore winds but also with smallest velocities (8.7 m.s^{-1}). On day 2 and day 4, at similar incident angle (46° and -41°, respectively), the wind velocity and *tke* were most likely the controlling factor for transport out of the measured parameters. They had approximately the same size of beach when measurements started, but a larger wind speed of 3.5 m.s^{-1} was associated with approximately doubled transport fluxes.

In no previous studies, such large differences between two dune foot catchers were observed, yet differences between C1 and C1.5 were considerable in Egmond (100% and 328%, respectively). Arens and van der Lee (1995) found that saltation height increases for a catcher on the upper slope (Figure 46, dark green curve) compared to the lower slope (Figure 46, light green), the total transport fluxes were however still smaller on the catcher on the lower slope (exact values unknown). The saltation height was only once higher at the dune foot (C1) than at the upper dune foot (C1.5) for perpendicular onshore winds, while the total transport fluxes were at all times higher at C1.5 than C1. For day 3, an in-depth comparison was possible between the two catchers on the dune foot (C1 and C1.5), because an additional ultrasonic anemometer was available (SA1.5). Since for all days, mass fluxes were greater on the upper dune foot (C1.5) than on the lower dune foot (C1) it was of particular interest to assess differences. Comparing the wind conditions for the two catchers showed that the wind magnitude at the upper catcher was somewhat larger with 11 m.s^{-1} compared to 9 m.s^{-1}. The *tke* was larger for C1 than C1.5 (2.9 m^2.s^{-1} and 1.9 m^2.s^{-1}, respectively), leading to a greater *r* at the lower dune foot (C1). From the available data, the greater wind speed at C1.5 was the only parameter that could have led to the larger mass flux of nearly fourfold. Possibly, the turbulent flows at the dune foot might (partly) be responsible for the transport through a zone of flow stagnation found in previous studies (Weaver and Wiggs, 2011; Chapman *et al.*, 2013). The large transport at C1.5 could however also be due to effects of the attached and deflected flow model as defined by Bauer *et al*. (2012) (Figure 47). The model suggests the occurrence of a strong alongshore flow vector at the base of the stoss slope. This wind flow develops under oblique onshore wind conditions and can potentially drive large sediment transport fluxes (Bauer *et al.*, 2012). Since sand catcher C1.5 was closer to the steep slope than C1, it is more likely to have measured alongshore sand transport than C1.

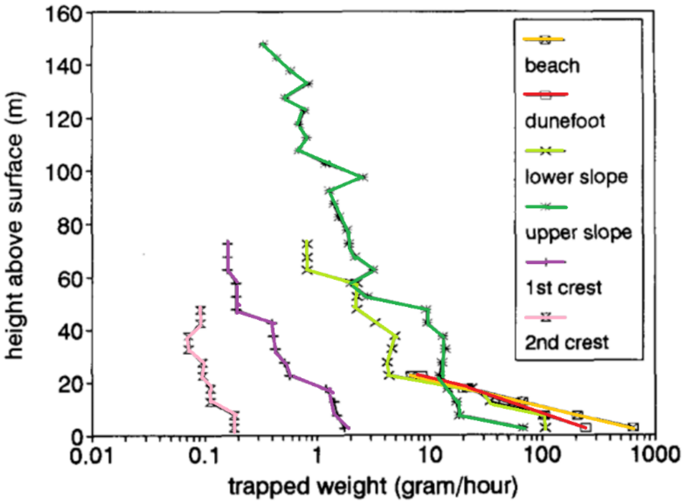

Figure 46. Sediment curved for different heights on a beach-dune, retrieved from (Arens and van der Lee, 1995). Traps were installed at different positions on the beach and the foredune and caught sand at different heights above the surface.

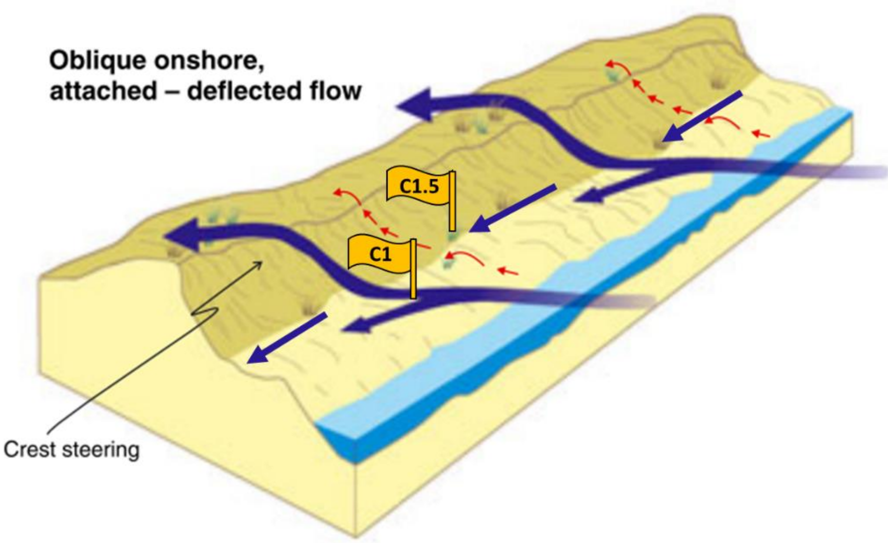

Figure 47. Conceptual model of flow–form interaction over large (> 8 m) foredunes for oblique onshore winds. Large solid arrows represent near-surface flows, modulated and steered by the local topography. Possible and high alongshore sand transport can result. Catcher C1.5 was closer to the steep slope than C1, therefore more likely to measure alongshore sand transport. Figure retrieved and modified of Bauer *et al.* (2012).

5.4.4. Morphological changes of the vegetated foredune

Gradients in fluxes at the sand catchers could subsequently be linked to morphological changes of the foredune profile. A volume gain of 0.58 m^3 was recorded, which is similar to the measured deposition of 0.52 m^3 for Greenwich dunes, although deposition patterns are different (Christiansen and Davidson-Arnott, 2004). Although the overall sediment budget of the foredune slope was positive, sedimentation varied clearly.

At the dune foot, sand accumulation could be the result of wind speed deceleration, as the dune foot was not vegetated. Vegetation started just landward of C1.5 with a cover of 50% (sand couch) and could be associated with the largest sediment accumulation. Vegetation cover increased with increasing height of the foredune and the dominant species shifted from sand couch to marram grass. Sedimentation was smaller on the slope and just behind the crest maximum erosion occurred. This was expected, since most sedimentation occurred already within the first few metres of the vegetation, which is commonly found amongst literature (Keijsers, De Groot and Riksen, 2015). For the other transects the vegetation limits caused similar sedimentation patterns, with largest sedimentation at the dune foot, which was characterised by the presence of embryo dunes. Vegetation covers of 1 - 10% caused the maximum sedimentation. A growing vegetation cover with height did not lead to an increased sedimentation (Figure 43), most likely due to the deposition within the first zone of vegetation. Since vegetation densities of 20 - 30% (Arens, 1996; Kuriyama, Mochizuki and Nakashima,

2005) or 5 – 85% (Keijsers *et al.*, 2012) are sufficient to trap most of the sediment, the findings of maximum sedimentation at 1 – 10% for 41.25 and 41.5 and 50% for 41.0 are typical. Some sedimentation on the upper slope and crest was possible despite the dense vegetation cover (20 – 70%), which might be due to spatial variations within the vegetation that affect transport rates and deposition (Bauer *et al.*, 2012; Davidson-Arnott *et al.*, 2012). The vegetation cover varied for the different transects and morphological changes as well. Especially transect 41.5 showed lower vegetation coverage and considerable erosion at the dune crest. This is most likely due to the presence of a large natural blow out directly next to it (north and landward) (Figure 48). A steep sand crater hindered the dune from growing in height and plants suffered more erosive stress, which may have resulted in a negative feedback mode.

Figure 48. Natural blow-out next and landward of transect 41.5, which might be responsible for the relatively large erosion at the dune crest.

At the study site, storms can cause severe dune erosion in the order of 5 - 40 $m^3.m^{-1}$ in several hours as in 2012 (Ruessink *et al.*, 2012). The dune erosion after storm might facilitate transport across the foredune. A vegetated part of the dune would be eroded and the novel presence of a dune ramp could facilitate transport across the slope as shown by Christiansen and Davidson-Arnott (2004). The findings of this study showed that most sedimentation occurred within the first vegetation zone so that a reduction in vegetation could be positive for dune growth. Regarding the quantities of sedimentation and erosion, rather large elevation changes were measured within five weeks of up to 30 cm. At the main study transect the dune profile was measured three times with a dGPS (point-wise measurements). This elevation data showed similar elevation changes in the order of tenth of centimetres. Pronounced sediment dynamics could be seen during the field work at various occasions. During a few days at the end of the campaign, the lower part of catcher C1.5 was buried and had to be dug out of about 20 cm. The sea-container that was placed for the crew and equipment showed considerable amounts of erosion and sedimentation (Figure 49).

Figure 49. Pronounced sediment dynamics occurred during the field campaign and were visual at e.g. the sea-container that was used for instrument storage.

The findings of this study allowed to complement the conceptual model that was at the basis of the study (Figure 50).

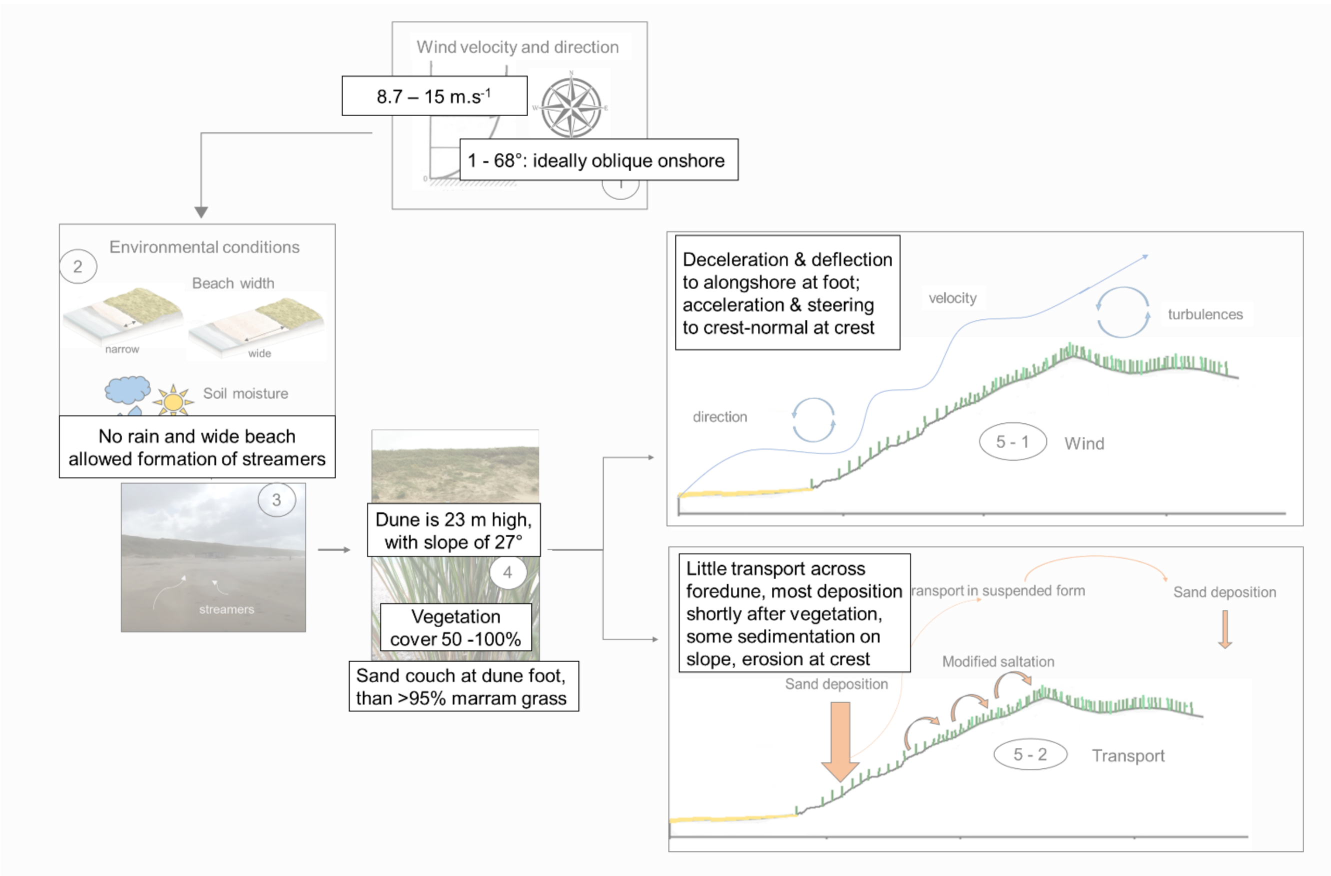

Figure 50. Conceptual model of answers to the formulated research questions and hypotheses.

It was hypothesised that depending on the incipient wind direction, airflows across the vegetated foredune would accelerate and deflect to more crest-perpendicular direction across the foredune, while turbulent flows were expected to decrease (hypothesis 1). The results showed this hypothesis was for the most part supported. Firstly, airflows are deflected to the alongshore (crest-parallel) at the dune foot, unless incident wind directions are highly oblique or alongshore. Moreover, a flow reduction for perpendicular and oblique onshore winds occurs at the dune foot, and only hereafter the wind is accelerated across the foredune and deflected to more crest-normal. While doing so, it turns more perpendicular to cross-shore than the undisturbed, initial wind (based on reference wind direction). The turbulent kinetic energy increased in absolute terms across the foredune, but decreased relatively to the wind speed due to streamline compression. However, it was not expected that the relative *tke* would be largest on the mid slope, which could be due to vegetation induced turbulences or topographic features of the dune. It was also not expected that for lower wind velocities, the general trends were often not applicable.

It was assumed that aeolian transport rates would decrease very fast, shortly after the first vegetation around the dune foot and that most sediment would be deposited around the dune foot, barely on the dune slope and not at all on the dune crest (hypothesis 2). This hypothesis was mostly supported since transport rates decreased by 99% across the foredune and largest deposition occurred within a few metres of the vegetation. Nevertheless, sedimentation was still measured across the foredune at high wind speeds and with either slightly oblique or highly oblique onshore directions, demonstrating the complexity of sand transport across the foredune and the effect of local topographic features, vegetation patterns and wind flows.

Hypothesis 3 was partly supported by the results. Although wind flows were not reduced due to the vegetation, vegetation trapped sediment and hindered further aeolian transport in form of saltation. Since there was only one species on the dune foot (sand couch grass) and one on the foredune slope (marram grass), no effects of varying species compositions were observed. Whether the vegetation cover was scarce (1 – 10%) or dense (50%) did not affect the rapid deposition behind the first vegetation line.

5.5. Project challenges and future recommendations

Overall, the data were abundant and allowed a holistic analysis. The wind data across the foredune could be enriched by placing two additional ultrasonic anemometers. Firstly, seaward from the dune foot to compare the wind across the dune with measurements of local but (topographically) undisturbed flows. Secondly, landward of the crest to link wind data with sand fluxes and sedimentation patterns that occur landward of the crest, since erosion was observed just behind the crest. Previous studies suggested that the reduced slope steepness for oblique onshore wind flows can have considerable implications for transport across the foredune. Therefore, it would be interesting to measure the slope profile at an angle of 45° from crest-normal. The differences in slope steepness for oblique onshore winds from north and south could be then taken into account in the analysis. Since it is likely that sand transport at the crest occurs in suspended form, higher sand catchers would be recommended for the dune slope and crest to see whether transport increases with height and above the vegetation canopy. The effect of vegetation was clearly visible, due to the sedimentation and erosion patterns of the three transects. The sharp decreases of sand fluxes across the foredune was most likely also owed to vegetation. However, it is challenging to directly link the changes across the foredune to the vegetation cover. Therefore, an *in situ* experiment along a study transect is recommended. This would allow to better link the effect of vegetation to actual sand transport quantities, as well as wind flows. Similar to Hesp (1989) the grass could be cut after half of the study period. Previous studies found that minor topographic changes and small variations of the wind conditions can result in different transport patterns. Cutting the vegetation would result in a real comparison between vegetated and less vegetated stoss site along the same profile. To resolve this, the use of a CFD model would also be recommended to compare the same dune profile under the same wind configurations with and without vegetation.

6. Conclusion

This study sought to answer three questions. Firstly, changes of wind flows across the foredune were examined. According to the results from this study, there appears to be a strong relationship of flow acceleration, deflection and relative *tke* (*r*) with incident angle of the wind flow. Results showed that perpendicular onshore winds were first decelerated at the dune foot and then greatly accelerated across the dune with little deflection. Oblique onshore winds were not as much accelerated but deflected the most to alongshore at the dune foot and to more crest-normal at the crest. Although *tke* seemed independent of the wind direction, *r* seemed independent on wind velocity and was largest for perpendicular onshore wind flows at the dune foot and for highly oblique to alongshore winds on the slope. For all findings, there was a slight asymmetry for wind flows approaching from the north and south, which is likely due to an inherently more turbulent wind from north. The findings could mostly be explained by the topographic forcing of the foredune to the wind flows. Aeolian sand transport and sedimentation pattern were also analysed. The recorded aeolian transport events showed that transport decreased considerably across the foredune. On average sand flux was 12.35 $g.m^{-1}.s^{-1}$ at the dune foot (100%), 40.52$g.m^{-1}.s^{-1}$ on the upper dune foot (328%), 2.08 $g.m^{-1}.s^{-1}$ (16.8%) on the mid slope and 0.18 $g.m^{-1}.s^{-1}$ (1.4%) at the crest. However, transport fluxes varied greatly for the different events, which was most likely due to varying wind velocity and differences in wind direction and, associated therewith, maximum fetch size. Lastly, vegetation assays were conducted to link the effect of vegetation with sand transport. The assays showed that the vegetation cover increased with height above NAP with largest cover usually on the crest. The presence of both scarcely vegetated (1 – 10%) embryo dunes and the vegetated dune slope (50% cover) lead to maximum sedimentation shortly behind the first vegetation line. The vegetation is related to transport reduction. Despite the increase in wind velocity, the sand transport decreases, most likely as a result of the presence of vegetation cover.

Although this study provides some interesting results, future research is needed to provide clearer conclusions about the sand transported across the foredune and further landward. This is particularly true for the quantification of sand fluxes that should to be recorded at high frequency simultaneously with wind flows supplemented by vegetation assays.

7. References

Aagaard, T. *et al.* (2005) 'Intertidal beach change during storm conditions; Egmond, The Netherlands', *Marine Geology*, 218(1–4), pp. 65–80. doi: 10.1016/j.margeo.2005.04.001.

Anderson, J. L. and Walker, I. J. (2006) 'Airflow and sand transport variations within a backshore-parabolic dune plain complex: NE Graham Island, British Columbia, Canada', *Geomorphology*, 77(1–2), pp. 17–34. doi: 10.1016/j.geomorph.2005.12.008.

Arens, S. M. (1996) 'Patterns of sand transport on vegetated foredunes', *Geomorphology*, 17(4), pp. 339–350. doi: 10.1016/0169-555X(96)00016-5.

Arens, S. M. (1996) 'Rates of aeolian transport on a beach in a temperate humid climate', *Geomorphology*, 17(1–3), pp. 3–18. doi: 10.1016/0169-555X(95)00089-N.

Arens, S. M. *et al.* (2013) 'Restoration of Dune Mobility in The Netherlands', (September), pp. 107–124. doi: 10.1007/978-3-642-33445-0_7.

Arens, S. M., Van Boxel, J. H. and Abuodha, J. O. Z. (2002) 'Changes in grain size of sand in transport over a foredune', *Earth Surface Processes and Landforms*, 27(11), pp. 1163–1175. doi: 10.1002/esp.418.

Arens, S. M., Van Kaam-Peters, H. M. E. and Van Boxel, J. H. (1995) 'Air-Flow Over Foredunes and Implications for Sand Transport', *Earth Surface Processes and Landforms*, 2, pp. 315–332.

Arens, S. M. and van der Lee, G. E. M. (1995) 'Saltation sand traps for the measurement of aeolian transport into the foredunes', *Soil Technology*, 8(1), pp. 61–74. doi: 10.1016/0933-3630(95)00007-5.

Baas, A. C. W. (2006) 'Wavelet power spectra of aeolian sand transport by boundary layer turbulence', *Geophysical Research Letters*, 33(5), pp. 1–4. doi: 10.1029/2005GL025547.

Barchyn, T. E. and Hugenholtz, C. H. (2013) 'Reactivation of supply-limited dune fields from blowouts: A conceptual framework for state characterization', *Geomorphology*. Elsevier B.V., 201, pp. 172–182. doi: 10.1016/j.geomorph.2013.06.019.

Bauer, B. O. *et al.* (2009) 'Aeolian sediment transport on a beach: Surface moisture, wind fetch, and mean transport', *Geomorphology*. Elsevier B.V., 105(1–2), pp. 106–116. doi: 10.1016/j.geomorph.2008.02.016.

Bauer, B. O. *et al.* (2012) 'Wind direction and complex sediment transport response across a beach-dune system', *Earth Surface Processes and Landforms*, 37(15), pp. 1661–1677. doi: 10.1002/esp.3306.

Bauer, B. O. and Davidson-Arnott, R. G. D. (2003) 'A general framework for modeling sediment supply to coastal dunes including wind angle, beach geometry, and fetch effects', *Geomorphology*, 49(1), pp. 89–108. doi: 10.1016/S0169-555X(02)00165-4.

Beniston, M. *et al.* (2007) 'Future extreme events in European climate: An exploration of regional climate model projections', *Climatic Change*, 81(SUPPL.1), pp. 71–95. doi: 10.1007/s10584-006-9226-z.

Blott, S. J. and Pye, K. (2001) 'Gradistat: A grain size distribution and statistics package for the analysis of unconsolidated sediments', *Earth Surface Processes and Landforms*, 26(11), pp. 1237–1248. doi: 10.1002/esp.261.

van Boxel, J. H., Sterk, G. and Arens, S. M. (2004) 'Sonic anemometers in aeolian sediment transport research', *Geomorphology*, 59(1–4), pp. 131–147. doi: 10.1016/j.geomorph.2003.09.011.

Chapman, C. *et al.* (2013) 'Reynolds stress and sand transport over a foredune', *Earth Surface Processes and Landforms*, 38(14), pp. 1735–1747. doi: 10.1002/esp.3428.

Chapman, C. A. *et al.* (2012) 'Turbulent Reynolds stress and quadrant event activity in wind flow over a coastal foredune', *Geomorphology*. Elsevier B.V., 151–152, pp. 1–12. doi: 10.1016/j.geomorph.2011.11.015.

Christiansen, M. B. and Davidson-Arnott, R. (2004) 'Rates of landward sand transport over the foredune at Skallingen, Denmark and the role of dune ramps', *Geografisk Tidsskrift*, 104(1), pp. 31–43. doi: 10.1080/00167223.2004.10649502.

Davidson-Arnott, R. *et al.* (2018) 'Sediment Budget Controls on Foredune Height: Comparing Simulation Model Results with Field Data', *Earth Surface Processes and Landforms*. doi: 10.1002/esp.4354.

Davidson-Arnott, R. G. D. *et al.* (2012) 'High-frequency sediment transport responses on a vegetated foredune', *Earth Surface Processes and Landforms*, 37(11), pp. 1227–1241. doi: 10.1002/esp.3275.

Delgado-Fernandez, I. (2011) 'Meso-scale modelling of aeolian sediment input to coastal dunes', *Geomorphology*. Elsevier B.V., 130(3–4), pp. 230–243. doi: 10.1016/j.geomorph.2011.04.001.

Dong, Z. *et al.* (2011) 'Equations for the near-surface mass flux density profile of wind-blown sediments', *Earth Surface Processes and Landforms*, 36(10), pp. 1292–1299. doi: 10.1002/esp.2151.

Dong, Z. B. *et al.* (2001) 'Aerodynamic roughness of fixed sandy beds', *Journal of Geophysical Research-Solid Earth*, 106(6), pp. 11001–11011.

van Duin, M. J. P. *et al.* (2004) 'Nourishing the shoreface: Observations and hindcasting of the Egmond case, The Netherlands', *Coastal Engineering*, 51(8–9), pp. 813–837. doi: 10.1016/j.coastaleng.2004.07.011.

Duran, O. and Moore, L. J. (2013) 'Vegetation controls on the maximum size of coastal dunes', *Proceedings of the National Academy of Sciences*, 110(43), pp. 17217–17222. doi: 10.1073/pnas.1307580110.

Environmental Agency Protection and (EPA) (2000) *Dune Management Report*.

Everard, M., Jones, L. and Watts, B. (2010) 'Have we neglected the societal importance of sand dunes? An ecosystem services perspective', *Aquatic Conservation: Marine and Freshwater Ecosystems*, 20(4), pp. 476–487. doi: 10.1002/aqc.1114.

Goldstein, E. B. and Moore, L. J. (2016) 'Stability and bistability in a one-dimensional model of coastal foredune height', *Journal of Geophysical Research: Earth Surface*, 121(5), pp. 964–977. doi: 10.1002/2015JF003783.

Goldstein, E. B., Moore, L. J. and Durán Vinent, O. (2017) 'Vegetation controls on maximum coastal foredune "hummockiness" and annealing time', *Earth Surface Dynamics Discussions*, (January), pp. 1–15. doi: 10.5194/esurf-2017-2.

Goossens, D. and Offer, Z. Y. (2000) 'Wind tunnel and field calibration of six aeolian dust samplers', *Atmospheric Environment*, 34(7), pp. 1043–1057. doi: 10.1016/S1352-2310(99)00376-3.

Gutiérrez, J. L. *et al.* (2011) 'Physical ecosystem engineers and the functioning of estuaries and coasts', in Heip, C. H. R., Philippart, C. J. M., and Middelburg, J. J. (eds) *Treatise on Estuarine and Coastal Science*. Elsevier, pp. 1–99.

Hesp, P. (1988) 'Morphology, dynamics and internal stratification of some established foredunes in southeast Australia', *Sedimentary Geology*, 55(1–2), pp. 17–41. doi: 10.1016/0037-0738(88)90088-7.

Hesp, P. (2002) 'Foredunes and blowouts: initiation, geomorphology and dynamics', *Geomorphology*, 48(1–3), pp. 245–268. doi: 10.1016/S0169-555X(02)00184-8.

Hesp, P. (2012) *Dune Coasts*, *Treatise on Estuarine and Coastal Science*. Elsevier Inc. doi: 10.1016/B978-0-12-374711-2.00310-7.

Hesp, P. A. (1989) 'A review of biological and geomorphological processes involved in the initiation and development of incipient foredunes', *Proceedings of the Royal Society of Edinburgh. Section B. Biological Sciences*, 96(January 1989), pp. 181–201. doi: 10.1017/S0269727000010927.

Hesp, P. A. *et al.* (2005) 'Flow dynamics over a foredune at Prince Edward Island, Canada', *Geomorphology*, 65(1–2), pp. 71–84. doi: 10.1016/j.geomorph.2004.08.001.

Hesp, P. A. *et al.* (2013) ‘Aeolian dynamics over a coastal foredune, Prince Edward Island, Canada’, *Earth Surface Processes and Landforms*, 38(13), pp. 1566–1575. doi: 10.1002/esp.3444.

Hesp, P. A. *et al.* (2015) ‘Flow deflection over a foredune’, *Geomorphology*, 230, pp. 51–63. doi: 10.1016/j.geomorph.2014.11.005.

Hilton, M., Duncan, M. and Jul, A. (2005) ‘Processes of Ammophila arenaria (Marram Grass) Invasion and Indigenous Species Displacement, Stewart Island, New Zealand’, *Journal of Coastal Research*, 211, pp. 175–185. doi: 10.2112/01041.1.

Horikawa, K. and Shen, W. (1960) ‘Sand Movement by wind action (on the characteristics of sand traps).’, *US Army Corps of Engineers, Beach Erosion Board, Technical Memo*, (119).

Keijsers, J. G. S. *et al.* (2012) ‘Connecting aeolian sediment transport with foredune development’, *NCK-days 2012: Crossing borders in Coastal Research: Jubilee Conference Proceedings*, pp. 153–156. doi: 10.3990/2.187.

Keijsers, J. G. S., De Groot, A. V. and Riksen, M. J. P. M. (2015) ‘Vegetation and sedimentation on coastal foredunes’, *Geomorphology*. Elsevier B.V., 228, pp. 723–734. doi: 10.1016/j.geomorph.2014.10.027.

Kumer, V. M. *et al.* (2016) ‘Turbulent kinetic energy estimates from profiling wind LiDAR measurements and their potential for wind energy applications’, *Renewable Energy*, 99, pp. 898–910. doi: 10.1016/j.renene.2016.07.014.

Kuriyama, Y., Mochizuki, N. and Nakashima, T. (2005) ‘Influence of vegetation on aeolian sand transport rate from a backshore to a foredune at Hasaki, Japan’, *Sedimentology*, 52(5), pp. 1123–1132. doi: 10.1111/j.1365-3091.2005.00734.x.

Mayaud, J. R. *et al.* (2017) ‘Modelling aeolian sand transport using a dynamic mass balancing approach’, *Geomorphology*. The Authors, 280, pp. 108–121. doi: 10.1016/j.geomorph.2016.12.006.

Miller, T. E. (2015) ‘Effects of disturbance on vegetation by sand accretion and erosion across coastal dune habitats on a barrier island’, *AoB PLANTS*, 7(1), pp. 1–10. doi: 10.1093/aobpla/plv003.

Milne, R. and Sawyer, J. W. D. (2002) *Coastal foredune vegetation in Wellington Conservancy: Current status and future management*.

Nickling, W. G. and Davidson-Arnott, R. G. D. (1990) ‘Aeolian sediment transport on beaches and coastal sand dunes’, *Proceedings of Symposium on Coastal Sand Dunes*, (June), pp. 1–35.

Petersen, P. S., Hilton, M. J. and Wakes, S. J. (2011) ‘Evidence of aeolian sediment transport across an Ammophila arenaria-dominated foredune, Mason Bay, Stewart Island’, *New Zealand Geographer*, 67(3), pp. 174–189. doi: 10.1111/j.1745-7939.2011.01210.x.

Provincie Noord-Holland (2012) *Atlas van de Natura 2000 duingebieden van Noord-Holland.* Haarlem.

R. M. Young Company (2001) ‘Model 81000 Ultrasonic Anemometer rev C031405’. USA.

Ruessink, B. G. *et al.* (2012) ‘Towards a process-based model to predict dune erosion along the Dutch Wadden coast’, *Geologie en Mijnbouw/Netherlands Journal of Geosciences*, 91(3), pp. 357–372. doi: 10.1017/S0016774600000494.

Ruessink, B. G. *et al.* (2017) ‘Coastal dune dynamics in response to excavated foredune notches’, *Aeolian Research*. Elsevier B.V. doi: 10.1016/j.aeolia.2017.07.002.

Ruessink, B. G., Kleinhans, M. G. and van den Beukel, P. G. L. (1998) ‘Observations of swash under highly dissipative conditions’, *Journal of Geophysical Research: Oceans*. Wiley-Blackwell, 103(C2), pp. 3111–3118. doi: 10.1029/97JC02791.

Ruggiero, P. *et al.* (2001) ‘Wave Runup, Extreme Water Levels and the Erosion of Coastal Properties Backing Beaches’, *Journal of Coastal Research*, 17(2), pp. 407–419.

Short, A. D. and Hesp, P. A. (1982) ‘Wave, beach and dune interactions in southeastern Australia’, *Marine Geology*, 48(3–4), pp. 259–284. doi: 10.1016/0025-3227(82)90100-1.

Sigren, J. M. *et al.* (2014) 'Coastal sand dunes and dune vegetation: restoration, erosion, and storm protection', *Shore & Beach*, 82(4), p. 5.

Stallins, J. A. (2003) 'Dune plant species diversity and function in two barrier island biogeomorphic system', *Plant Ecology*, 165(2), pp. 183–196.

Sterk, G. *et al.* (2012) 'Aeolian sediment mass fluxes on a sandy soil in Central Patagonia', *Catena*. Elsevier B.V., 95, pp. 112–123. doi: 10.1016/j.catena.2012.02.005.

Sterk, G. and Raats, P. a. C. (1996) 'Comparison of Models Describing the Vertical Distribution of Wind-Eroded Sediment', *Soil Science Society of America Journal*, 60(6), pp. 1914–1919.

de Vries, S. *et al.* (2012) 'Dune behavior and aeolian transport on decadal timescales', *Coastal Engineering*. Elsevier B.V., 67, pp. 41–53. doi: 10.1016/j.coastaleng.2012.04.002.

Walker, I. J. *et al.* (2006) 'Topographic Steering of Alongshore Airflow over a Vegetated Foredune: Greenwich Dunes, Prince Edward Island, Canada', *Journal of Coastal Research*, 225(225), pp. 1278–1291. doi: 10.2112/06A-0010.1.

Walker, I. J. *et al.* (2009) 'Mean Flow and Turbulence Responses in Airflow over Foredunes: New Insights from Recent Research.', *Journal of Coastal Research*, 1(56), pp. 366–370.

Walker, I. J. *et al.* (2017) 'Scale-dependent perspectives on the geomorphology and evolution of beach-dune systems', *Earth-Science Reviews*, 171(June 2016), pp. 220–253. doi: 10.1016/j.earscirev.2017.04.011.

Weaver, C. M. and Wiggs, G. F. S. (2011) 'Field measurements of mean and turbulent airflow over a barchan sand dune', *Geomorphology*. Elsevier B.V., 128(1–2), pp. 32–41. doi: 10.1016/j.geomorph.2010.12.020.

de Winter, R. C., Gongriep, F. and Ruessink, B. G. (2015) 'Observations and modeling of alongshore variability in dune erosion at Egmond aan Zee, the Netherlands', *Coastal Engineering*. Elsevier B.V., 99, pp. 167–175. doi: 10.1016/j.coastaleng.2015.02.005.

Wright, L. D. and Short, A. D. (1984) 'Morphodynamic variability of surf zones and beaches: A synthesis', *Marine Geology*, 56(1–4), pp. 93–118. doi: 10.1016/0025-3227(84)90008-2.

Zarnetske, P. L. *et al.* (2012) 'Biophysical feedback mediates effects of invasive grasses on coastal dune shape Published by : Ecological Society of America, 93(6), pp. 1439–1450.

Zarnetske, P. L. *et al.* (2015) 'Coastal foredune evolution: The relative influence of vegetation and sand supply in the US Pacific Northwest', *Journal of the Royal Society Interface*, 12(106). doi: 10.1098/rsif.2015.0017.

Zhang, K. Q., Douglas, B. C. and Leatherman, S. P. (2004) 'Global warming and coastal erosion', *Climatic Change*, 64(1–2), pp. 41–58. doi: 10.1023/b:clim.0000024690.32682.48.

8. Appendix

8.1. Details of instruments

Table A1. Position description and coordinates of SAs.

SA no.	Location	Position relative to reference (m)		
		X: Cross-shore	*Y: Alongshore*	*Z:Height +NAP*
SA1	Dune foot (bare beach)	-44.44	-230.30	3.8
SA2	Mid slope (patchy vegetation)	-61.54	-229.76	11.16
SA3	Dune top (dense vegetation)	-71.16	-229.21	17.75

Table A2. Heights from ground (cm) of all sand traps per sand catcher.

Trap	Catcher no.						
	1	1.5	2	3	4*	5*	6*
a	6.5	9.4	6.5	5.5	8.5	8.2	4.7
b	12.7	15.3	12.5	11.6	14.7	14.3	11
c	19	20	18.5	17.5	20.5	20.5	16.8
d	25	26.9	24.3	23.4	26.4	26.2	22.9
e	38.3	40.2	37.3	36.7	40	39.5	36.5
f	63.5	65	62.7	61.7	65.2	64.3	61.9

Table A3. Description of location and coordinates of sand catchers. Coordinates x, y and z represent cross-shore, alongshore and height coordinates, respectively. (*) indicates mobile catchers that were operational only once (11^{th} October).

Catcher No.	Location	Position relative to reference (m)		
		X: Cross-shore	*Y: Alongshore*	*Z:Height +NAP*
1	Height of embryo dunes (bare beach)	-40.16	-230.70	3.19
1.5	Dune foot (bare)	-52.14	-219.16	5.67
2	Mid slope (patchy vegetation)	-59.36	-219.50	10.57
3	Dune top (dense vegetation)	-70.27	-238.89	17.54

8.2. Vegetation assays

8.2.1. Main study transect

Pictures of quantification 1 – 19 not available. Quadrants 20 to 31 (mid slope to crest) were documented with images and are presented below:

			
20	21	22	23
			
24	25	26	27
			
28	29	30	31

8.2.2. Transect 41.25

At transect 41.25 the quadrants 1 – 8 were at the embryo dune, 9 – 12 (no image) were the bare dune foot and the remaining at the slope.

			
1	2	3	4
			
Embryo dune	5	6	7
			
8	13	14	15

			
16	17	18	19
			
20			

8.2.3. Transect 41.5

At transect 41.5 the quadrants 1 – 3 were at the embryo dune, 4 – 6 (no image) were the bare dune foot and the remaining at the slope.

			
1	2	3	7
			
8	9	10	11
			
12	13	14	15